Journal of Archaeological Science 86 (2017) 24–49

Contents lists available at ScienceDirect

Journal of Archaeological Science

journal homepage: http://www.elsevier.com/locate/jas

Radiogenic and "stable" strontium isotopes in provenance studies: A review and first results on archaeological wood from shipwrecks

Fadi Hajj [a, *], Anne Poszwa [a], Julien Bouchez [b], François Guérold [a]

[a] Laboratoire Interdisciplinaire des Environnements Continentaux, UMR 7360 CNRS, Université de Lorraine, 54506 Vandoeuvre-lès-Nancy, France
[b] Institut de Physique du Globe de Paris, UMR 7154 CNRS, Université Sorbonne-Paris Cité, 75238 Paris, France

ARTICLE INFO

Article history:
Received 4 January 2017
Received in revised form
18 June 2017
Accepted 2 September 2017

Keywords:
Wood provenance
Shipwrecks
Radiogenic and stable Sr isotopes
Site signature
Mass-dependent fractionation
Wood signature modification

ABSTRACT

Different approaches are used to study wood provenance, but most of them are based on tracers in wood that are generally controlled by climatic factors. The strontium isotopic ratio $^{87}Sr/^{86}Sr$ in trees and soils is related to the signature of the local bedrock. Despite being used in diverse archaeological studies, Sr isotopes have rarely been used to trace the provenance of archaeological wood and especially wood from shipwrecks. In addition, recent analytical advances have allowed the detection of mass-dependent fractionation of Sr isotopes during biogeochemical processes, as reflected in the variation of $\delta^{88/86}Sr$ values between different environmental materials. The $\delta^{88/86}Sr$ values could be used in conjunction with the $^{87}Sr/^{86}Sr$ isotope ratio to improve constraints on the sources of Sr in the archaeological materials being studied. This paper discusses the potential and limitations of using both of these Sr isotope ratios to trace the provenance of wood from shipwrecks. We review the $^{87}Sr/^{86}Sr$ and $\delta^{88/86}Sr$ variations in rocks, waters, soils, plants and other living organisms and discuss how to determine the local Sr isotopic signature of potential sites. We also compile a list of known wood *post mortem* modifications in seawater. Possible implications in terms of the modification of the original Sr isotope ratios of wood during storage in seawater are illustrated through preliminary observations. This paper points out some limitations and perspectives for using Sr isotopes in provenancing wood from shipwrecks, and suggests future research to test and apply this approach for tracing the origin of archaeological wood.

Contents

* Corresponding author.
E-mail address: fadi.hajj@univ-lorraine.fr (F. Hajj).

http://dx.doi.org/10.1016/j.jas.2017.09.005
0305-4403/

1. Introduction

The study of wood provenance (dendroprovenancing) can be applied for many purposes, including identifying the source of the construction wood used for building monuments, ancient houses and ships, understanding wood trading links in the past, and tracking illegal timber logging. Any physiological or chemical tracer of wood provenance must be highly specific of the geographic area of origin. Dendrochronology, wood anatomy, genetics and biogeochemical analyses are among the different tools that can be used to determine the provenance of wood. The wood in question needs to be compared with data on wood (or other biogeochemical compartments) from the potential sites of origin. Therefore, we need a comprehensive and large dataset on the tracer, at spatial scales varying from the region to the catchment or even the stand. However, in the case of archaeological wood, and regardless of the selected technique, some methods should be used with caution and adapted if processes such as diagenesis have modified the wood structure and/or composition during burial in soils or sediments.

Dendrochronology is the dating and study of annual rings in trees, representing the most common method developed so far for wood provenance studies. Trees respond to the climate by adapting their growth rate. As a result, trees growing in a given geographical location and experiencing similar environmental conditions (*e.g.* annual rainfall, air relative humidity, soil moisture, ground water availability) will display similar tree-ring patterns and typical pointer years. Dendrochronology has been used successfully to determine the origin of diverse wood materials *e.g.* wood from shipwrecks (Bonde and Christensen, 1993; Daly, 2007; Daly and Nymoen, 2008; Domínguez-Delmás et al., 2013), wine barrels (Eckstein et al., 1975), furniture and altarpieces (Haneca et al., 2005) as well as wooden foundation piles of historical buildings (Sass-Klaassen et al., 2008). The use of dendrochronology can be complicated in some cases when only short chronologies are available (Billamboz, 2003). Short tree-ring series (less than 60 years) yield lower correlation coefficients when cross-dated and lead to a higher probability of dating errors compared to longer chronologies, hence long tree-ring series are required to ensure a satisfactory interpretation. Another limitation can arise from the presence of various growth anomalies in the studied timber (Haneca et al., 2009). While extensive tree-ring databases are established in some regions (*e.g.* northern and central Europe), more data are needed in other regions to cover wider geographical areas and acquire longer chronologies (Domínguez-Delmás et al., 2015).

Alternatively, wood anatomy can serve to identify plant taxa to the genus level and sometimes to the species level. If the genus or species can be determined, and have small area of distribution linked to environmental conditions such as climate, this method might be suitable for wood provenance studies. In particular, Esteban et al. (2012) showed that the variation of anatomical features linked to provenance and microclimate conditions is greater than the variation within populations of *Pinus nigra* from 17 different regions in Spain. This observation shows the potential of using wood anatomy for provenance studies by matching the anatomical features of the examined wood with material from the site of origin. However, more studies are needed to validate this approach in other areas and with other species.

Genetics provides another tool for identifying the provenance of wood. For example, during the Quaternary glacial episodes, European forests were restricted to the Iberian, Italian, and Balkan peninsulas (Petit et al., 2003). Afterwards, the chloroplast DNA (cpDNA) lineages of European oaks became widely distributed due to post-glacial colonization outward from the different European refugia. This resulted in a clear geographical structure of cpDNA haplotypes (Deguilloux et al., 2004, 2003, Petit et al., 2002a, 2002b, 2002c). By characterizing the cpDNA haplotypes of oaks in Ireland, Kelleher et al. (2004) concluded that they matched the cpDNA of Iberian refugia out of which oaks migrated following the last glaciation. This method has a limitation when haplotypes are distributed over large areas. Moreover, when the wood comes from plantation trees, the DNA fingerprints do not match the natural distribution of DNA (Kagawa and Leavitt, 2010).

The compositions of cellulose, hemicellulose and lignin (Sandak et al., 2011), as well as other wood constituents such as so-called “wood extractives” (Miranda and Pereira, 2002) or monoterpenes (Smith et al., 1969) can be significantly different in relation to their specific geographical distribution. These variations in wood composition between geographical areas are linked to different environmental and climatic factors (Sandak et al., 2015). Clarke et al. (1997) found significant differences between cellulose and pentosan components in different species of *Eucalyptus* from different provenances. Rodrigues et al. (1998) showed variations in lignin content, which make it possible to trace the provenance of *Eucalyptus globulus*. These provenance studies using organic tracers are encouraging insofar as they reveal distinct organic compositions of certain species according to specific areas. However, further studies are needed to establish suitable species and organic component that could be used.

The isotopes of a given element show a shift in their relative abundances during biogeochemical cycling due to biological and physico-chemical processes – this phenomenon is known as “isotope fractionation”. In particular, climatic conditions influence the isotopic ratios of hydrogen (H), carbon (C) and oxygen (O), *i.e.* the main elements present in wood. While the signature of C isotopes in plants is linked to soil moisture and depends on relative humidity, temperature and precipitation (Francey and Farquhar, 1982; Saurer et al., 1995; Stuiver and Braziunas, 1987), the H and O isotope ratios are influenced by spatial variations of precipitation and humidity (Barbour, 2007; Bowen et al., 2005; Farquhar et al., 1997; McCarroll and Loader, 2004). As a result, the wood from growth-rings can record a specific isotopic fingerprint linked to the climatic factors at the original site of the tree (Leavitt, 1993). Kagawa et al. (2007) found a significant correlation between

latitude and the O or H isotope ratios in tree-rings. In a study on pinyon pines from the southwestern United States, Kagawa and Leavitt (2010) found that C isotope compositions were more closely linked to the site of origin than tree-ring width. This shows the potential for using these isotopes in dendroprovenance studies. Nevertheless, the isotopic composition of tree-rings can be influenced by fractionation effects involving biological or physico-chemical processes, but unrelated to climate or geographical factors, which could complicate the use of these tracers.

The methods mentioned above are based on physiological or biochemical tracers influenced more or less directly by climatic factors that are specific of a geographic region (longitude, latitude and elevation). As discussed previously, all of these methods show advantages as well as drawbacks in dendroprovenance studies. An alternative and complementary method is to use tracers which show less dependence on climate, such as inorganic constituents present in wood. The mineral composition of rocks and soils is mostly controlled by geology. Therefore, the abundance and isotopic signatures of elements released by the weathering of rocks, which then become available in the soil and which are taken up by trees, can also display significant local variations. Among these inorganic potential tracers, the relative abundance of the radiogenic strontium isotope (^{87}Sr) is very specific of rock type (Faure, 1986) and thus provides a powerful tracer of source materials. This explains why Sr isotopes were first applied around 30 years ago in environmental studies (Gosz et al., 1983; Graustein and Armstrong, 1983; Graustein, 1989), to investigate Earth surface processes such as weathering and erosion, as well as solute and sediment transport. In archaeology, Sr isotopes have been used to study human and animal diets and migrations (Ericson, 1985; Koch et al., 1995, 1992; Sealy et al., 1991). More recently, the detection of Sr isotope fractionation during biogeochemical and biomineralization processes (Fietzke and Eisenhauer, 2006; Ohno and Hirata, 2007) has opened new avenues for improving our understanding of the Sr cycle in the environment, while also providing a tool that could become useful for provenance studies.

In this review, we focus on Sr isotopes to show their potential as a tool for determining timber provenance and particularly when applied to wood from shipwrecks. We first establish the chemical properties of Sr and its range of isotopic variation amongst rocks and waters at the global scale. We then review existing data on Sr isotopic variations in soil and plant compartments compared to the underlying rocks, and discuss the potential of this tool to trace specific geographic source areas as well as the limits of this approach. We briefly summarize the results from studies using Sr isotope ratios to determine the origin of different biological materials. Only very few studies have used Sr isotopes to trace wood provenance, and especially archaeological wood from shipwrecks; hence, in the second part of this paper, we examine how the differences between wood from living trees and marine archaeological wood could hinder the use of Sr isotopes for determining the dendroprovenance of shipwrecks. In particular, we discuss the results of a new experiment of waterlogged wood contamination by seawater. Finally, we suggest potential lines of future research on marine archaeological wood from shipwrecks coupling ^{87}Sr/^{86}Sr and $\delta^{88/86}$Sr analyses.

2. The strontium cycle and its range of isotopic variation at the global scale

2.1. Chemical and isotopic properties of Sr

Strontium (Sr) is an ubiquitous alkaline-earth element and one of the most abundant trace elements in rocks and sediments. It is exclusively present in the oxidation state + II at the Earth's surface (*e.g.* dissolved Sr^{2+} in aqueous solutions). Strontium has four naturally occurring stable isotopes, with approximate abundances of 0.56% (^{84}Sr), 9.87% (^{86}Sr), 7.04% (^{87}Sr) and 82.53% (^{88}Sr). These four isotopes are stable (*i.e.* non-radioactive) and only ^{87}Sr is "radiogenic", meaning that it is produced by the radioactive decay of rubidium-87 (^{87}Rb), with a half-life of 4.9 10^{10} yrs. Therefore, if Rb is present in a given system, ^{87}Sr is added over the course of geological time to the "initial" amount of ^{87}Sr. Given that isotope ratios can be measured more precisely than absolute abundances, the isotope ratio ^{87}Sr/^{86}Sr (^{86}Sr usually being the stable isotope systematically used for reference) is systematically used as an index of this ^{87}Sr-enrichment. Owing to the relatively small abundances of ^{87}Rb and ^{87}Sr and the long half-life of ^{87}Rb, the total Rb and Sr inventories are considered to be only marginally affected by the radioactive decay of ^{87}Rb.

In addition to Rb radioactive decay, the relative abundance of Sr isotopes is affected by mass-dependent fractionation during biological and physico-chemical processes, similarly to O, C, H, or N. The term "mass-dependent" means that the magnitude of isotope fractionation is inversely related to the relative mass difference between the isotopes under consideration. This has two implications: (a) heavier elements (*e.g.* Sr) show less fractionation than the lighter elements (*e.g.* O); (b) for a given element, the fractionation will be highest for the two isotopes with the largest mass difference; in the case of Sr, the ^{88}Sr/^{86}Sr ratio will fractionate twice as much as the ^{87}Sr/^{86}Sr ratio (because 88−86 = 2 against 87−86 = 1; note that the largest mass-dependent fractionation would be observed for the ^{88}Sr/^{84}Sr ratio, but given the low abundance of ^{84}Sr, this ratio is never reported in practice except in studies on Sr isotopic anomalies in planetary materials; Moynier et al. (2012)). Actually, despite the fact that mass-dependent fractionation does affect the ^{87}Sr/^{86}Sr value during physico-chemical processes, in practice this effect is "normalized away" during measurement with mass spectrometers and subsequent data reduction. Therefore, the only cause for variation of measured ^{87}Sr/^{86}Sr ratios between different materials is ultimately due to the addition of ^{87}Sr through time due to the radioactive decay of ^{87}Rb, as explained above.

Although the measurement of differences in the ^{87}Sr/^{86}Sr value between natural materials has been possible for decades, only recent advances in mass spectrometry have allowed the detection of Sr mass-dependent fractionation (Fietzke and Eisenhauer, 2006; Halicz et al., 2008; Ma et al., 2013; Ohno et al., 2008; Ohno and Hirata, 2007; Shalev et al., 2013). The mass-dependent fractionation of Sr is quantified using the deviation of the ^{88}Sr/^{86}Sr value in the sample with respect to the value obtained from an international standard, and is expressed as:

$$\delta^{88/86}\mathrm{Sr}\ (‰) = [(^{88}\mathrm{Sr}/^{86}\mathrm{Sr})_{\ \mathrm{sample}} / (^{88}\mathrm{Sr}/^{86}\mathrm{Sr})_{\ \mathrm{SRM987}} - 1] \times 1000 \quad (1)$$

where SRM987 is the international isotopic standard for Sr (Sr carbonate provided by the National Institute for Standard and Technology (NIST), with an accepted ^{87}Sr/^{86}Sr value of 0.71024). The $\delta^{88/86}$Sr is expressed in ‰ units to magnify the low range of variation in the ^{88}Sr/^{86}Sr ratio. Its actual ^{88}Sr/^{86}Sr value (like that of any sample) is unimportant, because only relative shifts in ^{88}Sr/^{86}Sr ratios can be quantified.

2.2. Strontium isotopes in minerals and rocks

The ionic radius of Sr (0.113 nm) is close to that of calcium (Ca) (0.099 nm), which explains its substitution in many Ca-bearing minerals (calcite, apatite and plagioclase). Conversely, Rb (ionic radius of 0.152 nm) is an alkali element that easily substitutes for potassium (K) (ionic radius of 0.138 nm) in K-bearing minerals such as biotite, muscovite, phlogopite and K-feldspar. Therefore, the

$^{87}Sr/^{86}Sr$ ratio of K-bearing minerals is higher (more radiogenic) than that of Ca-bearing minerals having low K and Rb contents. Table 1 presents a compilation of Sr and Rb contents and $^{87}Sr/^{86}Sr$ values of minerals separated from granitic bedrocks at four different sites.

Since Sr is found in many different minerals, it is present in almost all rock types. The $^{87}Sr/^{86}Sr$ ratio in bulk rocks is highly variable according to the rock type, mineralogy and age (Capo et al., 1998; Faure, 1986; Faure and Mensing, 2005). Considering rocks with a similar age, the $^{87}Sr/^{86}Sr$ value of a rock rich in K-bearing minerals is more radiogenic compared with a rock rich in minerals with low K and Rb contents, such as Ca-bearing minerals. For minerals with a similar initial Rb/Sr content, the older rocks will have a higher Sr isotopic ratio than the younger rocks. To our knowledge, at present, no systematic study of $\delta^{88/86}Sr$ in different minerals has been carried out on igneous rocks to assess the potential mass-dependent fractionation of Sr isotopes.

Table 2 summarizes the range of bulk $^{87}Sr/^{86}Sr$ and $\delta^{88/86}Sr$ values in various rocks according to their type and age. Granitic rocks are the most enriched in Rb and have variable Sr contents. Through ^{87}Rb decay, ^{87}Sr contents are strongly increased in old granitic rocks over the time since their formation. Therefore, old granites have a very high $^{87}Sr/^{86}Sr$ value (for example: Precambrian granite from the Zuni–Bandera volcanic field near Grants, New Mexico yields values between 0.8043 and 0.8644; van der Hoven and Quade, 2002). In general, basaltic rocks have low Rb and high Sr contents, which therefore leads to lower $^{87}Sr/^{86}Sr$ values. Almost no decay of ^{87}Rb has occurred in young basaltic rocks since their formation, which explains their very low $^{87}Sr/^{86}Sr$ value (for example, basalts from the Zuni–Bandera volcanic field near Grants, New Mexico: Sr isotopic ratios measured on basaltic rocks show an average of 0.7053; van der Hoven and Quade, 2002) as these rocks basically inherit their $^{87}Sr/^{86}Sr$ signature from their source, the Earth mantle.

Although the range of $\delta^{88/86}Sr$ for different terrestrial rocks is small (andesite, basalt, gneiss, granite, granodiorite and quartz latite yield values between 0.20‰ and 0.35‰; Charlier et al., 2012; Moynier et al., 2010; Ohno and Hirata, 2007), a relative enrichment of the lighter isotopes has been observed for some rocks (*e.g.* $\delta^{88/86}Sr$ of ~ −0.20‰ for rhyolite glass; Charlier et al., 2012; and for potash granite; Ma et al., 2013; Ohno et al., 2008) suggesting that mass-dependent fractionation can be associated with the formation of Ca-bearing minerals during magma crystallization (Fig. 1; Table 2).

The $^{87}Sr/^{86}Sr$ ratio of sedimentary rocks is variable (Table 2), but usually ranges between the values obtained for granites and volcanic rocks. Sandstones, usually derived from magmatic rocks rich in Sr-free quartz, have $^{87}Sr/^{86}Sr$ ratios reflecting the occurrence of K-rich minerals (K-feldspars such as orthoclase, or mica) or Ca-rich minerals (plagioclase). Shales commonly display relatively high bulk $^{87}Sr/^{86}Sr$ values, as they are rich in fine, radiogenic minerals such as micas. Limestones that precipitate under marine conditions should accurately record the $^{87}Sr/^{86}Sr$ of the ocean at the time of their formation, since any Sr isotopic mass-dependent fractionation during precipitation is cancelled out through data reduction. Therefore, pure limestones yield $^{87}Sr/^{86}Sr$ ratios close to the values

Table 1
Sr and Rb contents (μg/g) and $^{87}Sr/^{86}Sr$ ratio of minerals in different granitic bedrocks from four sites: New Hampshire-USA (A) California-USA (B and C), Strengbach-France (D and E) and Göschenealp region- Switzerland (F). Data compiled from A: Bailey et al. (1996); B: Bullen et al. (1997); C: Kistler et al. (1986); D: Probst et al. (2000); E: Aubert et al. (2001); F: de Souza et al. (2010).

	A	B	C	D	E	F	Range
Apatite							
Sr	–	–	373–525	500	790.2	–	373–790.2
Rb	–	–	0.7–23.0	–	–	–	0.7–23.0
$^{87}Sr/^{86}Sr$	–	–	0.7059–0.7065	0.7090	0.7161	–	0.7059–0.7161
Biotite							
Sr	9.9	44–77	10.3–20.7	7.00	4.3	17–25	4.3–77
Rb	1719.3	20–380	508–1018	–	–	–	20–1719.3
$^{87}Sr/^{86}Sr$	2.5855	0.7128–0.7168	0.8611–0.8811	5.4000	5.8648	0.7296–0.8309	0.7128–5.8648
Chlorite							
Sr	32.4	–	–	–	–	–	32.4
Rb	27.2	–	–	–	–	–	27.2
$^{87}Sr/^{86}Sr$	0.7373	–	–	–	–	–	0.7373
Garnet							
Sr	1.6	–	–	–	–	–	1.6
Rb	7.7	–	–	–	–	–	7.7
$^{87}Sr/^{86}Sr$	0.7767	–	–	–	–	–	0.7767
Hornblende							
Sr	–	71–132	37–45.3	–	–	–	37–132
Rb	–	7.2–31	3.5–10.7	–	–	–	3.5–31
$^{87}Sr/^{86}Sr$	–	0.7067–0.7071	0.7061–0.7075	–	–	–	0.7061–0.7075
Feldspar							
Sr	–	352–509	636–1040	102.7	77.0	44–168	44–1040
Rb	–	150–380	212.5–360	–	–	–	150–380
$^{87}Sr/^{86}Sr$	–	0.7080–0.7093	0.7066–0.7076	0.7827	0.7975	0.7113–0.7550	0.7066–0.7975
Muscovite							
Sr	79.4	–	–	4.4	3.1	–	3.1–79.4
Rb	300.3	–	–	–	–	–	300.3
$^{87}Sr/^{86}Sr$	0.7731	–	–	7.4964	5.3686	–	0.7731–7.4964
Plagioclase							
Sr	–	616–809	508–1062	45.6	73.7	286–397	45.6–1062
Rb	–	34–123	1.6–37	–	–	–	1.6–123
$^{87}Sr/^{86}Sr$	–	0.7065–0.7073	0.7057–0.7065	0.7420	0.7743	0.7101–0.7402	0.7057–0.7743
Sphene							
Sr	–	–	34.8–48.0	–	–	–	34.8–48.0
Rb	–	–	1.9–3.6	–	–	–	1.9–3.6
$^{87}Sr/^{86}Sr$	–	–	0.7062–0.7066	–	–	–	0.7062–0.7066

Table 2
Range of Sr, Ca, Rb and K contents, $^{87}Sr/^{86}Sr$ and $\delta^{88/86}Sr$ (‰) values measured in different rock types. Mean $\delta^{88/86}Sr$ (‰) and number of samples is given in brackets.

Rock types	Sr (μg/g)	Ca (mg/g)	Rb (μg/g)	K (mg/g)	$^{87}Sr/^{86}Sr$ range	References for $^{87}Sr/^{86}Sr$	$\delta^{88/86}Sr$ (‰) range (Mean, n)	References for $\delta^{88/86}Sr$
Volcanic								
Basalt	390 to 620	76	30	8	0.7028 to 0.7063	a,d,e,g,j,k, o,p,q,s,t,u	0.08 to 0.42 (0.27, n = 93)	1,2,3,4,5,8, 9,10,11,13
Andesite	–	–	–	–	–	–	0.18 to 0.32 (0.26, n = 19)	1,4,9,10,11
Rhyolite	–	–	–	–	–	–	−0.19 to 0.18 (0.03, n = 5)	4
Other ultrabasic volcanic and metamorphic rocks	–	–	–	–	0.7038 to 0.7071	h	–	–
Various Lavas and Tephra	–	–	–	–	0.7036 to 0.7038	2	−0.02 to 0.27 (0.17, n = 9)	2
Plutonic								
Plutonic and metamorphic basic rocks (Gabbro)	–	–	–	–	0.7038 to 0.7057	1	0.10 to 0.28 (0.20, n = 4)	1
Plutonic and metamorphic acid rocks (Diorite, Gneiss, Granite and Granodiorite)	42 to 440	5 to 25	110 to 170	25 to 42	0.7107 to 0.8644	b,e,g,h,l,p,s	−0.20 to 0.37 (0.26, n = 64)	1,4,5,9,10,18
Sedimentary								
Limestone	101 to 2000	302 to 312	3 to 10	2.7 to 2.9	0.7062 to 0.7156	e,f,h,l,m,n,p,r,16	−0.42 to 0.38 (0.18, n = 280)	6,7,11,12,14, 15,16,17,18,19
Sandstone	20	39	60	11	0.7074 to 0.7536	d,m,n,r	–	–
Shales	–	–	–	–	0.7279 to 0.7547	r	–	–

Values of elements content and $^{87}Sr/^{86}Sr$ ratios compiled from (a) Altherr et al., 1990; (b) Bonhomme, 1967; (c) Brenot et al., 2008; (d) English et al., 2001; (e) Faure, 1986; (f) Goede et al., 1998; (g) Grupe et al., 2011; (h) Hodell et al., 2004; (i) Koepnick et al., 1985; (j) Kudo et al., 1972; (k) Laughlin et al., 1971; (l) Probst et al., 2000; (m) Rich et al., 2012; (n) Rich et al., 2015; (o) Shaw et al., 2003; (p) Song et al., 2015; (q) Stein and Hofmann, 1992; (r) Stueber et al., 1987; (s) van der Hoven and Quade, 2002; (t) Weinstein, 2000; (u) Weinstein et al., 2006; (1) Andrews et al., 2016; (2) Bullen and Chadwick, 2016; (16) Shalev et al., 2017.
Values of $\delta^{88/86}Sr$ (‰) compiled from (1) Andrews et al., 2016; (2) Bullen and Chadwick, 2016; (3) Chao et al., 2015; (4) Charlier et al., 2012; (5) de Souza et al., 2010; (6) Halicz et al., 2008; (7) Krabbenhöft et al., 2010; (8) Kramchaninov et al., 2012; (9) Ma et al., 2013; (10) Moynier et al., 2010; (11) Ohno and Hirata, 2007; (12) Ohno et al., 2008; (13) Pearce et al., 2015a; (14) Raddatz et al., 2013; (15) Rüggeberg et al., 2008; (16) Shalev et al., 2017 (17) Stevenson et al., 2014; (18) Stevenson et al., 2016; (19) Vollstaedt et al., 2014.

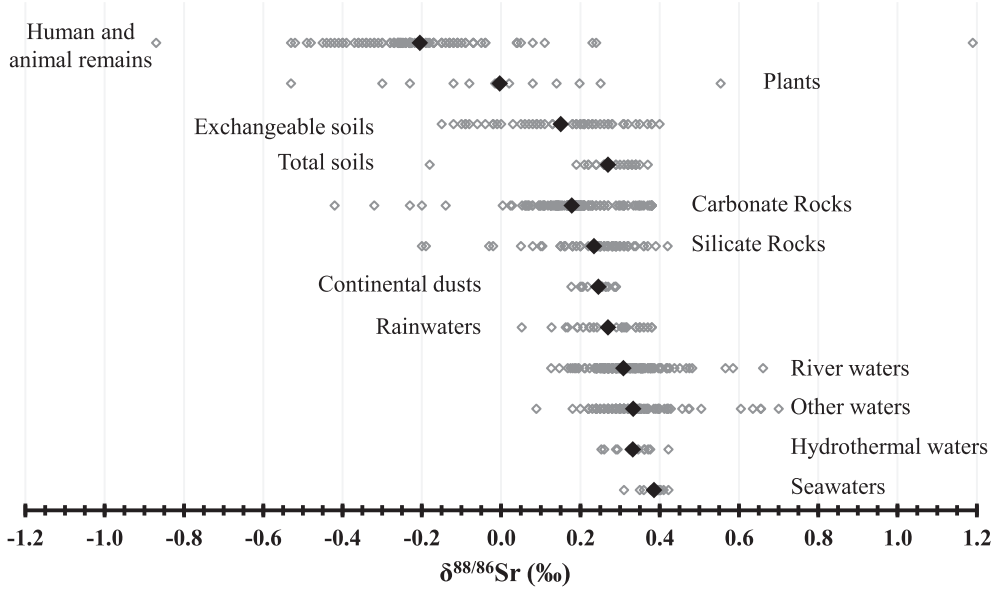

Fig. 1. Measured $\delta^{88/86}Sr$ (‰) of samples from different Earth compartments and the corresponding mean values. Seawater values include measurements from IAPSO standard and collected seawater samples. 'Other waters' values include glacial ice, porewater, cave waters, dissolved load subglacial flow and mud volcano fluid water. Data compiled from Andrews et al. (2016); Bullen and Chadwick, 2016; Chao et al., 2015; Charlier et al., 2012; de Souza et al., 2010; Fietzke and Eisenhauer, 2006; Halicz et al., 2008; Knudson et al., 2010; Krabbenhöft et al., 2010, 2009; Kramchaninov et al., 2012; Lewis et al., 2017; Liu et al., 2017; Ma et al., 2013; Moynier et al., 2010; Ohno et al., 2008; Ohno and Hirata, 2007; Pearce et al., 2015a, 2015b; Raddatz et al., 2013; Rüggeberg et al., 2008; Shalev et al., 2017; Stevenson et al., 2016, 2014; Voigt et al., 2015; Vollstaedt et al., 2014; Wei et al., 2013.

for modern or ancient seawater (Veizer, 1989; see section 2.4). Precipitation of carbonate and sulphate involves mass-dependent fractionation, with the lightest isotopes being preferentially transferred from solution to solids (Böhm et al., 2012; Fietzke and Eisenhauer, 2006; Raddatz et al., 2013; Rüggeberg et al., 2008; Shalev et al., 2017; Stevenson et al., 2014; Widanagamage et al., 2015, 2014), making authigenic sedimentary rocks isotopically lighter than seawater (*e.g.* $\delta^{88/86}Sr$ between 0.04 and 0.39‰ for Phanerozoic fossil carbonate samples, with a mean of 0.16‰ (Vollstaedt et al., 2014) as against 0.39‰ for seawater, see section 2.4) (Fig. 1). The lowest values (*i.e.* 0.04‰ and 0.07‰) were measured in fossils from the Permian and middle Triassic,

respectively, while the highest values (*i.e.* 0.36‰ and 0.39‰) were obtained in fossils from the Permian/Triassic transition. Raddatz et al. (2013) reported values ranging from 0.14‰ to 0.23‰ for coral samples from different locations along the European continental margin, while Rüggeberg et al. (2008) reported values ranging from 0.04‰ to 0.20‰. Carbonates from the Neoproterozoic yield $\delta^{88/86}$Sr ranging mainly from 0.20‰ to 0.38‰, with a few dolomites recording very low values down to −0.42‰ (Ohno et al., 2008). The authors attributed the anomalously low values to a combination of high influx from ancient continental crust with light $\delta^{88/86}$Sr (such as differentiated granitic rocks) and an enhanced isotopic fractionation related to high atmospheric CO_2 or higher precipitation rate. Terrestrial carbonates (*i.e.* speleothems, tufa and pedogenic carbonates) also showed $\delta^{88/86}$Sr values ranging from −0.20‰ to 0.12‰ (Halicz et al., 2008; Shalev et al., 2017).

2.3. Strontium isotopes in rivers

2.3.1. Controls on river dissolved $^{87}Sr/^{86}Sr$ and $\delta^{88/86}Sr$ values

During water-rock interactions at the Earth's surface, Sr is released from minerals and enters into solution as Sr^{2+}. As Sr is a fairly soluble element, it is only poorly re-incorporated into secondary weathering products (such as oxides or clays), except in young soils developed on volcanic substrates (Stewart et al., 1998). Since the $^{87}Sr/^{86}Sr$ ratio is not affected by mass-dependent fractionation, Sr^{2+} dissolved in rivers (as well as Sr potentially incorporated into neoformed materials in soils and later transported as river suspended sediment) should inherit the isotope signature of the minerals undergoing dissolution. This is best visible examining the isotope composition of small streams draining monolithological catchments. For example, the $^{87}Sr/^{86}Sr$ ratios of waters draining three different types of granites in the Vosges Mountains (Angéli, 2006) range between 0.712 and 0.728. According to the author, this variation is related to the mass fraction of orthoclase and albite in the three granites. Temporally, the $^{87}Sr/^{86}Sr$ of small streams can vary. For example, the $^{87}Sr/^{86}Sr$ measured regularly at different seasons in river water of the Strengbach catchment located in the Vosges Mountains varies between 0.72251 and 0.72530 related to the discharge rate affecting the Sr composition in the river (Aubert et al., 2002; Probst et al., 2000). At a larger scale, the river dissolved $^{87}Sr/^{86}Sr$ will result from the mixing between waters draining different rock types. For example, the dissolved $^{87}Sr/^{86}Sr$ values in waters from the Moselle river and its tributaries vary between 0.70815 and 0.72495 (Brenot et al., 2008). This wide range of variation is related to the large size of the Moselle River catchment draining the Vosges Mountains composed of magmatic rocks, as well as sedimentary terrains farther downstream. This spatial heterogeneity can lead to temporal variations: such temporal variation of $^{87}Sr/^{86}Sr$ ratio could be observed as in the study of Henchiri et al. (2016) on the Congo River, at Kinshasa (ratio varying from 0.71822 to 0.71941 during the year 2010) shown to be related to temporal variations in the lithological areas contributing to the weathering flux of the basin. Finally, in very large systems, heterogeneity in $^{87}Sr/^{86}Sr$ signatures have been observed within the river cross section itself, due to poor mixing of water masses from different tributaries (Bouchez et al., 2010).

Altogether, this results in large variations of $^{87}Sr/^{86}Sr$ signature in continental waters. Holland (1984) shows that $^{87}Sr/^{86}Sr$ signatures in river and lake waters vary between ca. 0.712 and 0.730 in Precambrian shield areas, between 0.706 and 0.709 in catchment areas dominated by limestone and between 0.704 and 0.706 in terrains dominated by young volcanic rocks. The $^{87}Sr/^{86}Sr$ of Ganges source waters analysed by Krishnaswami et al. (1992) fall in the range between 0.7300 and 0.7986, with the relatively high values being attributed to the weathering of ^{87}Sr-rich, old Precambrian granites and gneisses. Palmer and Edmond (1992) measured Sr isotope ratios ranging from 0.7059 to 0.9217 in waters of the Ganges, Orinoco and Amazon, three of the world's largest river basins. This large range of values is attributed to the fact that these basins include a wide variety of geological bedrocks. In the study cited above, the lowest value of 0.7059 corresponds to water sample from the Napo River in the Amazon basin influenced by weathering of the andesite and basalt rocks and the highest value of 0.9217 corresponds to water sample from the Parguaza River in the Orinoco basin draining the granite of the Guyana shield.

All these results indicate that the variation of riverwater $^{87}Sr/^{86}Sr$ values largely depends on the drained bedrock materials but are also affected by temporal and cross-section lateral variations. It should be noted that this does not mean that the dissolved $^{87}Sr/^{86}Sr$ ratio is equal to that of the bulk rock undergoing dissolution, as the different minerals of a given rock do not all weather at the same rate (see section 3.1), and differ in their initial $^{87}Sr/^{86}Sr$ signatures (Blum and Erel, 1997). In addition, it has been suggested that, in a given mineral, ^{87}Sr located in crystal defects formed during ^{87}Rb disintegration could be preferentially released during incipient mineral dissolution, thereby inducing an “apparent” fractionation during incipient rock weathering (Blum and Erel, 1997).

The $\delta^{88/86}$Sr value for river-dissolved Sr varies from 0.13‰ to 0.66‰ (Andrews et al., 2016; Krabbenhöft et al., 2010; Pearce et al., 2015a; Wei et al., 2013) (Fig. 1). At the scale of a given river basin, differences between $\delta^{88/86}$Sr values of river water and bedrock suggest that processes in the weathering zone fractionate Sr isotopes (see sections 3.1 and 3.2).

2.3.2. Global riverine input to the ocean

Apart from such large spatial variations, it is important for global Sr budgets to constrain the average $^{87}Sr/^{86}Sr$ of the dissolved load exported by rivers. Many authors measured the riverine Sr fluxes to the ocean and its global implications (*e.g.* Peucker-Ehrenbrink et al. (2010) and Wadleigh et al. (1985)). More recently, Pearce et al. (2015a) analysed water samples from small and large rivers in North and South America, Asia, Africa and Europe and found $^{87}Sr/^{86}Sr$ ratios between 0.70438 and 0.73723 yielding a global flux-weighted mean value of 0.71299. These values are consistent with previous results on the same rivers reported in other studies (Allègre et al., 2010; Gaillardet et al., 1999; Tipper et al., 2010, 2006; Vance et al., 2009).

The $\delta^{88/86}$Sr flux-weighted average (0.32‰; Krabbenhöft et al., 2010; Pearce et al., 2015a; 0.38‰; Wei et al., 2013) is close to the range of terrestrial rocks (generally around 0.30‰). This suggests that, at a large scale, processes which could fractionate Sr isotopes (*e.g.* plant uptake, clay formation, adsorption/desorption processes) do not significantly impact the Sr cycle. However, Shalev et al. (2017) calculated a ‘source’ (*i.e.* rock-derived) $\delta^{88/86}$Sr for global rivers of 0.22‰ based on the values of the $\delta^{88/86}$Sr composition of carbonates (0.16‰; Vollstaedt et al. (2014)), the $\delta^{88/86}$Sr composition of silicates (0.30‰; Charlier et al. (2012); Moynier et al. (2010)) and the proportion of Sr in rivers derived from the weathering of carbonates and silicates ~60% vs ~40% (percentage determined based on the $^{87}Sr/^{86}Sr$ of rivers; Pearce et al. (2015a)). This calculated $\delta^{88/86}$Sr of 0.22‰ is considerably lower than the measured $\delta^{88/86}$Sr for rivers (0.32‰; Krabbenhöft et al., 2010; Pearce et al., 2015a; 0.38‰; Wei et al., 2013). The increase of $\delta^{88/86}$Sr in rivers compared with their respective drainage basin was attributed by the authors to isotope fractionation by chemical weathering (preferential release of heavy Sr into solution; Pearce et al., 2015a), secondary mineralization during weathering (preferential precipitation of

light Sr into secondary minerals; Raddatz et al., 2013; Rüggeberg et al., 2008), calcium carbonate precipitation (Shalev et al., 2017), or plant uptake (Andrews et al., 2016; Bullen and Chadwick, 2016; de Souza et al., 2010).

2.4. Strontium isotopes in seawater

The two dominant sources of Sr in the oceanic geochemical budget are the hydrothermal fluids and the continental discharge through rivers and groundwater (Beck et al., 2013; Davis et al., 2003; Palmer and Edmond, 1989). Therefore, the modern seawater $^{87}Sr/^{86}Sr$ value is intermediate between the average $^{87}Sr/^{86}Sr$ of the continental crust (~0.716; Elderfield, 1986; Goldstein and Jacobsen, 1988; or taken as equivalent to the dissolved load of major rivers ~0.713; Pearce et al., 2015a) and the $^{87}Sr/^{86}Sr$ of oceanic basalts (~0.703; Albarède et al., 1981; Elderfield, 1986), which reflects supply from hydrothermal inputs and the weathering of volcanic islands. Seawater Sr has a residence time of ~2.5 Myrs (Broecker and Peng, 1982), much longer than the oceanic mixing time of ~1 kyrs (Broecker, 1963; Goldberg, 1963; Veizer, 1989). Because of the small Sr input flux in comparison to the amount of Sr in seawater (4.3×10^{10} mol yr^{-1} and 1.25×10^{17} mol, respectively; Richter and Turekian, 1993), changes in fluxes from the different sources to the sea will take more than 10 kyrs to affect the oceanic isotopic composition (McArthur, 1994). As a result, the seawater Sr isotopic ratios are spatially invariant but shift through geological time. The $^{87}Sr/^{86}Sr$ ratios measured in modern seawater vary between 0.7091 and 0.7092 (Burke et al., 1982; Capo and DePaolo, 1992; Goldstein and Jacobsen, 1987; Grupe et al., 2011; Hess et al., 1986; Hodell et al., 1990; Veizer, 1989). Groundwater discharge to the ocean has a $^{87}Sr/^{86}Sr$ ratio of 0.70890 (Beck et al., 2013), close to $^{87}Sr/^{86}Sr$ signature of the seawater 0.70918, and therefore has a limited leverage on seawater $^{87}Sr/^{86}Sr$ variations. During the Phanerozoic (542 Myrs to present), the Sr isotope composition of carbonates indicates that seawater $^{87}Sr/^{86}Sr$ ratio fluctuated between 0.707 and 0.709 (Burke et al., 1982), while late Proterozoic (850-550 Ma) carbonates indicate that seawater $^{87}Sr/^{86}Sr$ ranged from 0.70621 to 0.71860 (Derry et al., 1992). These variations through time are the result of modifications in the $^{87}Sr/^{86}Sr$ signature of the input fluxes to the oceans due to multiple geological and environmental factors. For example, the Sr dissolved fluxes and isotope ratios can change due to the increased continental relief caused by tectonic uplift and implicating intensified weathering (Li and Elderfield, 2013; Raymo et al., 1988; Richter et al., 1992) and the locally enhanced mineral weathering rates following glaciations (Armstrong, 1971; Blum and Erel, 1995; Hodell et al., 1990). The $\delta^{88/86}Sr$ of modern seawater is homogenous and is well established at $\delta^{88/86}Sr = 0.39‰$ (Liebetrau et al., 2009; Pearce et al., 2015a) (Fig. 1). However, because the $\delta^{88/86}Sr$ value is affected by mass-dependent fractionation, the magnitude of the output fluxes (such as carbonate precipitation), along with the associated isotope fractionation, also influence the $\delta^{88/86}Sr$ of seawater (Rüggeberg et al., 2008).

2.5. Sr in atmospheric deposition

Strontium in wet atmospheric deposition is mostly derived from seawater evaporation. Therefore, the atmospheric deposition has low $^{87}Sr/^{86}Sr$ ratios, very similar to the oceanic composition (~0.709) especially when near the coasts. This ratio varies with location (Fig. 2) according to the inputs of natural or anthropic dust to wet deposition. The $^{87}Sr/^{86}Sr$ values of rainwater samples range from a minimum of 0.70727 in the Azores (Pearce et al., 2015a), reaching values of 0.70880–0.71040 in the Tesuque watersheds of New Mexico (Graustein and Armstrong, 1983), 0.71122 and 0.71197 in China (Pearce et al., 2015a) and 0.70968 to 0.71326 in the Congo Basin (Négrel, 1992; Négrel et al., 1993; Pearce et al., 2015a). In France, rainwater samples from the Paris Basin yield a $^{87}Sr/^{86}Sr$ ratio between 0.70796 and 0.71093 (Négrel et al., 2007; Pearce et al., 2015b; Seimbille et al., 1989), with local values of 0.70944–0.70968 from two sites of the Lorraine plateau (Bedel et al., 2016), 0.70920–0.71314 in the Massif Central (Négrel and Roy, 1998) and 0.70964–0.71290 in the Strengbach catchment (Aubert et al., 2002; Probst et al., 2000). In Israel, the relatively low $^{87}Sr/^{86}Sr$ values between 0.70792 and 0.70923 found in wet atmospheric deposition are explained by the significant contribution of dust minerals derived from post-Jurassic carbonate rocks (Herut et al., 1993). In Sweden, on the other hand, where the bedrock is mainly composed of Precambrian granitoids and gneisses, the $^{87}Sr/^{86}Sr$ ratio of atmospheric deposition is higher than seawater, varying between 0.709 and 0.719 (Åberg et al., 1989; Wickman, 1996), with an increase in dust contamination from west to east. Gosz and Moore (1989) showed that the $^{87}Sr/^{86}Sr$ values in precipitation at a given location vary with the season, which could again be explained by temporary mixing of atmospheric dust with wet deposition.

Atmospheric dust (dry deposition) has a $^{87}Sr/^{86}Sr$ signature similar to the soils or bedrock from which it is derived. Loess is derived from glacial outwash plains or from desert environments, and generally displays $^{87}Sr/^{86}Sr$ values between 0.70964 and 0.71850 (continental loess from Banks Peninsula, New Zealand; Nanking, China; Kaiserstuhl, near Freiberg, Rhine Valley, West Germany; Kansas and Iowa, USA; Taylor et al., 1983). Pearce et al. (2015a) reported comparable values ranging globally between 0.70752 and 0.71802. In the case of Argentinian loess, the values range from 0.7059 to 0.7123 (Smith et al., 2003), while loess and dust from Patagonia, Africa, Australia, New Zealand and Antarctica ice-cores yield values between 0.70604 and 0.76336 (Basile et al., 1997; Grousset et al., 1992). In the latter study, the highest values were obtained from the Great Sandy Desert in Australia and the Kalahari Desert in South Africa. Many other studies measured the Sr radiogenic isotopes in ice-core dusts to successfully trace their provenance (*e.g.* Basile et al. (2001); Biscaye et al. (1997); Delmonte et al. (2004) and Svensson et al. (2000)) and reported values included in the $^{87}Sr/^{86}Sr$ range of variation for atmospheric dust illustrated on Fig. 3.

Chao et al. (2015) and Pearce et al. (2015a, 2015b) reported values of $\delta^{88/86}Sr$ in atmospheric deposition as being isotopically lighter than seawater, showing variations according to the location of the studied samples ($\delta^{88/86}Sr$ from 0.05‰ to 0.38‰ in rainwaters) (Fig. 1). Given the low volatility of Sr, little or no fractionation is expected through evaporation. Considering the large difference between the lowest $\delta^{88/86}Sr$ values in atmospheric deposition (*e.g.* $\delta^{88/86}Sr = 0.05‰$ in the Congo) and seawater (0.39‰), Pearce et al. (2015a) interpreted the lighter $\delta^{88/86}Sr$ values as being due to contamination from anthropogenic sources and/or the dissolution of dust in the atmosphere (such as loess with a $\delta^{88/86}Sr$ of 0.18‰–0.29‰; Fig. 1; Pearce et al., 2015a).

2.6. Variation of strontium isotopes at the global scale

Fig. 3 shows the variation of Sr isotope signatures in the different water compartments at the global scale. The average $^{87}Sr/^{86}Sr$ ratio of the dissolved riverine input to seawater is estimated as ~0.713 (Pearce et al., 2015a), which is significantly less radiogenic than the average $^{87}Sr/^{86}Sr$ value of the igneous continental crust (~0.716 according to Goldstein and Jacobsen, 1988) because of the influence of limestone weathering (Elderfield, 1986).

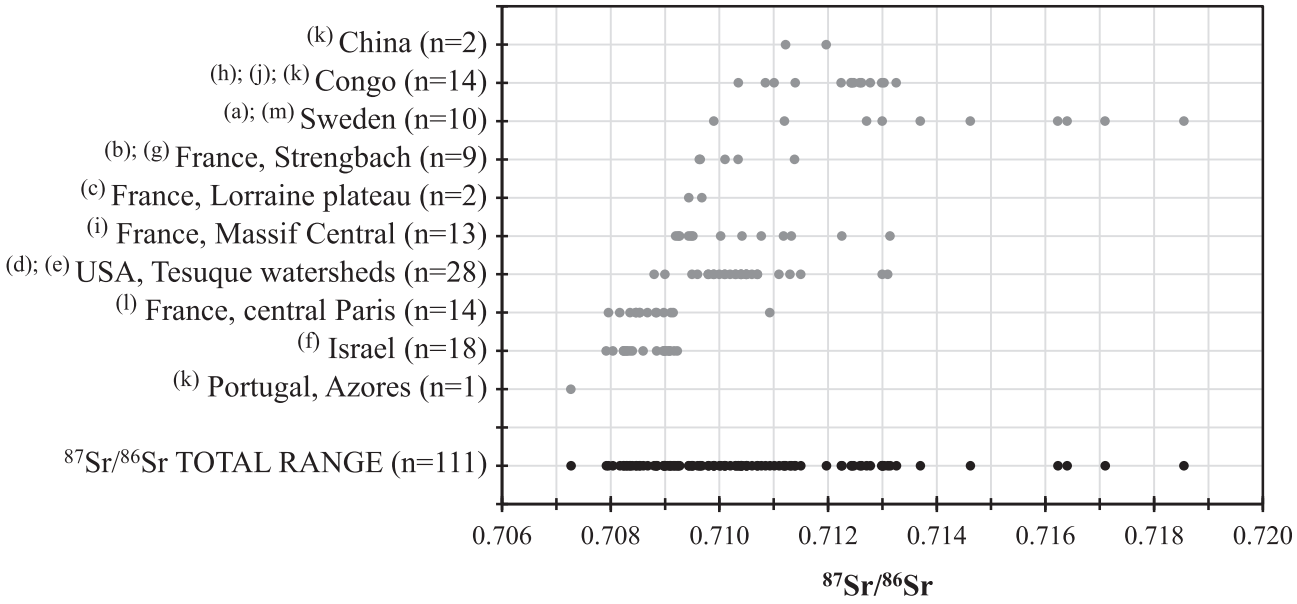

Fig. 2. The $^{87}Sr/^{86}Sr$ ratio of rainwater samples from different countries and range of variation of the values. Data compiled from (a) Åberg et al., 1989; (b) Aubert et al., 2002; (c) Bedel et al., 2016; (d) Gosz et al., 1983; (e) Graustein and Armstrong, 1983; (f) Herut et al., 1993; (g) Probst et al., 2000; (h) Négrel, 1992; (i) Négrel and Roy, 1998; (j) Négrel et al., 1993; (k) Pearce et al., 2015a; (l) Pearce et al., 2015b; (m) Wickman, 1996.

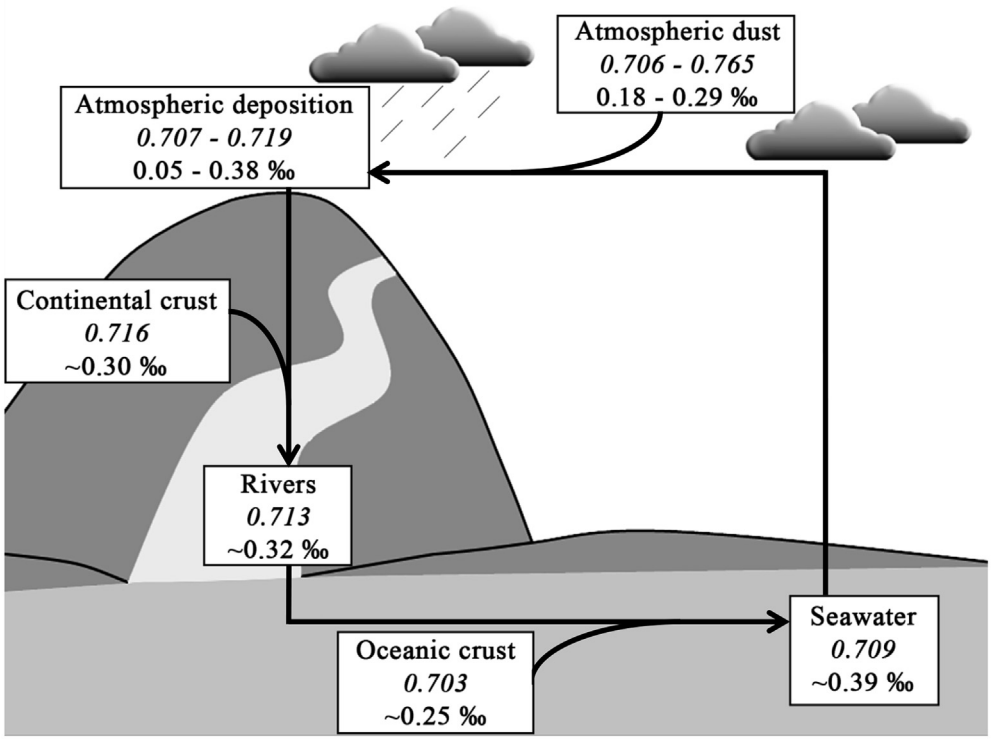

Fig. 3. Range of variation of $^{87}Sr/^{86}Sr$ ratios (values in italic) and $\delta^{88/86}Sr$ (‰) values in rocks, atmospheric dust and different water compartments at global scale.

The input of dissolved load from rivers ($^{87}Sr/^{86}Sr$ ~0.713) and the hydrothermal flux reflecting the oceanic crust signature (~0.703) are the main contributors to the Sr isotope composition of modern seawater (0.70918). The isotopic composition of atmospheric deposition (~0.707–0.719) is a mixture between the seawater signature (0.70918) and atmospheric dust (~0.706–0.765).

The average $\delta^{88/86}Sr$ of ~0.32‰ for riverine input (Krabbenhöft et al., 2010; Pearce et al., 2015a) is slightly heavier than the value of ~0.30‰ for average continental crust (Charlier et al., 2012; Moynier et al., 2010) due to isotope fractionation by chemical weathering (preferential release of heavy Sr into solution; Pearce et al., 2015a), secondary mineralization during weathering (preferential precipitation of light Sr as secondary minerals; Raddatz et al., 2013; Rüggeberg et al., 2008), calcium carbonate precipitation (Shalev et al., 2017), or plant uptake (Andrews et al., 2016; Bullen and Chadwick, 2016; de Souza et al., 2010). The $\delta^{88/86}Sr$ of

hydrothermal fluids, varying from 0.25‰ to 0.42‰, is heavier than oceanic crust (average ~0.25‰) due to preferential release of heavy Sr from the oceanic crust to hydrothermal fluids (Krabbenhöft et al., 2010; Pearce et al., 2015a). The $\delta^{88/86}$Sr of seawater, with an average of ~0.39‰, is heavier than the two major inputs of Sr to the ocean (*i.e.* riverine or hydrothermal) due to preferential precipitation of light Sr during marine carbonate formation leaving the seawater enriched in the heavier Sr isotopes. The $\delta^{88/86}$Sr of atmospheric deposition varies between 0.05‰ and 0.38‰, while the $\delta^{88/86}$Sr of atmospheric dust varies between 0.18‰ and 0.29‰ (Pearce et al., 2015a).

Considering the different inputs to the ocean, the Sr supply is controlled mainly by riverine discharge and to a lesser extent by groundwater and hydrothermal fluids (accounting for ~60%, ~29% and ~4%, respectively; Krabbenhöft et al., 2010), with 61% and 39% of riverine inputs derived from carbonate weathering and silicate weathering, respectively (Pearce et al., 2015a).

3. Can strontium isotopes be used as a reliable tracer of the geographical origins of materials and living organisms?

The reliability of Sr isotopes as a tracer of the provenance of archaeological material hinges on (i) measurable isotopic signatures characteristic of distinct geographical areas; (ii) sufficient homogeneity within these areas, implying they should not be too large; and (iii) the robustness of Sr isotope composition with respect to potential modifications during biological and physico-chemical processes - in other words, the isotopic signatures of biological materials should reflect those of rocks or soils.

As discussed below, these requirements are most likely best fulfilled by the $^{87}Sr/^{86}Sr$ ratio - under certain conditions - while the $\delta^{88/86}$Sr values have been shown to vary according to the trophic level (Knudson et al., 2010; Lewis et al., 2017) and might provide additional insight on the source of Sr for the archaeological material being studied (see section 3.2). It should be noted that most recently, few studies have aimed to establish “isoscapes” in order to predict variations of $^{87}Sr/^{86}Sr$ in rocks and rivers for provenance studies (Bataille et al., 2014; Bataille and Bowen, 2012; Brennan et al., 2016). While promising, this approach is still challenging to use in some regions due to the lack of data and inherent inaccuracies in the approach.

3.1. Isotopic signatures in different soil compartments at the site scale

Soil is the solid residue of rock weathering, and is composed of minerals and a small proportion of organic matter. Soil minerals are either derived from erosion of the rock (*i.e.* constituents that are most resistant to weathering) or have a secondary origin, as in the case of oxides, clays or pedogenic carbonates formed during water-rock interactions. Therefore, the bulk soil $^{87}Sr/^{86}Sr$ composition is influenced by the signature of the parent material, modified by the fact that some Sr has been lost from the more weatherable minerals. For example, if minerals with low $^{87}Sr/^{86}Sr$ ratios are preferentially weathered, bulk soils will show higher $^{87}Sr/^{86}Sr$ values compared to the parent rock (Fig. 4a), whereas preferential weathering of minerals with high $^{87}Sr/^{86}Sr$ ratios will lead to bulk soils with $^{87}Sr/^{86}Sr$ values lower than the parent rock (Fig. 4b).

Another factor that can influence Sr isotope signature in soils is the precipitation of secondary weathering products, even though these phases contain very little Sr in their structure. Their $^{87}Sr/^{86}Sr$ ratios will be similar to those of the dissolved Sr pool from which they precipitate, which is likely to be different from the local, surrounding solid soil. Finally, soil organic matter contains Sr derived from living biological material that can have a different isotope signature (see section 3.2). Fig. 5 presents some of the measured variations in $^{87}Sr/^{86}Sr$ ratio between rocks, superficial bulk soils, soil nutrient available pools and plant organs sampled at 28 sites from different countries and having different types of rocks (results from 9 articles showing complete data sets of $^{87}Sr/^{86}Sr$ on bulk soil, soil exchangeable pool and organs of plants growing on them; see references on Fig. 5 caption; site location and rock type are indicated in Table 3 and Fig. 5). The $^{87}Sr/^{86}Sr$ ratios of bulk rocks were measured only for the first four sites (Marchionni et al., 2016 (site 1), Song et al., 2015 (sites 2 to 4)). On sites 1 and 3, the $^{87}Sr/^{86}Sr$ ratios of rocks and bulk soils are closely similar and lie within the range of wet atmospheric deposition. On both of the other sites, the rock and bulk soil samples have distinct signatures. The granite bedrock on site 2 yields a higher $^{87}Sr/^{86}Sr$ value than the bulk soil, while the basalt bedrock on site 4 shows a lower $^{87}Sr/^{86}Sr$ value than the bulk soil, falling in the range of wet atmospheric deposition. This evolution of $^{87}Sr/^{86}Sr$ signatures between rocks and superficial bulk soils illustrates the preferential weathering of specific minerals, the possible precipitation of dissolved Sr (initially released from specific minerals combined with Sr from rain) in secondary minerals and mixing with organic matter. Finally, recent studies indicate that the light Sr isotopes are preferentially incorporated into secondary weathering products, making their $\delta^{88/86}$Sr values lower than in other soil compartments (Bullen and Chadwick, 2016; Chao et al., 2015; Halicz et al., 2008).

Like other cations, strontium released into soil water by weathering of minerals can be adsorbed onto the soil exchangeable complex, which is formed by the negative charges present at the surface of clay minerals and organic matter. This adsorbed Sr is called the “exchangeable Sr”, and represents an important pool as it is though that plants take up their nutrients, and consequently Sr, from this pool (see below). Several previous studies (*e.g.* Åberg et al., 1989; Gosz et al., 1983; Graustein and Armstrong, 1983; Graustein, 1989; Kennedy et al., 2002) highlight that the $^{87}Sr/^{86}Sr$ signature of exchangeable Sr in soils is the result of mixing (as no fractionation affects $^{87}Sr/^{86}Sr$ signatures) between two main sources: the weathering flux from bedrock and the atmospheric input. The Sr present in precipitation is deposited on the soil surface, whereas soil weathering releases Sr from mineral horizons at depth. As a result, the exchangeable Sr isotopic ratio may vary according to depth in the soil profile (Åberg, 1995; Dambrine et al., 1997; Miller et al., 1993; Poszwa et al., 2004, 2003, 2002; Wickman, 1996). Fig. 6 illustrates two kinds of $^{87}Sr/^{86}Sr$ ratio gradient formed in soil exchangeable pools: increasing with depth (soil developed on granitic rocks, Dambrine et al., 1997) and decreasing with depth (soils developed on glacial materials composed mainly of the local anorthosite bedrock with low $^{87}Sr/^{86}Sr$; Miller et al., 1993). At both sites, the signature of the deepest soil horizons is close to the bedrock isotopic signature. On the other hand, atmospheric deposition has a strong effect on the Sr isotopic ratio of surface soil horizons making their $^{87}Sr/^{86}Sr$ signature closer to the signature of the atmospheric deposition and more distinct from the rock signature.

The stable Sr composition of the soil exchangeable pool should also be the result of mixing between different sources (*e.g.* weathering fluxes and atmospheric deposition) but can in addition be affected by mass-dependent fractionation during adsorption and desorption to the negative charges of the organo-mineral complexes in the soil. To our knowledge, no systematic study was conducted to test the fractionation of Sr during these processes, thus their isotopic effect still remains uncertain. Bullen and Chadwick (2016) measured the exchangeable $\delta^{88/86}$Sr in seven soil depth profiles (Fig. 1). On five of the seven studied sites, the lightest isotope composition is observed in the shallowest soil

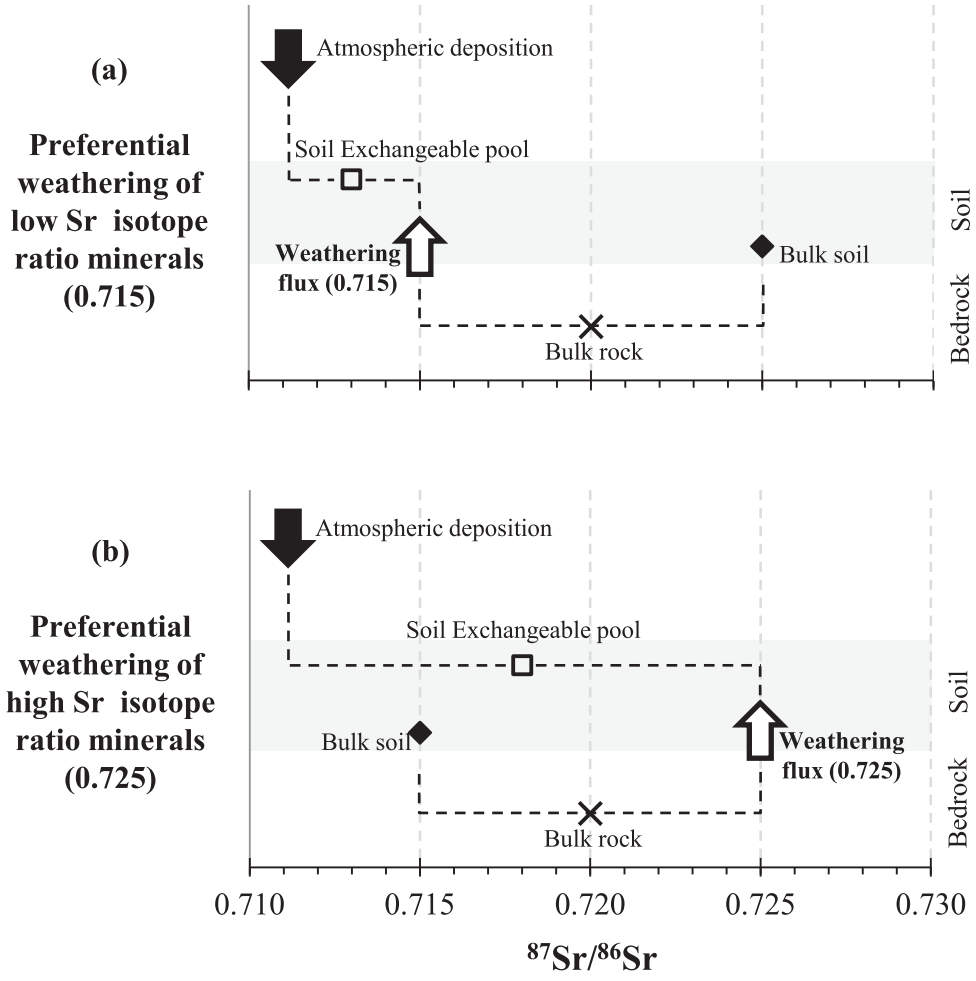

Fig. 4. Illustration of the Sr composition signature of rocks, bulk soils and soil exchangeable pool. The $^{87}Sr/^{86}Sr$ ratio for atmospheric deposition and other compartments are broad estimates and illustrative. Each end-member is considered to contribute 50% of the total Sr input. The soil "exchangeable" pool corresponds to the Sr fraction available for plants. This pool can be in equilibrium or not with the soil solution, depending on the type of water considered (capillary or gravitational water).

exchangeable pools (ranging from −0.15‰ to −0.09‰), with $\delta^{88/86}Sr$ values similar to those of plant tissues.

It should be emphasized that the definition of a "soil available pool" is not straightforward. This term often refers to an operationally defined pool accessed by means of extraction protocols, and the methods used can differ greatly between research groups and studies. Table 3 compiles the methods used to extract available Sr in soils from 28 sites (isotopic signatures are reported on Fig. 5). Most authors use salts to extract the soil-available Sr. Although this operationally-defined Sr is commonly associated with "exchangeable" Sr, some authors call this fraction "labile Sr" or "mobile Sr" (Table 3). The protocols used differ in terms of number and duration of extractions, as well as type of salt and molarity. Other methods allow the characterization of mobile cations that are not stored in organic and mineral structures. For example, Marchionni et al. (2016) used resin capsules in contact with soil and water for ten days, obtaining a fraction referred to as "bioavailable" Sr. Therefore, it is expected that the isotopic ratio of the available Sr varies according to the operational definition of the soil available pool, which, in turn, is related to the method used. Considering the 28 sites reported on Fig. 5, the $^{87}Sr/^{86}Sr$ ratio of the superficial soil available pool of 25 sites is clearly distinct from the results obtained on bulk soil, showing a trend towards atmospheric deposition. This confirms that the available pool of Sr in soil surface horizons (regardless of the method used to define the "available Sr") is supplied with Sr derived not only from the preferential weathering of specific rocks and bulk soil minerals, but also, and sometimes predominantly, from atmospheric deposition. Some authors have estimated the annual bio-available pool of individual trees by analysing the fine roots (<1 mm) sampled from each soil horizon below the trunk, assuming that their $^{87}Sr/^{86}Sr$ values reflect the signature of the soil available pool surrounding the roots (see, for example, Poszwa et al., 2004, 2002). Dambrine et al. (1997) found slight difference between the $^{87}Sr/^{86}Sr$ values in fine roots from the A1 horizon at three different sites and the corresponding soil available pools (respectively, 0.7160 and 0.7163; 0.7162 and 0.7158; 0.7173 and 0.7172). Similarly, Bedel et al. (2016) found closely similar Sr isotopic ratios between the fine roots and soil exchangeable pools at different depths at two different sites. These results suggest that fine roots could be used as an alternative material to estimate the time-averaged Sr signatures of soil available pools.

3.2. Strontium isotope composition of plants, animals and humans

Sr is a micro-nutrient which substitutes for Ca in plants, mainly in cell-wall components such as pectin, cellulose and lignin (Torre et al., 1992) or in plant leaves as Ca-oxalate crystals. Plants take up Sr that is available in the soil. The $^{87}Sr/^{86}Sr$ ratio measured in plants or other living organisms is unchanged by mass-dependent

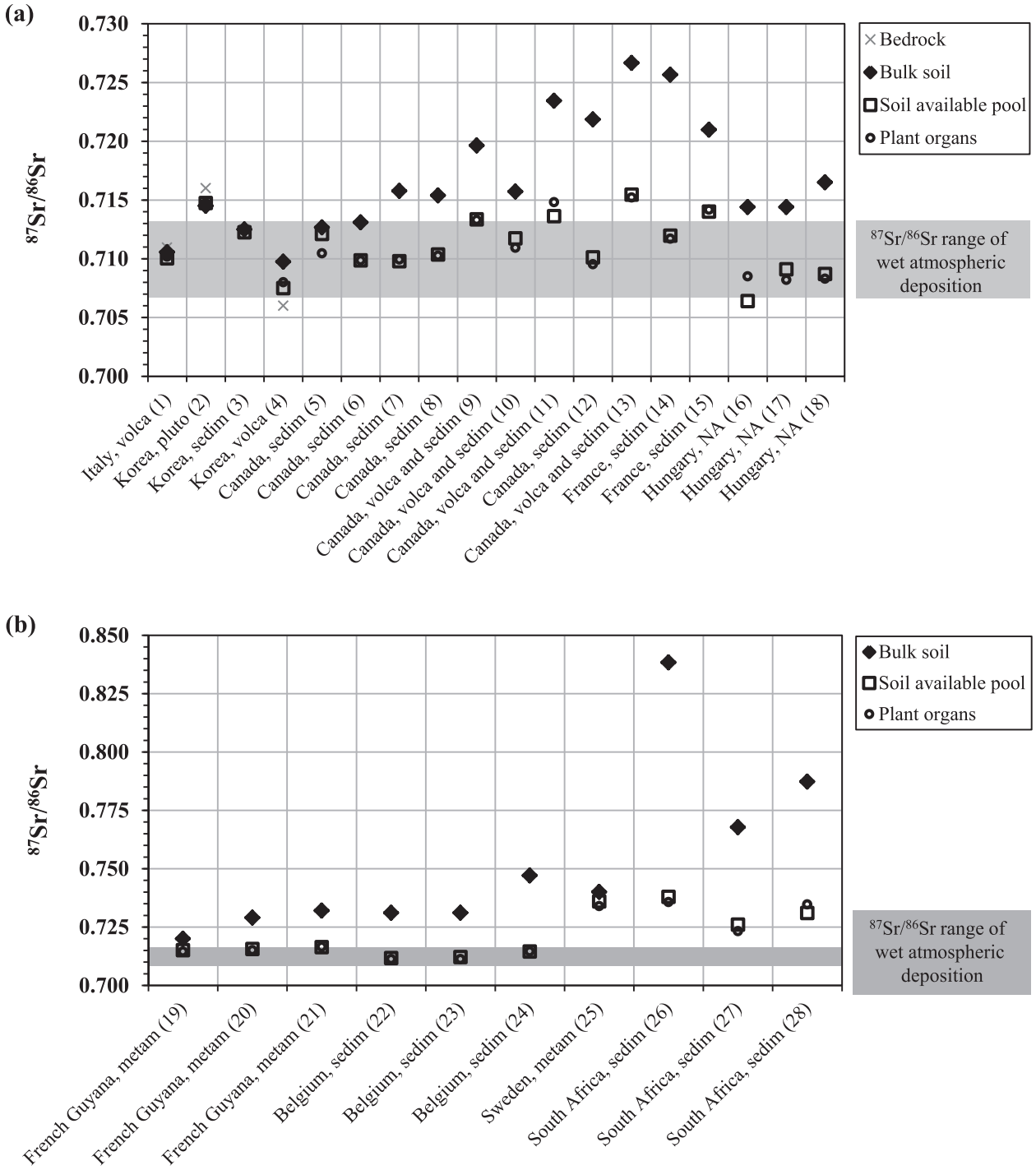

Fig. 5. Measured $^{87}Sr/^{86}Sr$ ratio ((a) values from 0.706 to 0.727 and (b) values from 0.711 to 0.838) in the bulk rock, bulk superficial soil horizon, available pool in the superficial soil horizon and different plant organs. Values are compiled from data of Marchionni et al. (2016) (site 1), Song et al., 2015 (sites 2 to 4), Vinciguerra et al., 2016 (sites 5 to 13), Bedel et al., 2016 (sites 14 and 15), Brunner et al., 2010 (sites 16 to 18), Poszwa et al., 2002 (sites 19 to 21), Drouet et al., 2005b (sites 22 to 24), Poszwa et al., 2004 (site 25) and Sillen et al., 1998 (sites 26 to 28). NA stands for Not Available, volca for volcanic rocks, pluto for plutonic rocks, sedim for sedimentary rocks and metam for metamorphic rocks. The range of $^{87}Sr/^{86}Sr$ ratio for wet atmospheric deposition (0.70727–0.71326) is indicated (in grey) on the Figure, but does not include the extremely high values measured for precipitation in Sweden (values reported by Åberg et al. (1989) and Wickman (1996), ranging up to 0.719; see Fig. 2).

fractionation during uptake or translocation, so it should be close to the value obtained for the soil bio-available pool. Several studies have shown systematic variations of $^{87}Sr/^{86}Sr$ with the geographical provenance of plants. Bong et al. (2012) found that the $^{87}Sr/^{86}Sr$ values in cabbage differed according to the geological characteristics of the region of origin. Song et al. (2015) reported that plants maintained the same $^{87}Sr/^{86}Sr$ values as measured in the bedrock, bulk soil, exchangeable pool and carbonate fraction (the latter being extracted with acetic acid). However, the plant $^{87}Sr/^{86}Sr$ isotope signature is often closer to the $^{87}Sr/^{86}Sr$ value of the soil available pool than the bulk soil. As discussed in the previous section, the $^{87}Sr/^{86}Sr$ ratio of the soil bio-available pool of a given site is only

Table 3
Protocol used, site location and rock type, and $^{87}Sr/^{86}Sr$ ratio measured in bedrock, bulk soil, soil available pool, and plant organs from 28 different sites ($^{87}Sr/^{86}Sr$ values are illustrated on Fig. 5). NA stands for Not Available.

Author	Name of soil fraction	Product of extraction	Site number	Region/country	Rock type	$^{87}Sr/^{86}Sr$			
						Bedrock	Bulk soil	Soil available pool	Plant organs
(a)	Bioavailable/ leached	Unibest resin capsule	1	central Italy	Volcanic rocks	0.71096	0.71056	0.71003	0.71018
(b)	Exchangeable	NH_4OAc, 1M	2	Gonju, Korea	Granite	0.71600	0.71450	0.71475	0.71475
			3	Yeongwol, Korea	Limestone	0.71250	0.71250	0.71225	0.71240
			4	Jeju, Korea	Basalt	0.70600	0.70975	0.70750	0.70800
(c)	Labile	NH_4NO_3 1N	5	Quebec province, Canada	sedimentary rocks	–	0.71267	0.71211	0.71046
			6	Quebec province, Canada	sedimentary rocks	–	0.71310	0.70986	0.70987
			7	Quebec province, Canada	sedimentary rocks	–	0.71578	0.70979	0.70994
			8	Quebec province, Canada	sedimentary rocks	–	0.71538	0.71036	0.71026
			9	Quebec province, Canada	Volcanic and sedimentary rocks	–	0.71964	0.71335	0.71330
			10	Quebec province, Canada	Volcanic and sedimentary rocks	–	0.71571	0.71174	0.71093
			11	Quebec province, Canada	Volcanic and sedimentary rocks	–	0.72345	0.71363	0.71482
			12	Quebec province, Canada	sedimentary rocks	–	0.72186	0.71012	0.70954
			13	Quebec province, Canada	Volcanic and sedimentary rocks	–	0.72666	0.71546	0.71522
(d)	Exchangeable	NH_4OAc, 1M	14	Clermont en Argonne, France	silicate sedimentary rocks	–	0.72567	0.71197	0.71171
			15	Azerailles, France	marls	–	0.72098	0.71402	0.71417
(e)	Bioavailable/ mobile	NH_4NO_3	16	Zsombó, Hungary	NA	–	0.71440	0.70640	0.70850
			17	Szeged, Hungary	NA	–	0.71440	0.70910	0.70820
			18	Mezöhedges, Hungary	NA	–	0.71650	0.70870	0.70830
(f)	Exchangeable	NH_4Cl, 1M	19	French Guyana	schist and pegmatite	–	0.72000	0.71510	0.71450
			20	French Guyana	schist and pegmatite	–	0.72900	0.71560	0.71510
			21	French Guyana	schist and pegmatite	–	0.73200	0.71640	0.71650
(g)	Labile pool	NH_4OAc, 1M	22	Belgium	Carbonated Pleistocene loess	–	0.73107	0.71173	0.71124
			23	Belgium	Carbonated Pleistocene loess	–	0.73111	0.71214	0.71124
			24	Belgium	Clastic shales and siltstones	–	0.74710	0.71451	0.71460
(h)	Exchangeable	NH_4Cl, 1M	25	Svartberget-Nyanget, Sweden	Gneiss	–	0.74001	0.73600	0.73400
(i)	Exchangeable	NA	26	Swartkrans, South Africa	Dolomite	–	0.83833	0.73791	0.73568
			27	Swartkrans, South Africa	Dolomite	–	0.76772	0.72605	0.72320
			28	Swartkrans, South Africa	Dolomite	–	0.78729	0.73098	0.73468

Values compiled from (a) Marchionni et al., 2016; (b) Song et al., 2015; (c) Vinciguerra et al., 2016; (d) Bedel et al., 2016; (e) Brunner et al., 2010; (f) Poszwa et al., 2002; (g) Drouet et al., 2005b; (h) Poszwa et al., 2004; (i) Sillen et al., 1998.

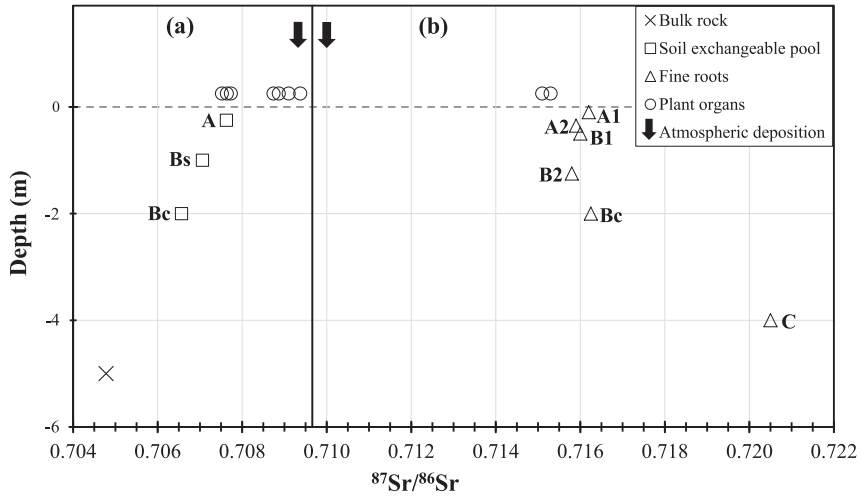

Fig. 6. Gradients of $^{87}Sr/^{86}Sr$ signature in soil exchangeable pools on (a) glacial materials composed mainly of anorthosite (Miller et al., 1993) and (b) granitic rocks (Dambrine et al., 1997). The letters correspond to the different soil horizons (A and A1: organo-mineral horizons; A2: eluvial horizon; B1 and B2: superficial structural mineral horizons; Bs: illuvial mineral horizon; Bc: deep mineral horizon; C: weathered rock). Atmospheric deposition and plant organs $^{87}Sr/^{86}Sr$ values from both studies are shown on the Figure. Horizon depths were not assigned in Miller et al. (1993), therefore, the depth values in Fig. 6 (a) should not be taken in consideration.

partly influenced by the underlying geological material (modulated by the preferential weathering of certain minerals). In addition, the isotopic composition is controlled by atmospheric Sr deposition on the ground surface. This is well illustrated by the data on Fig. 5.

Indeed, compared to bedrocks or bulk soils, the $^{87}Sr/^{86}Sr$ values of plants from all the sites represented here are shifted towards rainwater and close to the values measured in surface soil available pools. Some plant isotopic signatures are included in the range of rainwater $^{87}Sr/^{86}Sr$ ratios, while at other sites these ratios are clearly distinct, *e.g.* site 25 is located in Sweden where precipitation is very low and the weathering input is assumed to have a high $^{87}Sr/^{86}Sr$ value (Poszwa et al., 2004). This suggests that, in some contexts, the variability of plant $^{87}Sr/^{86}Sr$ values between sites is sufficient to distinguish different regions. In particular, Hodell et al. (2004) found significant $^{87}Sr/^{86}Sr$ differences between bedrock and plants but noted that this variability was not high enough to preclude the use of $^{87}Sr/^{86}Sr$ to distinguish between different regions.

Nevertheless, we should point out few limitations of this approach:

- The effect of atmospheric deposition is most striking for ecosystems developed under wet climates on deep and highly weathered soils (Hewawasam et al., 2013). In particular, tropical rainforests growing on different rock types can show tree $^{87}Sr/^{86}Sr$ signatures converging towards atmospheric deposition values, making it more difficult to distinguish the two sites with this approach. For example, on two sites in French Guyana, the $^{87}Sr/^{86}Sr$ values measured in leaf litter (representing the average leaf signature of the rainforest) are similar despite drastically different bedrock types: 0.713 on deep weathered soils developed from metavolcanic rocks at the Nouragues station (central French Guyana, site GP; Poszwa et al., 2009) and 0.7142 to 0.7164 on deep weathered soils developed from Paleoproterozoic schists and pegmatites at the Petit Saut site (northern coast of French Guyana, Poszwa et al., 2002).
- The presence of specific isotopic depth gradients could increase the range of variation of tree isotope signatures observed on the same site. On the sites reported on Fig. 6 (data from Miller et al., 1993; Dambrine et al., 1997), the isotopic ratio of plants is systematically close to that of the surface soil available pool. However, some plants with deep roots may have access to available Sr with a specific isotopic signature derived from deeper soil horizons than shallow-rooted plants. Besides, specific weathering in the root environment and intensive Sr recycling through litterfall could create specific gradients in the isotope composition under some species (case of spruce in Sweden, Poszwa et al., 2004). In this way, the isotopic signature of two neighboring trees (a Pine and a spruce) could be distinct according to their specific depth of uptake and their access to available pools of Sr with different signatures.
- In some agricultural contexts, the applied cultivation practices can impact the original and natural signature of the soils and vegetation. Techer et al. (2017) reported differences in Sr isotopic ratios between two sites (only 1 km apart) having the same bedrock but different agricultural practices. The irrigation degree and fertilization techniques were found to affect the $^{87}Sr/^{86}Sr$ value of soil exchangeable fraction (extracted using ammonium salt 1M NH_4NO_3), soil mobile fraction (extracted using acetic acid 1M AcOH) and the organs (*i.e.* branches, leaves and olives) of the studied olive trees growing on them.

Two recent studies (cited below) have shown differences in the $\delta^{88/86}Sr$ values between plants and their nutrient source pool, with plants having ^{86}Sr-enriched isotope compositions compared to the soils and rocks on which they grow (Fig. 1). De Souza et al. (2010) reported $\delta^{88/86}Sr$ values in plants lower by 0.20‰–0.50‰ than values measured in the corresponding bulk soils. Bullen and Chadwick (2016) analysed the seedling and an attached rock fragment sampled from a lava flow and found that the $\delta^{88/86}Sr$ of roots (−0.53‰), stem (−0.30‰) and foliage (−0.12‰) were lighter than in the lava fragment (0.24‰). In both studies, the lighter $\delta^{88/86}Sr$ in plants can be attributed either to a lighter Sr composition of the surface exchangeable pool available for the plant and/or preferential uptake of the lighter Sr isotopes. Andrews et al. (2016) also suggested fractionation during plant uptake to explain higher $\delta^{88/86}Sr$ of soil water compared to those expected from simple bedrock weathering leading to higher $\delta^{88/86}Sr$ values in rivers draining the Milford Sound region of Fiordland, New Zealand.

Humans and animals that feed on plants and other animals incorporate Sr into their bodies where it substitutes for Ca in the skeletal tissue minerals (Bentley, 2006; Bentley et al., 2004, 2003; Ericson, 1985; Hodell et al., 2004; Knudson et al., 2004; Price et al., 2002, 2000; Slovak and Paytan, 2011). The $^{87}Sr/^{86}Sr$ ratios in individual skeletons reflect the isotope composition of the plants and animals consumed, and thus record a site-specific signature (Fig. 7). Flockhart et al. (2015) measured the $^{87}Sr/^{86}Sr$ signatures in three associated trophic levels in a controlled greenhouse experiment and found no significant differences between the isotope composition of leachable Sr from soils, milkweed leaves and monarch butterfly wings. Blum et al. (2000) observed that the $^{87}Sr/^{86}Sr$ isotopic values remained unchanged between the soil exchangeable pools, leaves, caterpillars, snails and eggshells. The only exception occurs in the case of adult birds having a less radiogenic $^{87}Sr/^{86}Sr$ value than the lower trophic level, probably due to the low $^{87}Sr/^{86}Sr$ value of the food consumed in tropical winter habitats. Therefore, the $^{87}Sr/^{86}Sr$ signatures of animals and humans feeding on local nutrient sources reflect the isotope composition of available Sr at the site of residence. When the nutrients are drawn from several sources, the $^{87}Sr/^{86}Sr$ signature reflects mixing between the different sources.

Stable strontium isotopes have been shown to fractionate according to the trophic level, ranging from archaeological and modern small herbivores ($\delta^{88/86}Sr$ from −0.21‰ to 0.04‰; mean $\delta^{88/86}Sr = -0.09$‰; $n = 11$), through archaeological and modern large herbivores ($\delta^{88/86}Sr$ from −0.44‰ to 0.05‰; mean $\delta^{88/86}Sr = -0.21$‰; $n = 9$) to archaeological human remains ($\delta^{88/86}Sr$ from −0.87‰ to 1.19‰; mean $\delta^{88/86}Sr = -0.24$‰; $n = 58$), with lower $\delta^{88/86}Sr$ values being found at higher trophic levels (Fig. 1; Knudson et al., 2010). Similarly, lower values of $\delta^{88/86}Sr$ were identified in dental tissues of domestic pigs (from −0.26‰ to −0.18‰) compared to the diet (from 0.06‰ to 0.13‰) as a result of trophic level fractionation in a controlled feeding experiment (Lewis et al., 2017).

3.3. Characterizing the local Sr isotope signature of sites for wood provenance studies

When determining the provenance of plant materials, the $^{87}Sr/^{86}Sr$ ratio of the available pool in surface soil horizons generally represents the “local signature” of a potential site of origin, as there is usually a good correlation with the plant $^{87}Sr/^{86}Sr$ ratios (Fig. 5). However, because of the difficulty of precisely defining the isotopic signature of the Sr available pool and the possible presence of vertical gradients in isotope composition in soils, there may be differences in the $^{87}Sr/^{86}Sr$ signature between soil available pools and trees. In provenance studies, the best approach is to determine a site-specific local signature by analysing samples from the same type of studied material. For the study of wood provenance, it is thus preferable to determine regional isotopic signatures of Sr by analysing wood from living trees. Due to possible Sr isotopic variations between neighboring trees (*e.g.* presence of various geological materials and/or isotopic gradients in soils), it is appropriate to measure the $^{87}Sr/^{86}Sr$ of wood from several individuals to define the range of variation at the scale of a stand. However, this

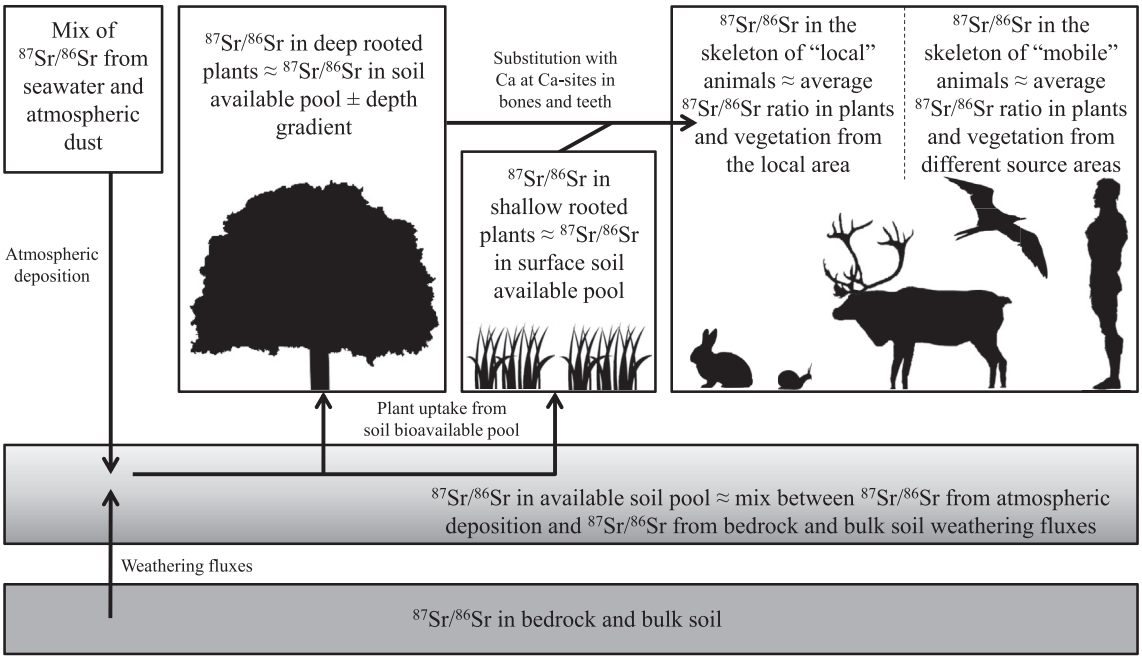

Fig. 7. Illustration of the links between the $^{87}Sr/^{86}Sr$ ratios in rocks, soils, vegetation and living organisms.

range of signatures may not be stable with time. Thus, we may wonder whether it is suitable to use modern local signatures to determine the provenance of historical materials.

Over the last hundred years, a decrease in $^{87}Sr/^{86}Sr$ ratios of soil available pools has been observed based on several studies using biological archives (references below). As in any ecosystem, weathering and atmospheric deposition are the two main natural sources of available Sr, the decrease in Sr isotopic ratios with time could be explained either by a variation of the inputs from these two sources or by the influence of an additional source. Drouet et al. (2005a) showed a temporal decrease in the $^{87}Sr/^{86}Sr$ isotope ratio of tree-rings from beech and oak growing on very acidic soils impoverished in exchangeable Ca due to the increased atmospheric acid deposition in the 1920s. A similar trend has been observed in tree-rings of spruce (Poszwa et al., 2003) and red spruce (Bullen and Bailey, 2005), also growing on acidic soils. The authors cited above put forward the hypothesis that acidic atmospheric deposition causes a deficiency in available Ca and mobilization of monomeric aluminium (Al_i) in the lower soil horizons. Due to this Ca depletion and/or Al_i toxicity affecting the fine roots, plant uptake from shallow soil available pools (characterized by lower $^{87}Sr/^{86}Sr$ at those sites) is enhanced. However, little time-variation of $^{87}Sr/^{86}Sr$ ratio was found in trees from forests growing on Ca-rich soils (Drouet et al., 2005a).

Åberg et al. (1990) interpreted a constant decrease of $^{87}Sr/^{86}Sr$ values in mussel shells between 1915 and 1985 as the result of surface water acidification. For the Slerebo River, located in Sweden, the slight decrease between 1945 and 1980 was followed by a sharp drop interpreted as due to the remarkable effect of river liming (Åberg, 1995), with the limestone used (with low $^{87}Sr/^{86}Sr$ value) representing a third source of Sr. This possible variation of $^{87}Sr/^{86}Sr$ signature with time is recorded in archives (such as shells or tree rings) but rarely in soils. Therefore, for dendroprovenance studies, it would be more appropriate to determine the past local $^{87}Sr/^{86}Sr$ signature by measuring the $^{87}Sr/^{86}Sr$ ratio of the oldest tree-rings of ancient trees. Since anthropogenic atmospheric acid inputs started less than a hundred years ago (whose effects are recorded in tree-rings that are even slightly older, see below), it should be possible to find and analyse such old trees. Another alternative is to use wood from archaeological buildings to determine past local $^{87}Sr/^{86}Sr$ values. Nevertheless, this implies that the wood should be dated and its local origin established.

In any case, to avoid any species-related variations, the local signature should be determined using trees of the same species as the studied material. In cases where the wood from living trees is not available at a given site, it may be possible to measure the local $^{87}Sr/^{86}Sr$ signature in (i) the soil exchangeable pool, which is close to the signature of trees (see Fig. 5) or (ii) the archaeological skeletal remains of small animals found in specific archaeological layers (Grupe et al., 2011), in case of a suspected Sr isotopic variation over time in the corresponding soils.

The Sr composition of a tree-ring undergoes continuous lateral equilibration as long as the tree-ring is active. This was demonstrated by Drouet et al. (2005a), who revealed the effect of liming on a beech stand by analysing tree-rings formed 50 years before the liming took place. Momoshima and Bondietti (1994) studied the distribution of the radionuclide ^{90}Sr in annual rings of different tree species. This radionuclide was found in rings dated as ca. 35 years (depending on the species) before the first deposition occurred in 1954. Even though these results suggest a lateral homogenization of the $^{87}Sr/^{86}Sr$ ratio between neighboring tree-rings, analyses should ideally be performed on a group of tree-rings rather than on an individual tree-ring, to avoid any effects due to seasonal or annual variations.

To summarize, the range of variation of a site-specific local isotopic signature should be defined at the scale of a stand. It needs to be established by measuring the $^{87}Sr/^{86}Sr$ in groups of old tree-rings from a large number of aged individuals.

4. Application of Sr isotopes to provenance studies

4.1. Provenance of foodstuffs and man-made products

By relating the $^{87}Sr/^{86}Sr$ signature in modern food products to their geographical origin, many authors have already shown the promising potential of this approach to studying the provenance of

food products. Several authors have pointed out the possibility of using $^{87}Sr/^{86}Sr$ ratio as a tracer of wine origin (Almeida and Vasconcelos, 2001; Dehelean and Voica, 2012; Durante et al., 2013; Lurton et al., 1999). Moreover, Barbaste et al. (2002), Di Paola-naranjo et al. (2011) and Masi and Castorina (2011) suggested that the application of Sr isotopes combined with other organic, inorganic, and isotopic data may be a promising tool for determining the fingerprints of wine origin. Even though Almeida and Vasconcelos (2004) reported significantly higher $^{87}Sr/^{86}Sr$ values in wines compared to the grape juices used for their production, Vinciguerra et al. (2015) have demonstrated that the $^{87}Sr/^{86}Sr$ isotope ratio of the wine is representative of the grapes from which it is made and that the winemaking process does not affect the Sr isotope ratio. Identifying the provenance of wine can be of importance to guarantee its authenticity (Durante et al., 2015; Marchionni et al., 2013; Martins et al., 2014) as well as detecting fraud in the wine trade (Petrini et al., 2015).

Similarly, $^{87}Sr/^{86}Sr$ signatures have been used in provenance studies of dairy products such as cheese (Fortunato et al., 2004; Pillonel et al., 2003) and butter (Rossmann et al., 2000), as well as beverages such as cider (García-Ruiz et al., 2007), olive oil (Medini et al., 2015) and orange juice (Rummel et al., 2010) or spices such as paprika (Brunner et al., 2010). Besides, $^{87}Sr/^{86}Sr$ ratios can be used to confirm the production area of rice (Kawasaki et al., 2002; Oda et al., 2001) and tomatoes (Trincherini et al., 2014), or determining the authenticity of food products such as high-quality coffee beans (Techer et al., 2011), medicinal efficient ginseng (Choi et al., 2008) and valuable varieties of asparagus (Swoboda et al., 2008). Archaeological food products can also be tested for geographic provenance. Benson et al. (2006b, 2003, 2009) and Benson (2010) measured $^{87}Sr/^{86}Sr$ signatures in archaeological maize and successfully determined the possible geographical origins for this dietary staple. The use of $^{87}Sr/^{86}Sr$ ratios has also been applied to provenance studies on other types of samples: glass raw materials (Degryse and Schneider, 2008; Freestone et al., 2003; Henderson et al., 2005) and building materials like gypsum and marble (Brilli et al., 2005; Gale et al., 1988). Benson et al. (2006a) combined Sr and O isotope analyses to successfully determine the origin of plants used to manufacture prehistoric textiles.

4.2. Migration of humans and animals in the past

Several studies have addressed historical and pre-historical human mobility by analysing $^{87}Sr/^{86}Sr$ ratios in human skeletons (Bentley et al., 2003), tooth enamel (Price et al., 2012) or skeletal bone and tooth enamel at the same time (Bentley et al., 2004; Ezzo et al., 1997; Grupe et al., 1997; Hodell et al., 2004; Knudson et al., 2004; Price et al., 1994a, 1994b; Slovak et al., 2009). In other studies, $^{87}Sr/^{86}Sr$ measurements have been combined with other analyses (elemental concentrations and isotopic analysis of oxygen and lead) to determine human residential mobility and migration (Knudson and Price, 2007; Montgomery et al., 2005; Price et al., 1998; Shaw et al., 2016). Beard and Johnson (2000) analysed the Sr isotopic composition of skeletal material and tooth enamel to determine the birth region and geographic mobility of humans and animals. The $^{87}Sr/^{86}Sr$ values along with other isotopic analysis (C; N and O) were used on mammoth and mastodon tooth enamel (Hoppe, 2004; Hoppe et al., 1999) to investigate their mobility and migration, and on elephant ivory and bone samples (van der Merwe et al., 1990) to identify the region where the animal lived. Strontium isotope ratio $^{87}Sr/^{86}Sr$ have been successfully used to discriminate salmon from different sites, thus showing potential for the determination of natal origins (Martin et al., 2013).

It should be noted that diagenetic processes can hamper studies on the provenance of archaeological materials: Sr from the burial environment can replace or become mixed with the original Sr composition of these materials. The diagenetic modification of the initial $^{87}Sr/^{86}Sr$ signature of archaeological human and animal remains has been shown to be a potential issue (Budd et al., 2000; Koch et al., 1992; Nelson et al., 1986; Trickett et al., 2003; Tuross et al., 1989). Indeed, bones and teeth are subject to *post mortem* diagenesis, and Sr from the burial environment can be incorporated into the mineralized tissue and modify the original biogenic Sr composition. It is thus preferable to use tooth enamel, since this less porous tissue is less affected by diagenesis. Several sequential extraction protocols have been developed to resolve the problem of Sr contamination in bones and teeth (Hedman et al., 2009; Hoppe et al., 2003; Nielsen-Marsh and Hedges, 2000; Price et al., 1992; Sillen and Sealy, 1995).

4.3. Provenance of archaeological wood

Despite the numerous applications using Sr isotopes to study human and animal mobility and provenance of food or other materials, only few studies so far have focused on the provenance of archaeological wood using their $^{87}Sr/^{86}Sr$ ratio. In two case studies, $^{87}Sr/^{86}Sr$ signatures were analysed to trace the provenance of archaeological wood found in the Chaco Canyon, New Mexico. English et al. (2001) analysed the $^{87}Sr/^{86}Sr$ ratios of living trees (spruce and fir), rocks, soils and stream waters from three potential source areas for the Chaco Canyon timbers to determine the signature of the felling sites. These authors also measured the $^{87}Sr/^{86}Sr$ values of several archaeological wood samples from six great houses in Chaco Canyon to determine their provenance. The source of the timber was successfully determined, and they found that trees from two of the three studied sites (Chuska Mountains and San Mateo Mountains) were felled at the same time, with twice as many beams being sourced in the Chuska Mountains rather than from the San Mateo Mountains. Reynolds et al. (2005) extended the $^{87}Sr/^{86}Sr$ analyses to ponderosa pine (*Pinus ponderosa*) and more sites in the Chaco Canyon. Even though most of the ponderosa pine yield $^{87}Sr/^{86}Sr$ values matching the data from the Chuska Mountains (in accordance with the results of English et al. (2001) on spruce and fir), many others matched the $^{87}Sr/^{86}Sr$ signatures of three sites that were not taken into account by English et al. (2001).

The preliminary studies of Rich et al. (2015, 2012) report the $^{87}Sr/^{86}Sr$ signatures of cedar wood from different forests in Lebanon, Cyprus and Turkey to test the feasibility of tracing the provenance of archaeological cedar timber from ancient East Mediterranean ships. These authors (*op. cit.*) demonstrate the possibility of discriminating the Sr signatures for different sources of timbers, except in the case of two sites where the $^{87}Sr/^{86}Sr$ values overlap. Rich et al. (2015) concluded that, combined with other dendroprovenance techniques, this approach would yield more accurate results for determining the source of timbers. In a subsequent study, Rich et al. (2016) used $^{87}Sr/^{86}Sr$ ratios to investigate the provenance of cedar wood from three different shipwrecks. The potential sites of origin for the timber were analysed in the previous studies of Rich et al. (2015, 2012). To our knowledge, the study of Rich et al. (2016) is the only one to date that aims to trace the origin of wood from shipwrecks using Sr isotopes. Although these authors succeeded in determining the origin of timbers from one shipwreck located on land (Carnegie boat), the origin for the two others (Uluburun shipwreck and Athlit ram) remains unknown. The two non-provenanced shipwrecks sunk off the coast and have Sr isotopic signatures (0.70921 for the Uluburun shipwreck and 0.70891 for the Athlit ram) close to the seawater signature (0.70918). The $^{87}Sr/^{86}Sr$ values of the Uluburun shipwreck do not match any of the sampled forests, while the results from the Athlit

ram narrow the possible provenance to two different forests having overlapping ranges of Sr isotopic ratio. However, these isotope signatures could also be, at least partially, the results of seawater-derived Sr incorporated into the archaeological wood.

A further issue that remains unresolved is the potential modification of the Sr isotopic composition of archaeological wood from shipwrecks, which takes place in relation to marine biogeochemical processes. In the following section, this issue is addressed in the context of $^{87}Sr/^{86}Sr$ and $\delta^{88/86}Sr$ values.

5. The potential of Sr isotopes to trace the provenance of archaeological wood from shipwrecks

5.1. Modification of waterlogged wood by living organisms

Wood is composed essentially of lignin, cellulose and hemicellulose in different proportions depending on the tree species. Wood decomposition is inevitable, but the degree of alteration depends on the environmental conditions of the timber (Blanchette, 2000). Physico-chemical factors (moisture, temperature, O and N availability) affect the activity of the microbial decomposers (bacterial and fungal communities) and detritivores (invertebrates) causing the degradation of wood. Wood in waterlogged conditions can show signs of degradation within few days after waterlogging. In some other cases, in the absence of oxygen (especially at the sea bottom or in fine sediments), condition which slows down decomposers degradation, wood can survive for centuries with minimum alteration.

Shipworms are the main agent of physical degradation of wood under waterlogged conditions. These marine bivalves of the *Teredinidae* family contain dense communities of intracellular bacteria contributing to the digestion of the wood (Betcher et al., 2012; Distel et al., 2002a, 2002b; Elshahawi et al., 2013; Eriksen et al., 2015). These bivalves perforate the wood when it is exposed in water or buried in shallow sediment (Fig. 8), which can complicate dendrochronological and anatomical studies used to determine timber provenance. Shipworms can enhance the chemical contamination of timber by boring holes, which increases the surface of contact with other organisms (*e.g.* microbial decomposers) and environmental "contaminants" (seawater elements).

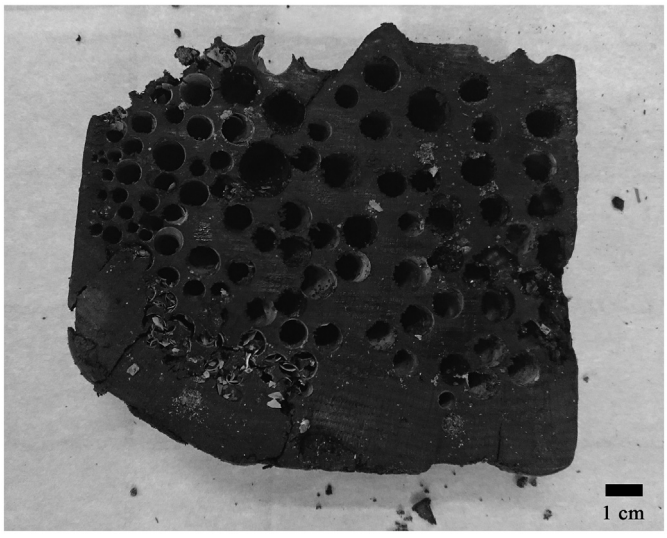

Fig. 8. Photograph of an oak wood sample from the Ribadeo shipwreck illustrating alteration by shipworms.

Microbial activity has an effect on the chemical structure of the wood, with fungal decay found mostly in timber of terrestrial environments, whereas timber from aquatic environments is mainly subject to bacterial decomposition (Björdal et al., 1999; Blanchette et al., 1991). Among the different types of fungal decay of wood, brown-rot and white-rot fungi are associated with non-waterlogged conditions, while soft-rot fungi are associated with waterlogged conditions (Blanchette, 2003). The soft-rot fungi can degrade cellulose, hemicellulose and lignin, thereby softening the wood surface. Additionally, wood-inhabiting microorganisms requiring high levels of moisture are linked mostly to waterlogged wood (Blanchette, 2000). This latter author reported that the most advanced stages of decay in terrestrial timber from ancient great houses (Chaco Canyon, New Mexico) are found in locations where the wood is exposed to weather. Parts of the wood protected from moisture are relatively free of decay and remain in good condition. Bacterial decomposition of wood can take place even in anoxic environments (Sandak et al., 2014). Bacterial attack on waterlogged wood from shipwrecks is considered as the main cause of the depletion of wood carbohydrates (Blanchette, 2000). The decay of organic compounds in wood can complicate dendroprovenance studies. The modification of C and O contents and isotope signatures can occur during wood burial. For example, archaeological oak specimens dated at approximately 6000 years and preserved in a shallow marine setting show distinct ^{13}C-enriched carbon, mainly due to alteration of the chemical composition of the wood (polysaccharides and lignin; van Bergen and Poole, 2002). Importantly, different pools of Sr in the waterlogged wood (such as bio-minerals formed during the life of the tree compared to marine neoformed minerals) could have different Sr isotope signatures (in $^{87}Sr/^{86}Sr$ or $\delta^{88/86}Sr$), so the release of Sr from some of these pools during selective degradation will lead to an apparent isotope fractionation that will hinder the use of Sr isotopes as a provenance tool.

Furthermore, external compounds can also be added to the wood over time. For example, several studies have quantified the accumulation of iron (Fe) and sulphur (S) in wood from shipwrecks. Analyses carried out on different shipwrecks show that the concentrations of these elements are higher on the surface and lower towards the centre of the samples (Fors et al., 2014, 2012, 2008; Fors and Sandström, 2006). Other studies on the Swedish warship Vasa found an accumulation of S compounds in the wood of the shipwreck (Sandström et al., 2005, 2002a, 2002b). This superficial contamination results in further degradation of the timber due to the oxidation of Fe and S, and the formation of acids. The formation of S-bearing phases (for example gypsum) could lead to the incorporation of Sr from the environment, with a different isotope composition both in terms of $^{87}Sr/^{86}Sr$ and $\delta^{88/86}Sr$. In section 5.2, we provide an example of such alteration of the initial Sr isotope signal.

5.2. New data on the modification of the "initial" Sr isotope ratio of wood during waterlogging

As seawater is relatively Sr-rich (~7.89 ppm; Palmer and Edmond, 1989), there is a significant risk that Sr from seawater will become incorporated over time into archaeological wood, thus obscuring the "initial" Sr isotope composition. Such an effect could in particular complicate the interpretation of $^{87}Sr/^{86}Sr$ signatures in terms of provenance, as regions underlain by carbonate rocks have $^{87}Sr/^{86}Sr$ values of 0.708–0.709, close to the value for present-day seawater. In that respect, $\delta^{88/86}Sr$ could help distinguish between the two effects (carbonate source region vs. seawater-derived Sr incorporation), since their effect on the bulk wood $\delta^{88/86}Sr$ would in theory be drastically different. To address these possibilities, we

performed two sets of measurements that are reported here: (1) Sr isotope ratios were measured on archaeological wood from a shipwreck, as a function of distance from the centre to the outer part of the wood chunk; (2) Sr isotope ratios were determined in non-marine archaeological wood reacted with seawater for three months. Strontium isotope analyses were combined with chemical and mineralogical analyses of wood structure by microscopy to assist interpretation of the results.

Archaeological oak wood from a 16th-century shipwreck in Ribadeo Bay, north-western Spain, was analysed to determine its $^{87}Sr/^{86}Sr$ and $\delta^{88/86}Sr$ values. Ten 1-cm-wide samples were collected systematically from side to side passing through the center of the timber. The samples were oven-dried at 60 °C and then grinded at 0.5 mm before being digested. Strontium from wood digests was separated using Eichrom Sr-SPEC resin and $^{87}Sr/^{86}Sr$ and $\delta^{88/86}Sr$ were measured on a Multi-Collector Plasma Source Mass Spectrometer (MC-ICP-MS; Neptune Thermo Electron) at the Institut de Physique du Globe de Paris (see appendix 1. for methodological information).

The $^{87}Sr/^{86}Sr$ values measured at the surface of the wood range between 0.70909 and 0.70916 (Table 4; Fig. 9), very close to the seawater ratio of 0.70918 (Pearce et al., 2015a), whereas the signature at the centre of the timber is lower (0.70871 and 0.70883). This difference indicates that Sr from seawater most likely contaminated the external parts of the timber, with little or no contamination from seawater at the centre. This interpretation can be supported by the $\delta^{88/86}Sr$ results showing values on the surface (0.32‰ and 0.23‰) closer to the seawater signature (0.39‰; Pearce et al. (2015a)) than at the centre of the sample (~0.19‰). Wood samples from the surface were studied also by Scanning Electron Microscope (SEM) at the PTEF-EEF Centre INRA-Lorraine (Plateforme Technique d'Ecologie Forestière) (see Appendix 1. for more detail on SEM analyses). Crystals at the wood surface and in wood pores were observed on the SEM image (Fig. 10a and c). Oxalates are the most widely distributed minerals known to be formed during the life of a tree (*i.e.* "biominerals"). Calcium-oxalate formation is of major importance in many plant species, since it plays a role in Ca regulation in tissues and organs (Franceschi and Nakata, 2005). While Ca-oxalate crystals show various sizes and morphologies (Baran and Monje, 2008), the crystals observed in the Ribadeo sample do not seem to correspond to the most common types of Ca-oxalate crystal shapes. Moreover, some S is detected in the EDS spectra of these crystals (Fig. 10b and d) reducing their possibility of being Ca-oxalate crystals. Therefore, it is unlikely that they were present during the life of the tree. As Ca is also detected in these crystals, they would appear to have a marine origin and should therefore contain some Sr (although Sr was not detected). These results suggest that, after a long period of

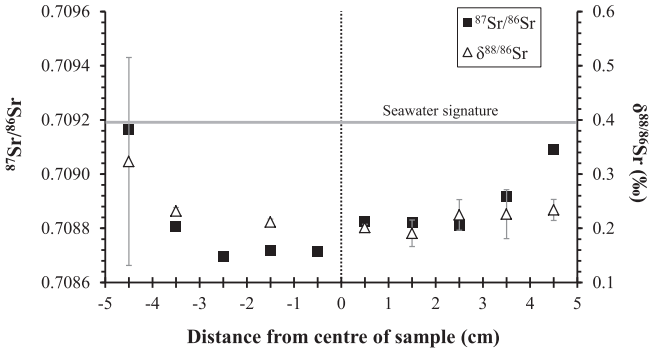

Fig. 9. Measured $^{87}Sr/^{86}Sr$ and $\delta^{88/86}Sr$ (‰) values along cross-section of an archaeological timber from the Ribadeo shipwreck. Seawater signature is indicated (grey line; 0.70918 and 0.39‰; Pearce et al. (2015a)) on the Figure. Error bars correspond to the 95% CI for $\delta^{88/86}Sr$ values.

waterlogging in seawater, marine Sr can be included in neoformed crystals in wood (during immersion in seawater or during drying after sample collection) thus modifying its bulk Sr isotope composition. The recent studies of AlKhatib and Eisenhauer (2017a, 2017b) and Liu et al. (2017) reported Sr fractionation during the formation of calcite and aragonite crystals, with light Sr isotope being preferentially incorporated into solid crystals. This fractionation during crystal formation can explain the lower $\delta^{88/86}Sr$ value measured in wood sample from the Ribadeo shipwreck ($\delta^{88/86}Sr$ of 0.32‰ for the most contaminated surface sample ShiTra01 as suggested by its $^{87}Sr/^{86}Sr$ ratio close to seawater signature) compared to the previously reported seawater signature of 0.39‰.

Another test experiment was carried out on 16th-century continental archaeological wood collected from the Segovia cathedral in central Spain. Fifteen sub-samples of the wood were measured for their Sr contents and initial isotopic composition, with five samples each corresponding to 10 tree-ring periods and covering 50 consecutive years, and the other ten samples corresponding to 10 individual tree-rings. Three other sub-samples were placed in seawater for three months and then analysed for Sr content and isotopic ratios. The results are shown in Table 5. The initial archaeological wood $^{87}Sr/^{86}Sr$ ratios range from 0.71314 to 0.71399, with a mean value of 0.71376 ± 0.00012 (95% CI). Values obtained for stable isotopes $\delta^{88/86}Sr$ vary between 0.07 and 0.18‰ with a mean $\delta^{88/86}Sr$ of 0.12‰ ± 0.02 (95% CI). The mean Sr content measured in wood is 1.6 μg/g ± 0.1 (95% CI). Isotopic signatures obtained in the three separate sub-samples analysed after waterlogging ranged from 0.709297 to 0.709302 (as regards $^{87}Sr/^{86}Sr$) and from 0.46 to 0.55‰ (as regards $\delta^{88/86}Sr$), with respective mean values of 0.70930 ± 0.5 10^{-5} (95% CI) and 0.49‰ ± 0.10 (95% CI) and

Table 4
Mean Sr content, $^{87}Sr/^{86}Sr$ and $\delta^{88/86}Sr$ (‰) values measured in transect samples from an archaeological wood from shipwreck. Column yield (%) was indicated in the table.

	Samples	Distance from centre	Sr (μg/g)	$^{87}Sr/^{86}Sr$	95% CI	$\delta^{88/86}Sr$ (‰)	95% CI (‰)	Yield (%)
Transect samples (n = 10)	ShiTra01	−4.5 cm	49.36	0.709165	0.000004	0.32	0.38	96
	ShiTra02	−3.5 cm	35.01	0.708808	0.000023	0.23	0.01	95
	ShiTra03	−2.5 cm	53.84	0.708695	0.000003	–	–	–
	ShiTra04	−1.5 cm	28.59	0.708716	0.000019	0.21	0.01	89
	ShiTra05	−0.5 cm	28.26	0.708714	0.000011	–	–	–
	ShiTra06	0.5 cm	26.19	0.708827	0.000015	0.20	0.01	98
	ShiTra07	1.5 cm	29.57	0.708822	0.000015	0.19	0.05	92
	ShiTra08	2.5 cm	31.26	0.708810	0.000009	0.22	0.06	97
	ShiTra09	3.5 cm	21.56	0.708919	0.000012	0.23	0.09	101
	ShiTra10	4.5 cm	17.87	0.709091	0.000007	0.23	0.04	108
Seawater[a] (n = 4)	**Mean**		**-**	**0.709177**	**0.000008**	**0.39**	**0.01**	**-**

[a] Data from Pearce et al. (2015a) corresponding to IAPSO seawater standard and samples from the Atlantic Ocean, Indian Ocean and Pacific Ocean.

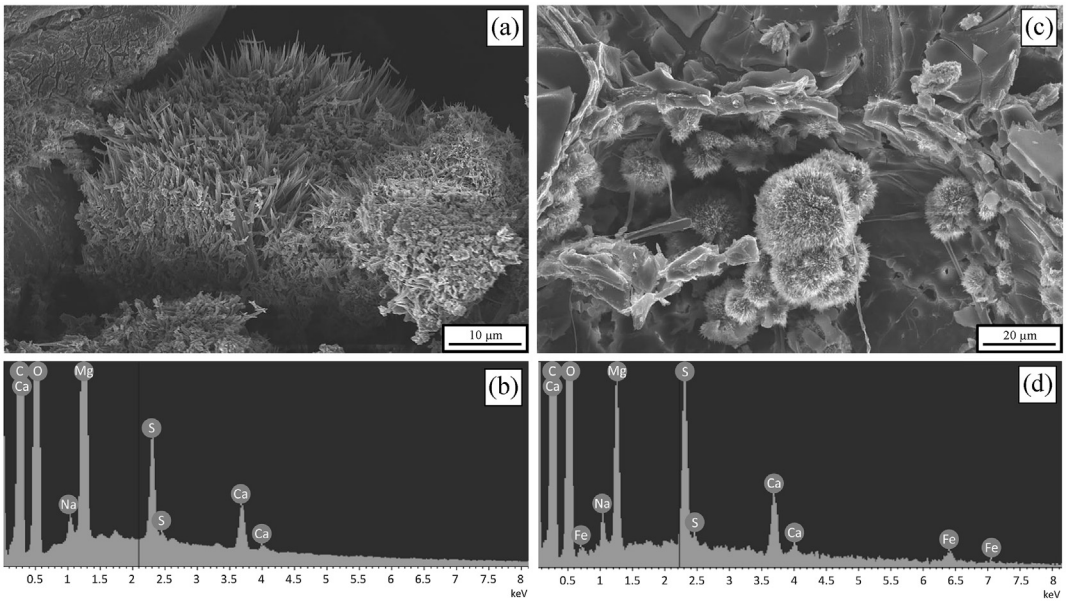

Fig. 10. Scanning Electron Microscope images of two different crystals (a and c) in a sample of archaeological wood from the Ribadeo shipwreck, with corresponding EDS spectra indicating elemental composition (b and d, respectively).

Table 5
Mean Sr content, $^{87}Sr/^{86}Sr$ and $\delta^{88/86}Sr$ (‰) values measured in archaeological wood from Segovia cathedral before and after being waterlogged in seawater for three months. The before waterlogging samples correspond to (i) ten tree-ring periods (CatPer01 to 05) and (ii) individual tree-rings (CatInd01 to 10). The samples (CatAft01 to 03) correspond to the three sub-samples analysed after waterlogging in seawater. Column yield (%) was indicated in the table. The measured seawater was collected from Berck-sur-Mer (Pas-de-Calais, France).

	Samples	Sr (µg/g)	$^{87}Sr/^{86}Sr$	95% CI	$\delta^{88/86}Sr$ (‰)	95% CI (‰)	Yield (%)
Before waterlogging (n = 15)	CatPer01	1.61	0.713890	0.000062	0.12	0.03	98
	CatPer02	1.52	0.713698	0.000042	0.08	0.09	100
	CatPer03	1.53	0.713137	0.000006	–	–	–
	CatPer04	1.41	0.713632	0.000044	0.07	0.06	99
	CatPer05	1.52	0.713630	0.000051	–	–	–
	CatInd01	1.54	0.713861	0.000039	0.12	0.04	95
	CatInd02	1.59	0.713861	0.000042	0.12	0.07	96
	CatInd03	1.64	0.713934	0.000071	0.09	0.07	93
	CatInd04	1.77	0.713985	0.000020	0.18	0.07	98
	CatInd05	1.69	0.713937	0.000027	0.13	0.06	95
	CatInd06	1.59	0.713918	0.000052	–	–	–
	CatInd07	1.69	0.713909	0.000059	0.13	0.02	96
	CatInd08	1.48	0.713454	0.000033	0.17	0.06	104
	CatInd09	1.46	0.713773	0.000051	0.15	0.18	93
	CatInd10	1.43	0.713745	0.000019	0.10	0.11	97
	Mean	**1.6 (0.1)**	**0.713758**	**0.000121**	**0.12**	**0.02**	
After waterlogging (n = 3)	CatAft01	16.33	0.709302	0.000005	0.46	–	88
	CatAft02	15.88	0.709300	0.000013	0.55	0.20[a]	91
	CatAft03	15.88	0.709297	0.000022	0.47	0.19	87
	Mean	**16.0 (0.5)**	**0.709300**	**0.000005**	**0.49**	**0.10**	
Seawater	SeaWat01	–	0.709276	0.000004	0.39	0.00	–

[a] This value corresponds to the long-term 2SD of SRM1515 and not the 95% CI of the sample (see Appendix 1 for the detail).

a mean Sr content of 16.0 µg/g ± 0.5 (95% CI). The radiogenic Sr isotopic signature in reacted wood is virtually indistinguishable from the measured seawater Sr isotopic signature ($^{87}Sr/^{86}Sr$ = 0.70928), while the measured $\delta^{88/86}Sr$ in wood is slightly higher (0.49‰) than the measured $\delta^{88/86}Sr$ of seawater (0.39‰). This might reflect isotope fractionation during marine Sr adsorption with the heavier ^{88}Sr being preferentially adsorbed on the wood surface. Although we lack constraints to ascertain this hypothesis, we note that a similar enrichment of heavy isotopes during adsorption has been experimentally observed for barium, another alkali element (van Zuilen et al., 2016). The Segovia cathedral wood samples were also studied by X-ray Diffraction (XRD, D2 Phaser) and SEM before and after being placed in seawater. However, these analyses failed to show the presence of crystals in the wood before and after marine waterlogging (data not shown). This experiment highlights the rapid contamination of wood with marine Sr after a short storage in seawater. This contamination completely modifies the original isotopic composition towards a seawater signature. As no minerals were found in the waterlogged wood, we assume that marine Sr was adsorbed into the wood and is present in these 3 samples in an exchangeable form.

Fig. 11 illustrates the processes causing the measured isotopic variations in our shipwreck and cathedral samples and the

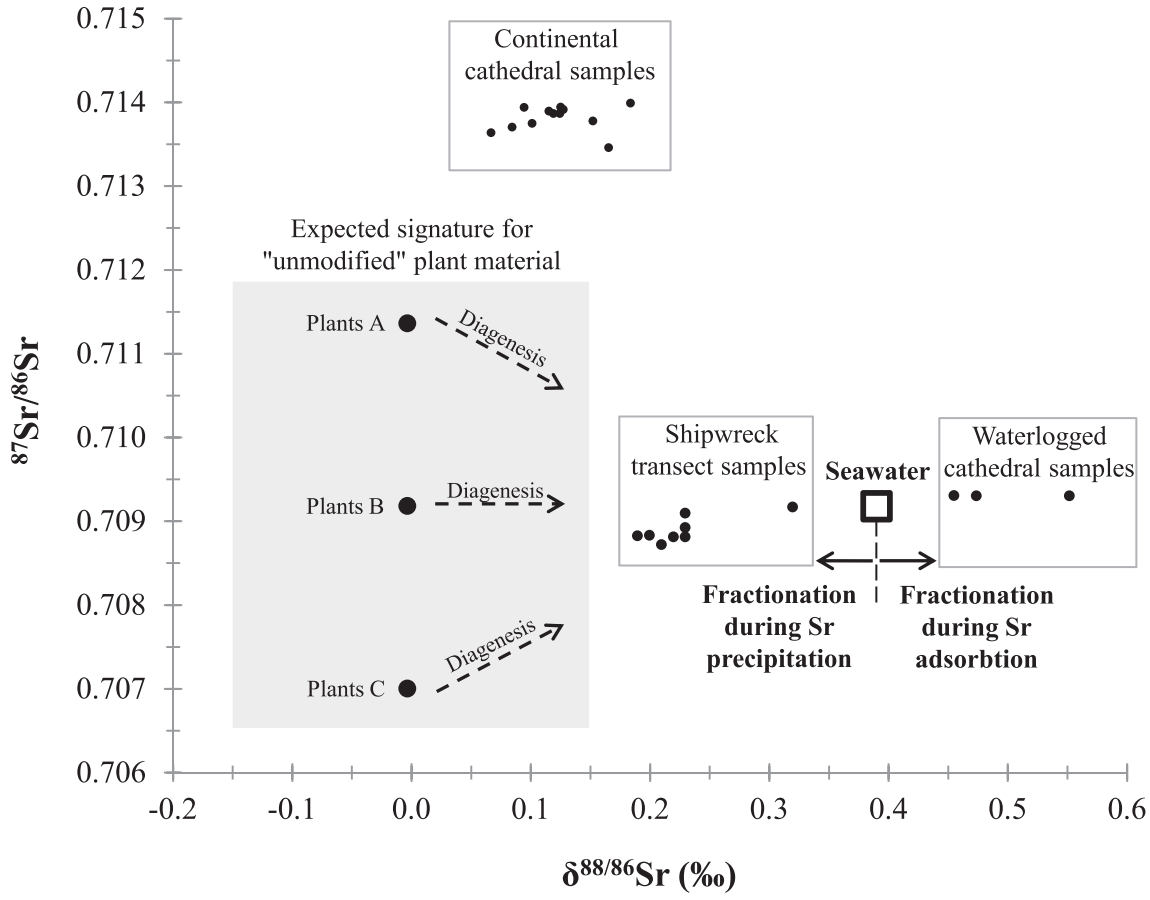

Fig. 11. Illustrative plot of $^{87}Sr/^{86}Sr$ versus $\delta^{88/86}Sr$ showing seawater signature (Pearce et al., 2015a), expected "unmodified" living plants signature and the signature of samples from the shipwreck transect and waterlogged cathedral (this study). Plants A, plants B and Plants C have $\delta^{88/86}Sr$ corresponding to the mean value of data reported in Andrews et al. (2016); Bullen and Chadwick (2016) and de Souza et al. (2010) (n = 13). The corresponding $^{87}Sr/^{86}Sr$ ratio are theoretical values illustrating three different contexts of origin; A: on silicate rocks; B: on carbonate rocks; C: on volcanic rocks. The dashed arrows show the direction of expected $^{87}Sr/^{86}Sr$ and $\delta^{88/86}Sr$ modifications (diagenesis) during waterlogging of a modern wood sample. The full line arrows show the direction of seawater $\delta^{88/86}Sr$ fractionation during Sr precipitation (enrichement in light ^{86}Sr) and during Sr adsorption (enrichement in heavy ^{88}Sr) on the waterlogged wood.

hypothetical variation of the signature in wood from living trees due to potential seawater contamination. Because relatively small $\delta^{88/86}Sr$ differences are expected in wood from trees growing over carbonate rocks and those growing over silicate rocks (*e.g.* Plants A, Plants B, Plants C and continental cathedral wood samples), the seawater contamination will affect their $\delta^{88/86}Sr$ similarly by enriching the wood with heavier ^{88}Sr isotopes. Contrarily, their $^{87}Sr/^{86}Sr$ signature will be affected distinctly as function of the bedrock underneath. Wood on silicate rocks (*e.g.* Plants A and continental cathedral samples) will have their $^{87}Sr/^{86}Sr$ ratio decreasing towards 0.70918 (modern seawater signature) while wood on limestone and basaltic rocks (*e.g.* Plants C) will have their $^{87}Sr/^{86}Sr$ ratio increasing towards seawater $^{87}Sr/^{86}Sr$ value. Moreover, while wood on limestone having $^{87}Sr/^{86}Sr$ signature close to that of seawater cannot be differentiated from seawater by comparing their radiogenic Sr signatures, their $\delta^{88/86}Sr$ will have very distinct values (*e.g.* Plants B). Fig. 11 also illustrates that fractionation during marine Sr adsorption would results in higher $\delta^{88/86}Sr$ values in waterlogged wood compared to seawater (*e.g.* waterlogged cathedral samples; this study) and fractionation during marine Sr precipitation would imply lower $\delta^{88/86}Sr$ values in wood compared to seawater (*e.g.* surface sample from the shipwreck transect; this study). The shipwreck samples from the center of the transect (ShiTra04 to 07; Table 4) show less contamination compared to the surface samples as regards $^{87}Sr/^{86}Sr$ (~0.7087 compared to 0.7092 for the most contaminated surface sample and for seawater) and $\delta^{88/86}Sr$ (~0.19‰ compared to 0.32‰ for the most contaminated wood surface sample and 0.39‰ for seawater). This $\delta^{88/86}Sr$ value of ~0.19‰ (ShiTra04 to 07) is closer to the signature of "non-contaminated" wood from the continental cathedral samples (0.12‰ ± 0.02; 95% CI; n = 12; see Table 5) and the different plant organs signature (0.00‰ ± 0.16; 95% CI; n = 13; Andrews et al. (2016); Bullen and Chadwick (2016); de Souza et al. (2010)). This plot suggests that the coupling between $^{87}Sr/^{86}Sr$ and $\delta^{88/86}Sr$ values have the potential to help future studies on dendroprovenance.

The preliminary results described here suggest that the surface of wood placed in seawater is rapidly contaminated by marine Sr. However, Sr substitutes for Ca mainly in plant cell wall constituents such as pectin, cellulose and lignin. Pectins are water soluble and can be relatively rapidly degraded by decomposition processes. Therefore, Sr in archaeological wood is contained mainly in the cell wall bonded to the lignin and cellulose. FTIR analyses on the archaeological wood from a shipwreck show a well-preserved lignin fingerprint typical of the studied type of wood despite the significant depletion of carbohydrates (Traoré et al., 2016). Therefore, specific molecules may be selected for Sr analysis to avoid or reduce the degree of contamination. As applied in the case of skeletal material (Price et al., 1992), a procedure of non-biogenic Sr removal should be developed for wood to access the original wood

Sr isotopic signature.

6. Conclusion and future prospects

Cutting-edge analytical techniques are yielding new insights in archaeological and historical studies. While dendrochronology remains the most commonly used tool for tracing wood provenance, it can be combined with other approaches such as anatomy, genetics, organic and inorganic analyses, as well as isotope analyses, to increase the accuracy and precision of results. Nevertheless, all these methods are influenced more or less directly by climatic factors specific to a given geographic area, which vary in relation to longitude, latitude and elevation. In this respect, the analysis of Sr isotopes in wood offers a unique opportunity to discriminate more clearly between different wood sources. Strontium is an element ubiquitous in rocks and released into waters and soils by weathering processes, then incorporated into the hard tissue of living organisms (humans, animals and plants). As physicochemical and biological processes do not affect the measured $^{87}Sr/^{86}Sr$, this ratio in plants reflects the local isotopic composition of the soil available pool which supplies nutrients, as well as Sr, to plants. In a similar manner, humans and animals show a $^{87}Sr/^{86}Sr$ signature in their tissues that is close to that of the food they have consumed, which is itself derived from plants yielding the same local $^{87}Sr/^{86}Sr$ isotopic signature. Recent advances in mass spectrometry now allow the detection of Sr isotopes mass-dependent fractionation, measured as $\delta^{88/86}Sr$; some recent studies demonstrate significant variations of $\delta^{88/86}Sr$ values between plant and soil compartments, which can help to distinguish between different sources of archaeological material.

Despite several applications of this tool to study human and animal mobility and the provenance of food and other plant products, few studies have focused on the provenance of archaeological wood using Sr isotopic composition. One difficulty arises from the fact that the local signature of a potential site of origin corresponds to the $^{87}Sr/^{86}Sr$ signature of the soil available pool at this site, which is only partly derived from the underlying geological substrate. Indeed, this signature in some cases is mainly controlled by atmospheric Sr fluxes entering the soil surface. As the Sr isotope signature of rainwater has a narrow range of variation, overlaps in local signatures can make it difficult to distinguish sites using this approach. Our review points out the lack of integrated studies reporting the variation of $^{87}Sr/^{86}Sr$ signatures in rocks, bulk soils, soil available pools and plants (and animals) from the same site. In addition, the $^{87}Sr/^{86}Sr$ signature of the soil available pool could be variable laterally and/or vertically within a site and may have changed through time. This highlights the need to characterize the local signature of a site taking into account a large number of samples to minimize the spatial heterogeneity and define the range of variation within the site. It could be interesting to characterize the local historical Sr signature using the same type of material (tree wood for studying the provenance of timber from shipwrecks) and, if possible, having the same age as the studied material. In addition, future studies should aim at a better understanding of the respective contributions of rocks and atmospheric deposition in various geological, climatic and pedogenetic contexts, to establish the local Sr isotopic signature of a site. More generally, maps should be compiled showing local Sr isotopic signatures.

Another major obstacle for the application of the Sr isotopes as a tracer of archaeological wood from shipwrecks is the diagenetic modification of the original signature of the timber. This is due to the physical degradation caused by shipworms, as well as the fungal and bacterial decomposition of wood and modification of its chemical composition by adsorption and precipitation of elements from the marine environment. To determine the provenance of wood sampled from shipwrecks using this method, more research should be undertaken to identify the degree and type of contamination of the waterlogged wood. Finally, a dedicated protocol needs to be developed for the elimination of marine Sr and the restoration of the original wood Sr signature. Our preliminary results suggest that stable Sr isotopes could be used to validate protocols and provide evidence of marine contamination.

Acknowledgments

This work was supported in the framework of the Initial Training Network (ITN) Marie Curie Actions project 'For-SEAdiscovery' [grant numbers PITN-GA-2013-607545]. More details on this project are available at http://forseadiscovery.eu/. We thank P. Burckel, L. Faure, P. Louvat, J. Moureau and J. Dallas for analytical help at IPGP. We are especially grateful to Dr M.S.N Carpenter for correcting the English style and grammar. We would also like to thank two anonymous reviewers for their constructive comments that improved previous version of this manuscript.

Appendix A. Supplementary data

Supplementary data related to this article can be found at https://doi.org/10.1016/j.jas.2017.09.005.

References

Åberg, G., 1995. The use of natural strontium isotopes as tracers in environmental studies. Water Air Soil Pollut. 79, 309–322. http://dx.doi.org/10.1007/BF01100444.

Åberg, G., Jacks, G., Joseph Hamilton, P., 1989. Weathering rates and 87Sr/86Sr ratios: an isotopic approach. J. Hydrol. 109, 65–78. http://dx.doi.org/10.1016/0022-1694(89)90007-3.

Åberg, G., Jacks, G., Wickman, T., Hamilton, P.J., 1990. Strontium isotopes in trees as an indicator for calcium availability. Catena 17, 1–11. http://dx.doi.org/10.1016/0341-8162(90)90011-2.

Albarède, F., Michard, A., Minster, J.F., Michard, G., 1981. 87Sr/86Sr ratios in hydrothermal waters and deposits from the East Pacific Rise at 21°N. Earth Planet. Sci. Lett. 55, 229–236. http://dx.doi.org/10.1016/0012-821X(81)90102-3.

AlKhatib, M., Eisenhauer, A., 2017a. Calcium and strontium isotope fractionation during precipitation from aqueous solutions as a function of temperature and reaction rate; II. Aragonite,. Geochim. Cosmochim. Acta 209, 320–342. http://dx.doi.org/10.1016/j.gca.2017.04.012.

AlKhatib, M., Eisenhauer, A., 2017b. Calcium and strontium isotope fractionation in aqueous solutions as a function of temperature and reaction rate; I. Calcite. Geochim. Cosmochim. Acta 209, 296–319. http://dx.doi.org/10.1016/j.gca.2016.09.035.

Allègre, C.J., Louvat, P., Gaillardet, J., Meynadier, L., Rad, S., Capmas, F., 2010. The fundamental role of island arc weathering in the oceanic Sr isotope budget. Earth Planet. Sci. Lett. 292, 51–56. http://dx.doi.org/10.1016/j.epsl.2010.01.019.

Almeida, C.M., Vasconcelos, M.T.S., 2001. ICP-MS determination of strontium isotope ratio in wine in order to be used as a fingerprint of its regional origin. J. Anal. At. Spectrom. 16, 607–611. http://dx.doi.org/10.1016/j.foodchem.2014.07.043.

Almeida, C.M.R., Vasconcelos, M.T.S.D., 2004. Does the winemaking process influence the wine 87Sr/86Sr? A case study. Food Chem. 85, 7–12. http://dx.doi.org/10.1016/j.foodchem.2003.05.003.

Altherr, R., Henjes-Kunst, F., Baumann, A., 1990. Asthenosphere versus lithosphere as possible sources for basaltic magmas erupted during formation of the Red Sea: constraints from Sr, Pb and Nd isotopes. Earth Planet. Sci. Lett. 96, 269–286. http://dx.doi.org/10.1016/0012-821X(90)90007-K.

Andrews, M.G., Jacobson, A.D., Lehn, G.O., Horton, T.W., Craw, D., 2016. Radiogenic and stable Sr isotope ratios (87Sr/86Sr, δ88/86Sr) as tracers of riverine cation sources and biogeochemical cycling in the Milford Sound region of Fiordland, New Zealand. Geochim. Cosmochim. Acta 173, 284–303. http://dx.doi.org/10.1016/j.gca.2015.10.005.

Angéli, N., 2006. Évolution de la composition chimique des ruisseaux vosgiens. Analyse rétrospective et effet d'un amendement calco-magnésien. UHP Nancy I, Nancy.

Armstrong, R.L., 1971. Glacial erosion and the variable isotopic composition of strontium in sea water. Nat. Phys. Sci. 230, 132–133. http://dx.doi.org/10.1038/physci230132a0.

Aubert, D., Probst, A., Stille, P., Viville, D., 2002. Evidence of hydrological control of Sr behavior in stream water (Strengbach catchment, Vosges mountains, France). Appl. Geochem. 17, 285–300. http://dx.doi.org/10.1016/S0883-2927(01)00080-4.

Aubert, D., Stille, P., Probst, A., 2001. REE fractionation during granite weathering and removal by waters and suspended loads: Sr and Nd isotopic evidence. Geochim. Cosmochim. Acta 65, 387–406. http://dx.doi.org/10.1016/S0016-7037(00)00546-9.

Bailey, S.W., Hornbeck, J.W., Driscoll, C.T., Gaudette, E., 1996. Calcium inputs and transport in a base-poor forest ecosystem as interpreted by Sr isotopes. Water Resour. Res. 32, 707–719.

Baran, E.J., Monje, P.V., 2008. Oxalate biominerals. In: Sigel, A., Sigel, H., Sigel, R.K.O. (Eds.), Biomineralization: from Nature to Application, pp. 219–254. http://dx.doi.org/10.1002/9780470986325.ch7.

Barbaste, M., Robinson, K., Guilfoyle, S., Medina, B., Lobinski, R., 2002. Precise determination of the strontium isotope ratios in wine by inductively coupled plasma sector field multicollector mass spectrometry (ICP-SF-MC-MS). J. Anal. At. Spectrom. 17, 135–137. http://dx.doi.org/10.1039/b109559p.

Barbour, M.M., 2007. Stable oxygen isotope composition of plant tissue: a review. Funct. Plant Biol. 34, 83–94. http://dx.doi.org/10.1071/FP06228.

Basile, I., Grousset, F.E., Revel, M., Petit, J.R., Biscaye, P.E., Barkov, N.I., 1997. Patagonian origin of glacial dust deposited in East Antarctica (Vostok and Dome C) during glacial stages 2, 4 and 6. Earth Planet. Sci. Lett. 146, 573–589. http://dx.doi.org/10.1016/S0012-821X(96)00255-5.

Basile, I., Petit, J.R., Touron, S., Grousset, F.E., Barkov, N., 2001. Volcanic layers in Antarctic (Vostok) ice cores: source identification and atmospheric implications. J. Geophys. Res. 106, 31915–31931. http://dx.doi.org/10.1029/2000JD000102.

Bataille, C.P., Bowen, G.J., 2012. Mapping 87Sr/86Sr variations in bedrock and water for large scale provenance studies. Chem. Geol. 304–305, 39–52. http://dx.doi.org/10.1016/j.chemgeo.2012.01.028.

Bataille, C.P., Brennan, S.R., Hartmann, J., Moosdorf, N., Wooller, M.J., Bowen, G.J., 2014. A geostatistical framework for predicting variations in strontium concentrations and isotope ratios in Alaskan rivers. Chem. Geol. 389, 1–15. http://dx.doi.org/10.1016/j.chemgeo.2014.08.030.

Beard, B.L., Johnson, C.M., 2000. Strontium isotope composition of skeletal material can determine the birth place and geographic mobility of humans and animals. J. Forensic Sci. 45, 1049–1061. http://dx.doi.org/10.1520/JFS14829J.

Beck, A.J., Charette, M.A., Cochran, J.K., Gonneea, M.E., Peucker-Ehrenbrink, B., 2013. Dissolved strontium in the subterranean estuary - implications for the marine strontium isotope budget. Geochim. Cosmochim. Acta 117, 33–52. http://dx.doi.org/10.1016/j.gca.2013.03.021.

Bedel, L., Poszwa, A., van der Heijden, G., Legout, A., Aquilina, L., Ranger, J., 2016. Unexpected calcium sources in deep soil layers in low-fertility forest soils identified by strontium isotopes (Lorraine plateau, eastern France). Geoderma 264, 103–116. http://dx.doi.org/10.1016/j.geoderma.2015.09.020.

Benson, L., Cordell, L., Vincent, K., Taylor, H., Stein, J., Farmer, G.L., Futa, K., 2003. Ancient maize from Chacoan great houses: where was it grown? Proc. Natl. Acad. Sci. 100, 13111–13115. http://dx.doi.org/10.1073/pnas.2135068100.

Benson, L., Hattori, E.M., Taylor, H.E., Poulson, S.R., Jolie, E.A., 2006a. Isotope sourcing of prehistoric willow and tule textiles recovered from western Great Basin rock shelters and caves - proof of concept. J. Archaeol. Sci. 33, 1588–1599. http://dx.doi.org/10.1016/j.jas.2006.02.012.

Benson, L., Stein, J., Taylor, H., Friedman, R., Windes, T.C., 2006b. The agricultural productivity of Chaco Canyon and the source (s) of pre-Hispanic maize found in Pueblo Bonito. In: Histories of Maize: Multidisciplinary Approaches to the Prehistory, Linguistics, Biogeography, Domestication, and Evolution of Maize. Elsevier/Academic Press, Amsterdam, pp. 289–314. http://dx.doi.org/10.1016/B978-012369364-8/50273-4.

Benson, L.V., 2010. Who provided maize to Chaco Canyon after the mid-12th-century drought? J. Archaeol. Sci. 37, 621–629. http://dx.doi.org/10.1016/j.jas.2009.10.027.

Benson, L.V., Stein, J.R., Taylor, H.E., 2009. Possible sources of archaeological maize found in Chaco Canyon and Aztec Ruin, New Mexico. J. Archaeol. Sci. 36, 387–407. http://dx.doi.org/10.1016/j.jas.2008.09.023.

Bentley, R.A., 2006. Strontium isotopes from the earth to the archaeological skeleton: a review. J. Archaeol. Method Theory 13, 135–187. http://dx.doi.org/10.1007/s10816-006-9009-x.

Bentley, R.A., Krause, R., Price, T.D., Kaufmann, B., 2003. Human mobility at the early Neolithic settlement of Vaihingen, Germany: evidence from strontium isotope analysis. Archaeometry 45, 471–486. http://dx.doi.org/10.1111/1475-4754.00122.

Bentley, R.A., Price, T.D., Stephan, E., 2004. Determining the "local" 87Sr/86Sr range for archaeological skeletons: a case study from Neolithic Europe. J. Archaeol. Sci. 31, 365–375. http://dx.doi.org/10.1016/j.jas.2003.09.003.

Betcher, M.A., Fung, J.M., Han, A.W., O'Connor, R., Seronay, R., Concepcion, G.P., Distel, D.L., Haygood, M.G., 2012. Microbial distribution and abundance in the digestive system of five shipworm species (Bivalvia: Teredinidae). PLoS One 7, e45309. http://dx.doi.org/10.1371/journal.pone.0045309.

Billamboz, A., 2003. Tree rings and wetland occupation in southwest Germany between 2000 and 500 BC: dendroarchaeology beyond dating in tribute to F.H. Schweingruber. Tree-Ring Res. 59, 37–49.

Biscaye, P.E., Grousset, F.E., Revel, M., Van Der Gaast, S., Zielinski, G.A., Vaars, A., Kukla, G., 1997. Asian provenance of glacial dust (stage 2) in the Greenland ice sheet project 2 ice core, summit. Greenl. J. Geophys. Res. 102, 26765–26781. http://dx.doi.org/10.1029/97JC01249.

Björdal, C.G., Nilsson, T., Daniel, G., 1999. Microbial decay of waterlogged archaeological wood found in Sweden. Applicable to archaeology and conservation. Int. Biodeterior. Biodegr. 43, 63–73. http://dx.doi.org/10.1016/S0964-8305(98)00070-5.

Blanchette, R.A., 2003. Deterioration in historic and archaeological woods from terrestrial sites. Microb. Ecol. 328–347.

Blanchette, R.A., 2000. A review of microbial deterioration found in archaeological wood from different environments. Int. Biodeterior. Biodegr. 46, 189–204. http://dx.doi.org/10.1016/S0964-8305(00)00077-9.

Blanchette, R.A., Cease, K.R., Abad, A.R., Sams, G.K., Simpson, E., Koestler, R.J., 1991. Biodeterioration of archaeological wood. In: Biodeterioration and Biodegradation 8: Proceedings of the 8th International Biodeterioration and Biodegradation Symposium, Windsor, Ontario, Canada, 26-31 August 1990, pp. 385–388.

Blum, J.D., Erel, Y., 1997. Rb-Sr isotope systematics of a granitic soil chronosequence: the importance of biotite weathering. Geochim. Cosmochim. Acta 61, 3193–3204. http://dx.doi.org/10.1016/S0016-7037(97)00148-8.

Blum, J.D., Erel, Y., 1995. A silicate weathering mechanism linking increases in marine 87Sr/86Sr with global glaciation. Nature. http://dx.doi.org/10.1038/373415a0.

Blum, J.D., Taliaferro, E.H., Weisse, M.T., Holmes, R.T., 2000. Changes in Sr/Ca, Ba/Ca and 87Sr/86Sr ratios between trophic levels in two forest ecosystems in the northeastern U.S.A. Biogeochemistry 49, 87–101. http://dx.doi.org/10.1023/A:1006390707989.

Böhm, F., Eisenhauer, A., Tang, J., Dietzel, M., Krabbenhöft, A., Kisakürek, B., Horn, C., 2012. Strontium isotope fractionation of planktic foraminifera and inorganic calcite. Geochim. Cosmochim. Acta 93, 300–314. http://dx.doi.org/10.1016/j.gca.2012.04.038.

Bonde, N., Christensen, A.E., 1993. Dendrochronological dating of the viking age ship burials at Oseberg, Gokstad and Tune, Norway. Antiquity 67, 575–583. http://dx.doi.org/10.1017/S0003598X00045774.

Bong, Y.S., Shin, W.J., Gautam, M.K., Jeong, Y.J., Lee, A.R., Jang, C.S., Lim, Y.P., Chung, G.S., Lee, K.S., 2012. Determining the geographical origin of Chinese cabbages using multielement composition and strontium isotope ratio analyses. Food Chem. 135, 2666–2674. http://dx.doi.org/10.1016/j.foodchem.2012.07.045.

Bonhomme, M., 1967. Ages radiométriques de quelques granites des Vosges moyennes. Bull.. du Serv. la Cart. géologique d'Alsace Lorraine 20, 101–106.

Bouchez, J., Lajeunesse, E., Gaillardet, J., France-Lanord, C., Dutra-Maia, P., Maurice, L., 2010. Turbulent mixing in the Amazon River: the isotopic memory of confluences. Earth Planet. Sci. Lett. 290, 37–43. http://dx.doi.org/10.1016/j.epsl.2009.11.054.

Bowen, G.J., Wassenaar, L.I., Hobson, K.A., 2005. Global application of stable hydrogen and oxygen isotopes to wildlife forensics. Oecologia 143, 337–348. http://dx.doi.org/10.1007/s00442-004-1813-y.

Brennan, S.R., Torgersen, C.E., Hollenbeck, J.P., Fernandez, D.P., Jensen, C.K., Schindler, D.E., 2016. Dendritic network models: improve isoscapes and quantifying influence of landscape and in-stream processes on strontium isotopes in rivers. Geophys. Res. Lett. 43, 5043–5051. http://dx.doi.org/10.1002/2016GL068904.

Brenot, A., Cloquet, C., Vigier, N., Carignan, J., France-Lanord, C., 2008. Magnesium isotope systematics of the lithologically varied Moselle river basin, France. Geochim. Cosmochim. Acta 72, 5070–5089. http://dx.doi.org/10.1016/j.gca.2008.07.027.

Brilli, M., Cavazzini, G., Turi, B., 2005. New data of 87Sr/86Sr ratio in classical marble: an initial database for marble provenance determination. J. Archaeol. Sci. 32, 1543–1551. http://dx.doi.org/10.1016/j.jas.2005.04.007.

Broecker, W.S., 1963. A preliminary evaluation of uranium series inequilibrium as a tool for absolute age measurement on marine carbonates. J. Geophys. Res. 68, 2817–2834.

Broecker, W.S., Peng, T.H., 1982. Tracers in the Sea. Lamont-Doherty Geol. Obs., Palisades, NY.

Brunner, M., Katona, R., Stefánka, Z., Prohaska, T., 2010. Determination of the geographical origin of processed spice using multielement and isotopic pattern on the example of Szegedi paprika. Eur. Food Res. Technol. 231, 623–634. http://dx.doi.org/10.1007/s00217-010-1314-7.

Budd, P., Montgomery, J., Barreiro, B., Thomas, R.G., 2000. Differential diagenesis of strontium in archaeological human dental tissues. Appl. Geochem. 15, 687–694. http://dx.doi.org/10.1016/S0883-2927(99)00069-4.

Bullen, T., Chadwick, O., 2016. Ca, Sr and Ba stable isotopes reveal the fate of soil nutrients along a tropical climosequence in Hawaii. Chem. Geol. 422, 25–45. http://dx.doi.org/10.1016/j.chemgeo.2015.12.008.

Bullen, T., White, A., Blum, A., Harden, J., Schulz, M., 1997. Chemical weathering of a soil chronosequence on granitoid alluvium: II. Mineralogic and isotopic constraints on the behavior of strontium. Geochim. Cosmochim. Acta 61, 291–306. http://dx.doi.org/10.1016/S0016-7037(96)00344-4.

Bullen, T.D., Bailey, S.W., 2005. Identifying calcium sources at an acid deposition-impacted spruce forest: a strontium isotope, alkaline earth element multitracer approach. Biogeochemistry 74, 63–99. http://dx.doi.org/10.1007/s10533-004-2619-z.

Burke, W.H., Denison, R.E., Hetherington, E.A., Koepnick, R.B., Nelson, H.F., Otto, J.B., 1982. Variation of seawater 87Sr/86Sr throughout Phanerozoic time. Geology 10, 516–519. http://dx.doi.org/10.1130/0091-7613(1982)10<516:VOSSTP>2.0.CO;2.

Capo, R.C., DePaolo, D.J., 1992. Homogeneity of Sr isotopes in the oceans. EOS, Trans. Am. Geophys. Union 73, 272.

Capo, R.C., Stewart, B.W., Chadwick, O.A., 1998. Strontium isotopes as tracers of ecosystem processes: theory and methods. Geoderma 82, 197–225. http://dx.doi.org/10.1016/S0016-7061(97)00102-X.

Chao, H.C., You, C.F., Liu, H.C., Chung, C.H., 2015. Evidence for stable Sr isotope

fractionation by silicate weathering in a small sedimentary watershed in southwestern Taiwan. Geochim. Cosmochim. Acta 165, 324–341. http://dx.doi.org/10.1016/j.gca.2015.06.006.
Charlier, B.L.A., Nowell, G.M., Parkinson, I.J., Kelley, S.P., Pearson, D.G., Burton, K.W., 2012. High temperature strontium stable isotope behaviour in the early solar system and planetary bodies. Earth Planet. Sci. Lett. 329–330, 31–40. http://dx.doi.org/10.1016/j.epsl.2012.02.008.
Choi, S.M., Lee, H.S., Lee, G.H., Han, J.K., 2008. Determination of the strontium isotope ratio by ICP-MS ginseng as a tracer of regional origin. Food Chem. 108, 1149–1154. http://dx.doi.org/10.1016/j.foodchem.2007.11.079.
Clarke, C.R.E., Garbutt, D.C.F., Pearce, J., 1997. Growth and wood properties of provenances and trees of nine Eucalypt species. Appita J. 50, 121–130.
Daly, A., 2007. The Karschau ship, Schleswig-Holstein: dendrochronological results and timber provenance. Int. J. Naut. Archaeol. 36, 155–166. http://dx.doi.org/10.1111/j.1095-9270.2006.00103.x.
Daly, A., Nymoen, P., 2008. The Bøle ship, Skien, Norway - research history, dendrochronology and provenance. Int. J. Naut. Archaeol. 37, 153–170. http://dx.doi.org/10.1111/j.1095-9270.2007.00157.x.
Dambrine, E., Loubet, M., Vega, J.A., Lissarague, A., 1997. Localisation of mineral uptake by roots using Sr isotopes. Plant Soil 192, 129–132. http://dx.doi.org/10.1023/A:1004294820733.
Davis, A.C., Bickle, M.J., Teagle, D.A.H., 2003. Imbalance in the oceanic strontium budget. Earth Planet. Sci. Lett. 211, 173–187. http://dx.doi.org/10.1016/S0012-821X(03)00191-2.
de Souza, G.F., Reynolds, B.C., Kiczka, M., Bourdon, B., 2010. Evidence for mass-dependent isotopic fractionation of strontium in a glaciated granitic watershed. Geochim. Cosmochim. Acta 74, 2596–2614. http://dx.doi.org/10.1016/j.gca.2010.02.012.
Degryse, P., Schneider, J., 2008. Pliny the Elder and Sr-Nd isotopes: tracing the provenance of raw materials for Roman glass production. J. Archaeol. Sci. 35, 1993–2000. http://dx.doi.org/10.1016/j.jas.2008.01.002.
Deguilloux, M.F., Pemonge, M.H., Bertel, L., Kremer, A., Petit, R.J., 2003. Checking the geographical origin of oak wood: Molecular and statistical tools. Mol. Ecol. 12, 1629–1636. http://dx.doi.org/10.1046/j.1365-294X.2003.01836.x.
Deguilloux, M.F., Pemonge, M.H., Petit, R.J., 2004. DNA-based control of oak wood geographic origin in the context of the cooperage industry. Ann. For. Sci. 61, 97–104. http://dx.doi.org/10.1051/forest.
Dehelean, A., Voica, C., 2012. Determination of lead and strontium isotope ratios in wines by inductively coupled plasma mass spectrometry. Rom. J. Phys. 57, 1194–1203.
Delmonte, B., Basile-Doelsch, I., Petit, J.R., Maggi, V., Revel-Rolland, M., Michard, A., Jagoutz, E., Grousset, F., 2004. Comparing the Epica and Vostok dust records during the last 220,000 years: stratigraphical correlation and provenance in glacial periods. Earth-Science Rev. 66, 63–87. http://dx.doi.org/10.1016/j.earscirev.2003.10.004.
Derry, L.A., Kaufman, A.J., Jacobsen, S.B., 1992. Sedimentary cycling and environmental change in the late Proterozoic: evidence from stable isotopes. Geochim. Cosmochim. Acta 56, 1317–1329.
Di Paola-naranjo, R.D., Baroni, M.V., Podio, N.S., Rubinstein, R., Fabani, M.P., Badini, G., Inga, M., Ostera, A., Cagnoni, M., Gallegos, E., Gautier, E., Peral-García, P., Hoogewerf, J., Wunderlin, D.A., 2011. Fingerprints for main varieties of Argentinean wines: terroir differentiation by inorganic, organic, and stable isotopic analyses coupled to chemometrics. J. Agric. Food Chem. 59, 7854–7865.
Distel, D.L., Beaudoin, D.J., Morrill, W., 2002a. Coexistence of multiple proteobacterial endosymbionts in the gills of the wood-boring bivalve Lyrodus pedicellatus (Bivalvia: Teredinidae). Appl. Environ. Microbiol. 68, 6292–6299. http://dx.doi.org/10.1128/AEM.68.12.6292.
Distel, D.L., Morrill, W., Maclaren-Toussaint, N., Franks, D., Waterbury, J., 2002b. Teredinibacter turnerae gen. nov., sp. nov., a dinitrogen-fixing, cellulolytic, endosymbiotic gamma-proteobacterium isolated from the gills of wood-boring molluscs (Bivalvia: Teredinidae). Int. J. Syst. Evol. Microbiol. 52, 2261–2269.
Domínguez-Delmás, M., Alejano-Monge, R., Van Daalen, S., Rodríguez-Trobajo, E., García-González, I., Susperregi, J., Wazny, T., Jansma, E., 2015. Tree-rings, forest history and cultural heritage: current state and future prospects of dendroarchaeology in the Iberian Peninsula. J. Archaeol. Sci. 57, 180–196. http://dx.doi.org/10.1016/j.jas.2015.02.011.
Domínguez-Delmás, M., Nayling, N., Wazny, T., Loureiro, V., Lavier, C., 2013. Dendrochronological dating and provenancing of timbers from the arade 1 shipwreck. Port. Int. J. Naut. Archaeol. 42, 118–136. http://dx.doi.org/10.1111/j.1095-9270.2012.00361.x.
Drouet, T., Herbauts, J., Demaiffe, D., 2005a. Long-term records of strontium isotopic composition in tree rings suggest changes in forest calcium sources in the early 20th century. Glob. Chang. Biol. 11, 1926–1940. http://dx.doi.org/10.1111/j.1365-2486.2005.01034.x.
Drouet, T., Herbauts, J., Gruber, W., Demaiffe, D., 2005b. Strontium isotope composition as a tracer of calcium sources in two forest ecosystems in Belgium. Geoderma 126, 203–223. http://dx.doi.org/10.1016/j.geoderma.2004.09.010.
Durante, C., Baschieri, C., Bertacchini, L., Bertelli, D., Cocchi, M., Marchetti, A., Manzini, D., Papotti, G., Sighinolfi, S., 2015. An analytical approach to Sr isotope ratio determination in Lambrusco wines for geographical traceability purposes. Food Chem. 173, 557–563. http://dx.doi.org/10.1016/j.foodchem.2014.10.086.
Durante, C., Baschieri, C., Bertacchini, L., Cocchi, M., Sighinolfi, S., Silvestri, M., Marchetti, A., 2013. Geographical traceability based on 87Sr/86Sr indicator: a first approach for PDO Lambrusco wines from Modena. Food Chem. 141, 2779–2787. http://dx.doi.org/10.1016/j.foodchem.2013.05.108.
Eckstein, D., van Es, W.A., Hollstein, E., 1975. Beitrag zu Datierung der frühmittelalterlichen Siedlung Dorestad, Holland. Ber. van Rijksd. voor het Oudheidkd. Bodemonderz 25, 165–175.
Elderfield, H., 1986. Strontium isotope stratigraphy. Palaeogeogr. Palaeoclimatol. Palaeoecol. 57, 71–90. http://dx.doi.org/10.1016/0031-0182(86)90007-6.
Elshahawi, S.I., Trindade-Silva, A.E., Hanora, A., Han, A.W., Flores, M.S., Vizzoni, V., Schrago, C.G., Soares, C.A., Concepcion, G.P., Distel, D.L., Schmidt, E.W., Haygood, M.G., 2013. Boronated tartrolon antibiotic produced by symbiotic cellulose-degrading bacteria in shipworm gills. Proc. Natl. Acad. Sci. 110, E295–E304. http://dx.doi.org/10.1073/pnas.1213892110.
English, N.B., Betancourt, J.L., Dean, J.S., Quade, J., 2001. Strontium isotopes reveal distant sources of architectural timber in Chaco Canyon. New Mex. Proc. Natl. Acad. Sci. 98, 11891–11896. http://dx.doi.org/10.1073/pnas.211305498.
Ericson, J., 1985. Strontium isotope characterization in the study of prehistoric human ecology. J. Hum. Evol. 14, 503–514.
Eriksen, A.M., Gregory, D., Shashoua, Y., 2015. Selective attack of waterlogged archaeological wood by the shipworm, Teredo navalis and its implications for in-situ preservation. J. Archaeol. Sci. 55, 9–15. http://dx.doi.org/10.1016/j.jas.2014.12.011.
Esteban, L.G., Martín, J.A., de Palacios, P., Fernández, F.G., 2012. Influence of region of provenance and climate factors on wood anatomical traits of Pinus nigra Arn. subsp. salzmannii. Eur. J. For. Res. 131, 633–645. http://dx.doi.org/10.1007/s10342-011-0537-x.
Ezzo, J.A., Johnson, C.M., Price, T.D., 1997. Analytical perspective on prehistoric migration: a case study from east-central Arizona. J. Archaeol. Sci. 24, 447–466.
Farquhar, G.D., Henry, B.K., Styles, J.M., 1997. A rapid on-line technique for determination of oxygen isotope composition of nitrogen-containing organic matter and water. Rapid Commun. Mass Spectrom. 11, 1554–1560. http://dx.doi.org/10.1002/(SICI)1097-0231(199709)11:14<1554::AID-RCM980>3.0.CO;2-I.
Faure, G., 1986. Principles of Isotope Geology, second ed.
Faure, G., Mensing, T.M., 2005. Isotopes: Priciples and Applications. John Wiley & Sons Inc.
Fietzke, J., Eisenhauer, A., 2006. Determination of temperature-dependent stable strontium isotope (88Sr/86Sr) fractionation via bracketing standard MC-ICP-MS. Geochem. Geophys. Geosyst. 7 http://dx.doi.org/10.1029/2006GC001243.
Flockhart, D.T., Kyser, T.K., Chipley, D., Miller, N.G., Norris, D.R., 2015. Experimental evidence shows no fractionation of strontium isotopes (87Sr/86Sr) among soil, plants, and herbivores: implications for tracking wildlife and forensic science. Isot. Environ. Health Stud. 51, 372–381. http://dx.doi.org/10.1080/10256016.2015.1021345.
Fors, Y., Grudd, H., Rindby, A., Jalilehvand, F., Sandström, M., Cato, I., Bornmalm, L., 2014. Sulfur and iron accumulation in three marine-archaeological shipwrecks in the Baltic sea: the Ghost, the crown and the sword. Sci. Rep. 4, 4222. http://dx.doi.org/10.1038/srep04222.
Fors, Y., Jalilehvand, F., Damian Risberg, E., Björdal, C., Phillips, E., Sandström, M., 2012. Sulfur and iron analyses of marine archaeological wood in shipwrecks from the Baltic Sea and Scandinavian waters. J. Archaeol. Sci. 39, 2521–2532. http://dx.doi.org/10.1016/j.jas.2012.03.006.
Fors, Y., Nilsson, T., Risberg, E.D., Sandström, M., Torssander, P., 2008. Sulfur accumulation in pinewood (Pinus sylvestris) induced by bacteria in a simulated seabed environment: implications for marine archaeological wood and fossil fuels. Int. Biodeterior. Biodegr. 62, 336–347. http://dx.doi.org/10.1016/j.ibiod.2007.11.008.
Fors, Y., Sandström, M., 2006. Sulfur and iron in shipwrecks cause conservation concerns. Chem. Soc. Rev. 35, 399–415. http://dx.doi.org/10.1039/b507010b.
Fortunato, G., Mumic, K., Wunderli, S., Pillonel, L., Bosset, J.O., Gremaud, G., 2004. Application of strontium isotope abundance ratios measured by MC-ICP-MS for food authentication. J. Anal. At. Spectrom. 19, 227–234. http://dx.doi.org/10.1039/b307068a.
Franceschi, V.R., Nakata, P.A., 2005. Calcium oxalate in plants: formation and function. Annu. Rev. Plant Biol. 56, 41–71. http://dx.doi.org/10.1146/annurev.arplant.56.032604.144106.
Francey, R.J., Farquhar, G.D., 1982. An explanation of 13C/12C variations in tree rings. Nature 297, 28–31. http://dx.doi.org/10.1038/297028a0.
Freestone, I.C., Leslie, K.A., Thirlwall, M., Gorin-Rosen, Y., 2003. Strontium isotopes in the investigation of early glass production: Byzantine and early islamic glass from the near East. Archaeometry 45, 19–32. http://dx.doi.org/10.1111/1475-4754.00094.
Gaillardet, J., Dupré, B., Allègre, C.J., 1999. Geochemistry of large river suspended sediments: silicate weathering or recycling tracer? Geochim. Cosmochim. Acta 63, 4037–4051. http://dx.doi.org/10.1016/S0016-7037(99)00307-5.
Gale, N.H., Einfalt, H.C., Hubberten, H.W., Jones, R.E., 1988. The sources of Mycenaean gypsum. J. Archaeol. Sci. 15, 57–72. http://dx.doi.org/10.1016/0305-4403(88)90019-2.
García-Ruiz, S., Moldovan, M., Fortunato, G., Wunderli, S., García Alonso, J.I., 2007. Evaluation of strontium isotope abundance ratios in combination with multi-elemental analysis as a possible tool to study the geographical origin of ciders. Anal. Chim. Acta 590, 55–66. http://dx.doi.org/10.1016/j.aca.2007.03.016.
Goede, A., McCulloch, M., McDermott, F., Hawkesworth, C., 1998. Aeolian contribution to strontium and strontium isotope variations in a Tasmanian speleothem. Chem. Geol. 149, 37–50. http://dx.doi.org/10.1016/S0009-2541(98)00035-7.
Goldberg, E.D., 1963. The oceans as a chemical system. sea 2, 645–701.
Goldstein, S.J., Jacobsen, S.B., 1988. Nd and Sr isotopic systematics of river water suspended material: implications for crustal evolution. Earth Planet. Sci. Lett.

87, 249–265. http://dx.doi.org/10.1016/0012-821X(88)90013-1.
Goldstein, S.J., Jacobsen, S.B., 1987. The Nd and Sr isotopic systematics of river-water dissolved material: implications for the sources of Nd and Sr in seawater. Chem. Geol. Isot. Geosci. Sect. 66, 245–272. http://dx.doi.org/10.1016/0168-9622(87)90045-5.
Gosz, J.R., Brookins, D.G., Moore, D.I., 1983. Using strontium isotope ratios to estimate inputs to ecosystems. Bioscience 33, 23–30. http://dx.doi.org/10.2307/1309240.
Gosz, J.R., Moore, D.I., 1989. Strontium isotope studies of atmospheric inputs to forested watersheds in New Mexico. Biogeochemistry 8, 115–134. http://dx.doi.org/10.1007/BF00001316.
Graustein, W., Armstrong, R., 1983. The use of strontium-87/strontium-86 ratios to measure atmospheric transport into forested watersheds. Sci. (80-.) 219, 289–292.
Graustein, W.C., 1989. 87Sr/86Sr ratios measure the sources and flow of strontium in terrestrial ecosystems. In: Stable Isotopes in Ecological Research, pp. 491–512. http://dx.doi.org/10.1007/978-1-4612-3498-2_28.
Grousset, F.E., Biscaye, P.E., Revel, M., Petit, J.R., Pye, K., Joussaume, S., Jouzel, J., 1992. Antarctic (Dome C) ice-core dust at 18 k.y. B.P.: isotopic constraints on origins. Earth Planet. Sci. Lett. 111, 175–182.
Grupe, G., Price, T.D., Schröter, P., Söllner, F., Johnson, C.M., Beard, B.L., 1997. Mobility of Bell Beaker people revealed by strontium isotope ratios of tooth and bone: a study of southern Bavarian skeletal remains. Appl. Geochem. 12, 517–525. http://dx.doi.org/10.1016/S0883-2927(98)00073-0.
Grupe, G., Von Carnap-Bornheim, C., Söllner, F., 2011. Stable strontium isotope mapping for provenance studies in archaeology - different material, different signals? Bull. Schweiz. Ges. für Anthr. 17, 67–76.
Halicz, L., Segal, I., Fruchter, N., Stein, M., Lazar, B., 2008. Strontium stable isotopes fractionate in the soil environments? Earth Planet. Sci. Lett. 272, 406–411. http://dx.doi.org/10.1016/j.epsl.2008.05.005.
Haneca, K., de Boodt, R., Herremanas, V., de Pauw, H., Van Acker, J., van de Velde, C., Beeckman, H., 2005. Late Gothic altarpieces as sources of information on medieval wood use: a dendrochronological and art historical survey. IAWA J. 26, 273–298.
Haneca, K., Čufar, K., Beeckman, H., 2009. Oaks, tree-rings and wooden cultural heritage: a review of the main characteristics and applications of oak dendrochronology in Europe. J. Archaeol. Sci. 36, 1–11. http://dx.doi.org/10.1016/j.jas.2008.07.005.
Hedman, K.M., Curry, B.B., Johnson, T.M., Fullagar, P.D., Emerson, T.E., 2009. Variation in strontium isotope ratios of archaeological fauna in the Midwestern United States: a preliminary study. J. Archaeol. Sci. 36, 64–73. http://dx.doi.org/10.1016/j.jas.2008.07.009.
Henchiri, S., Gaillardet, J., Dellinger, M., Bouchez, J., Spencer, R.G., 2016. Riverine dissolved lithium isotopic signatures in low-relief central Africa and their link to weathering regimes. Geophys. Res. Lett. 43, 4391–4399. http://dx.doi.org/10.1002/2013GL058740.Received.
Henderson, J., Evans, J.A., Sloane, H.J., Leng, M.J., Doherty, C., 2005. The use of oxygen, strontium and lead isotopes to provenance ancient glasses in the Middle East. J. Archaeol. Sci. 32, 665–673. http://dx.doi.org/10.1016/j.jas.2004.05.008.
Herut, B., Starinsky, A., Katz, A., 1993. Strontium in rainwater from Israel: sources, isotopes and chemistry. Earth Planet. Sci. Lett. 120, 77–84. http://dx.doi.org/10.1016/0012-821X(93)90024-4.
Hess, J., Bender, M.L., Schilling, J.G., 1986. Evolution of the ratio of strontium-87 to strontium-86 in seawater from cretaceous to present. Sci. (80-.) 231, 979–984. http://dx.doi.org/10.1126/science.231.4741.979.
Hewawasam, T., von Blanckenburg, F., Bouchez, J., Dixon, J.L., Schuessler, J.A., Maekeler, R., 2013. Slow advance of the weathering front during deep, supply-limited saprolite formation in the tropical Highlands of Sri Lanka. Geochim. Cosmochim. Acta 118, 202–230. http://dx.doi.org/10.1016/j.gca.2013.05.006.
Hodell, D.A., Mead, G.A., Mueller, P.A., 1990. Variation in the strontium isotopic composition of seawater (8 Ma to present): implications for chemical weathering rates and dissolved fluxes to the oceans. Chem. Geol. Isot. Geosci. Sect. 80, 291–307. http://dx.doi.org/10.1016/0168-9622(90)90011-Z.
Hodell, D.A., Quinn, R.L., Brenner, M., Kamenov, G., 2004. Spatial variation of strontium isotopes (87Sr/86Sr) in the Maya region: a tool for tracking ancient human migration. J. Archaeol. Sci. 31, 585–601. http://dx.doi.org/10.1016/j.jas.2003.10.009.
Holland, H.D., 1984. The Chemical Evolution of the Atmosphere and Oceans. Princeton Univ. Press, Princeton, N. J.
Hoppe, K.A., 2004. Late Pleistocene mammoth herd structure, migration patterns, and Clovis hunting strategies inferred from isotopic analyses of multiple death assemblages. Paleobiology 30, 129–145. http://dx.doi.org/10.1666/0094-8373(2004)030<0129:LPMHSM>2.0.CO;2.
Hoppe, K.A., Koch, P.L., Furutani, T.T., 2003. Assessing the preservation of biogenic strontium in fossil bones and tooth enamel. Int. J. Osteoarchaeol 13, 20–28. http://dx.doi.org/10.1002/oa.663.
Hoppe, K.A., Koch, P.L., Carlson, R.W., Webb, S.D., 1999. Tracking mammoths and mastodons: reconstruction of migratory behavior using strontium isotope ratios. Geology 27, 439–442. http://dx.doi.org/10.1130/0091-7613(1999)027<0439.
Kagawa, A., Kuroda, K., Abe, H., Fujii, T., Itoh, Y., 2007. Stable isotopes and inorganic elements as potential indicators of geographic origin of Southeast Asian timber. In: Fujii, T. (Ed.), Proceedings of the International Symposium on Development of Improved Methods to Identify Shorea Species Wood and its Origin. Forestry and Forest Products Research Institute, Tsukuba, pp. 39–44.
Kagawa, A., Leavitt, S.W., 2010. Stable carbon isotopes of tree rings as a tool to pinpoint the geographic origin of timber. J. Wood Sci. 56, 175–183. http://dx.doi.org/10.1007/s10086-009-1085-6.
Kawasaki, A., Oda, H., Hirata, T., 2002. Determination of strontium isotope ratio of brown rice for estimating its provenance. Soil Sci. Plant Nutr. 48, 635–640. http://dx.doi.org/10.1080/00380768.2002.10409251.
Kelleher, C.T., Hodkinson, T.R., Kelly, D.L., Douglas, G.C., 2004. Characterisation of chloroplast DNA haplotypes to reveal the provenance and genetic structure of oaks in Ireland. For. Ecol. Manage 189, 123–131. http://dx.doi.org/10.1016/j.foreco.2003.07.032.
Kennedy, M.J., Hedin, L.O., Derry, L.A., 2002. Decoupling of unpolluted temperate forests from rock nutrient sources revealed by natural 87Sr/86Sr and 84Sr tracer addition. Proc. Natl. Acad. Sci. 99, 9639–9644. http://dx.doi.org/10.1073/pnas.152045499.
Kistler, R.W., Chappell, B.W., Peck, D.L., Bateman, P.C., 1986. Isotopic variation in the Tuolumne intrusive suite, central sierra Nevada, California. Contrib. Mineral. Pet. 94, 205–220. http://dx.doi.org/10.1007/BF00592937.
Knudson, K., Price, T., Buikstra, J., Blom, D., 2004. The use of strontium isotope analysis to investigate Tiwanaku migration and mortuary ritual in Bolivia and Peru. Archaeometry 46, 5–18. http://dx.doi.org/10.1111/j.1475-4754.2004.00140.x.
Knudson, K.J., Price, T.D., 2007. Utility of multiple chemical techniques in archaeological residential mobility studies: case studies from Tiwanaku- and Chiribaya-affiliated sites in the Andes. Am. J. Phys. Anthropol. 132, 25–39. http://dx.doi.org/10.1002/ajpa.
Knudson, K.J., Williams, H.M., Buikstra, J.E., Tomczak, P.D., Gordon, G.W., Anbar, A.D., 2010. Introducing δ88/86Sr analysis in archaeology: a demonstration of the utility of strontium isotope fractionation in paleodietary studies. J. Archaeol. Sci. 37, 2352–2364. http://dx.doi.org/10.1016/j.jas.2010.04.009.
Koch, P.L., Halliday, A.N., Walter, L.M., Stearley, R.F., Huston, T.J., Smith, G.R., 1992. Sr isotopic composition of hydroxyapatite from recent and fossil salmon: the record of lifetime migration and diagenesis. Earth Planet. Sci. Lett. 108, 277–287. http://dx.doi.org/10.1016/0012-821X(92)90028-T.
Koch, P.L., Heisinger, J., Moss, C., Carlson, R.W., Fogel, M.L., Behrensmeyer, A.K., 1995. Isotopic tracking of change in diet and habitat use in African elephants. Sci. (80-.). http://dx.doi.org/10.1126/science.267.5202.1340.
Koepnick, R.B., Burke, W.H., Denison, R.E., Hetherington, E.A., Nelson, H.F., Otto, J.B., Waite, L.E., 1985. Construction of the seawater curve for the cenozoic and cretaceous: supporting data. Chem. Geol. Isot. Geosci. Sect. 58, 55–81. http://dx.doi.org/10.1016/0168-9622(85)90027-2.
Krabbenhöft, A., Eisenhauer, A., Böhm, F., Vollstaedt, H., Fietzke, J., Liebetrau, V., Augustin, N., Peucker-Ehrenbrink, B., Müller, M.N., Horn, C., Hansen, B.T., Nolte, N., Wallmann, K., 2010. Constraining the marine strontium budget with natural strontium isotope fractionations (87Sr/86Sr*, δ88/86Sr) of carbonates, hydrothermal solutions and river waters. Geochim. Cosmochim. Acta 74, 4097–4109. http://dx.doi.org/10.1016/j.gca.2010.04.009.
Krabbenhöft, A., Fietzke, J., Eisenhauer, A., Liebetrau, V., Böhm, F., Vollstaedt, H., 2009. Determination of radiogenic and stable strontium isotope ratios (87Sr/86Sr; δ88/86Sr) by thermal ionization mass spectrometry applying an 87Sr/84Sr double spike. J. Anal. At. Spectrom. 24, 1267–1271. http://dx.doi.org/10.1039/b906292k.
Kramchaninov, A.Y., Chernyshev, I.V., Shatagin, K.N., 2012. Isotope analysis of strontium by multicollector inductively-coupled plasma mass spectrometry: high-precision combined measurement of 88Sr/86Sr and 87Sr/86Sr isotope ratios. J. Anal. Chem. 67, 1084–1092. http://dx.doi.org/10.1134/S1061934812140067.
Krishnaswami, S., Trivedi, J.R., Sarin, M.M., Ramesh, R., Sharma, K.K., 1992. Strontium isotopes and rubidium in the Ganga-Brahmaputra river system: weathering in the Himalaya, fluxes to the Bay of Bengal and contributions to the evolution of oceanic 87Sr/86Sr. Earth Planet. Sci. Lett. 109, 243–253. http://dx.doi.org/10.1016/0012-821X(92)90087-C.
Kudo, A.M., Brookins, D.G., Laughlin, A.W., 1972. Sr isotopic disequilibrium in lherzolites from the Puerco necks, New Mexico. Earth Planet. Sci. Lett. 15, 291–295. http://dx.doi.org/10.1016/0012-821X(72)90175-6.
Laughlin, A.W., Brookins, D.G., Kudo, A.M., Causey, J.D., 1971. Chemical and strontium isotopic investigations of ultramafic inclusions and basalt, Bandera Crater, New Mexico. Geochim. Cosmochim. Acta 35, 107–113. http://dx.doi.org/10.1016/0016-7037(71)90108-6.
Leavitt, S., 1993. Environmental information from 13C/12C ratios in wood. In: Swart, P.K. (Ed.), Climate Change in Continental Isotopic Records. Geophysical Monograph 78. American Geophysical Union, Washington, DC, pp. 325–331.
Lewis, J., Pike, A.W.G., Coath, C.D., Evershed, R.P., 2017. Strontium concentration, radiogenic (87Sr/86Sr) and stable (δ88Sr) strontium isotope systematics in a controlled feeding study. Star. Sci. Technol. Archaeol. Res. 3, 53–65. http://dx.doi.org/10.1080/20548923.2017.1303124.
Li, G., Elderfield, H., 2013. Evolution of carbon cycle over the past 100 million years. Geochim. Cosmochim. Acta 103, 11–25. http://dx.doi.org/10.1016/j.gca.2012.10.014.
Liebetrau, V., Eisenhauer, A., Krabbenhöft, A., Fietzke, J., Böhm, F., Rüggeberg, A., Guers, K., 2009. New perspectives on the marine Sr-isotope record: δ88/86Sr, 87Sr/86Sr* and δ44/40Ca signatures of aragonitic molluscs throughout the last 27 Ma. Geochim. Cosmochim. Acta 73, A762.
Liu, H.C., You, C.F., Zhou, H., Huang, K.F., Chung, C.H., Huang, W.J., Tang, J., 2017. Effect of calcite precipitation on stable strontium isotopic compositions: insights from riverine and pool waters in a karst cave. Chem. Geol. 456, 85–97.

http://dx.doi.org/10.1016/j.chemgeo.2017.03.008.
Lurton, L., Lancelot, J., Herreiras, J., Verdoux, P., 1999. Authentification de vins de la Vallée du Rhône à l'aide du rapport 87Sr/86Sr de leur terroir d'origine. In: XXIVeme Congrès Mondial de la Vigne et du Vin. Mayence, 5–9 juillet.
Ma, J.L., Wei, G.J., Liu, Y., Ren, Z.Y., Xu, Y.G., Yang, Y.H., 2013. Precise measurement of stable (δ88/86Sr) and radiogenic (87Sr/86Sr) strontium isotope ratios in geological standard reference materials using MC-ICP-MS. Chin. Sci. Bull. 58, 3111–3118. http://dx.doi.org/10.1007/s11434-013-5803-5.
Marchionni, S., Braschi, E., Tommasini, S., Bollati, A., Cifelli, F., Mulinacci, N., Mattei, M., Conticelli, S., 2013. High-precision 87Sr/86Sr analyses in wines and their use as a geological fingerprint for tracing geographic provenance. J. Agric. Food Chem. 61, 6822–6831. http://dx.doi.org/10.1021/jf4012592.
Marchionni, S., Buccianti, A., Bollati, A., Braschi, E., Cifelli, F., Molin, P., Parotto, M., Mattei, M., Tommasini, S., Conticelli, S., 2016. Conservation of 87Sr/86Sr isotopic ratios during the winemaking processes of "Red" wines to validate their use as geographic tracer. Food Chem. 190, 777–785. http://dx.doi.org/10.1016/j.foodchem.2015.06.026.
Martin, J., Bareille, G., Berail, S., Pecheyran, C., Daverat, F., Bru, N., Tabouret, H., Donard, O., 2013. Spatial and temporal variations in otolith chemistry and relationships with water chemistry: a useful tool to distinguish Atlantic salmon Salmo salar parr from different natal streams. J. Fish. Biol. 82, 1556–1581. http://dx.doi.org/10.1111/jfb.12089.
Martins, P., Madeira, M., Monteiro, F., De Sousa, R.B., Curvelo-García, A.S., Catarino, S., 2014. 87Sr/86Sr ratio in vineyard soils from Portuguese denominations of origin and its potential for origin authentication. J. Int. Des. Sci. la Vigne Du. Vin 48, 21–29.
Masi, U., Castorina, F., 2011. Sr isotopes and Romagna wines: an opportunity for better trading? EQA-International J. Environ. Qual. 7, 41–48. http://dx.doi.org/10.6092/issn.2281-4485/3832.
McArthur, J.M., 1994. Recent trends in strontium isotope stratigraphy. Terra Nov. 6, 331–358. http://dx.doi.org/10.1111/j.1365-3121.1994.tb00507.x.
McCarroll, D., Loader, N.J., 2004. Stable isotopes in tree rings. Quat. Sci. Rev. 23, 771–801. http://dx.doi.org/10.1016/j.quascirev.2003.06.017.
Medini, S., Janin, M., Verdoux, P., Techer, I., 2015. Methodological development for 87Sr/86Sr measurement in olive oil and preliminary discussion of its use for geographical traceability of PDO Nîmes (France). Food Chem. 171, 78–83. http://dx.doi.org/10.1016/j.foodchem.2014.08.121.
Miller, E.K., Blum, J.D., Friedland, A.J., 1993. Determination of soil exchangeable-cation loss and weathering rates using Sr isotopes. Nature 362, 438–441. http://dx.doi.org/10.1038/362438a0.
Miranda, I., Pereira, H., 2002. Variation of pulpwood quality with provenances and site in Eucalyptus globulus. Ann. For. Sci. 59, 283–291. http://dx.doi.org/10.1051/forest.
Momoshima, N., Bondietti, E.A., 1994. The radial distribution of 90Sr and 137Cs in trees. J. Environ. Radioact. 22, 93–109. http://dx.doi.org/10.1016/0265-931X(94)90016-7.
Montgomery, J., Evans, J.A., Powlesland, D., Roberts, C.A., 2005. Continuity or colonization in Anglo-Saxon England? Isotope evidence for mobility, subsistence practice, and status at West Heslerton. Am. J. Phys. Anthropol. 126, 123–138. http://dx.doi.org/10.1002/ajpa.20111.
Moynier, F., Agranier, A., Hezel, D.C., Bouvier, A., 2010. Sr stable isotope composition of Earth, the Moon, Mars, Vesta and meteorites. Earth Planet. Sci. Lett. 300, 359–366. http://dx.doi.org/10.1016/j.epsl.2010.10.017.
Moynier, F., Day, J.M.D., Okui, W., Yokoyama, T., Bouvier, A., Walker, R.J., Podosek, F.A., 2012. Planetary-scale strontium isotopic heterogeneity and the age of volatile depletion of early Solar System materials. Astrophys. J. 758, 45–51. http://dx.doi.org/10.1088/0004-637X/758/1/45.
Négrel, P., 1992. Utilisation des isotopes du strontium, des alcalins et alcalino-terreux pour la détermination des bilans des éléments chimiques dans les fleuves: Apports atmosphériques, altération des roches. Univ. Paris 7.
Négrel, P., Allègre, C.J., Dupré, B., Lewin, E., 1993. Erosion sources determined by inversion of major and trace element ratios and strontium isotopic ratios in river: the Congo Basin case. Earth Planet. Sci. Lett. 120, 59–76. http://dx.doi.org/10.1016/0012-821X(93)90023-3.
Négrel, P., Guerrot, C., Millot, R., 2007. Chemical and strontium isotope characterization of rainwater in France: influence of sources and hydrogeochemical implications. Isot. Environ. Health Stud. 43, 179–196.
Négrel, P., Roy, S., 1998. Chemistry of rainwater in the Massif Central (France): a strontium isotope and major element study. Appl. Geochem. 13, 941–952. http://dx.doi.org/10.1016/S0883-2927(98)00029-8.
Nelson, B.K., DeNiro, M.J., Schoeninger, M.J., De Paolo, D.J., Hare, P.E., 1986. Effects of diagenesis on strontium, carbon, nitrogen and oxygen concentration and isotopic composition of bone. Geochim. Cosmochim. Acta 50, 1941–1949. http://dx.doi.org/10.1016/0016-7037(86)90250-4.
Nielsen-Marsh, C.M., Hedges, R.E., 2000. Patterns of diagenesis in bone II: effects of acetic acid treatment and the removal of diagenetic CO3 2−. J. Archaeol. Sci. 27, 1151–1159. http://dx.doi.org/10.1006/jasc.1999.0537.
Oda, H., Kawasaki, A., Hirata, T., 2001. Determination of the geographic origin of brown-rice with isotope ratios of 11B/10B and 87Sr/86Sr. Anal. Sci. 17 (Suppl. e), i1627–i1630.
Ohno, T., Hirata, T., 2007. Simultaneous determination of mass-dependent isotopic fractionation and radiogenic isotope variation of strontium in geochemical samples by multiple collector-ICP-mass spectrometry. Anal. Sci. 23, 1275–1280. http://dx.doi.org/10.2116/analsci.23.1275.
Ohno, T., Komiya, T., Ueno, Y., Hirata, T., Maruyama, S., 2008. Determination of 88Sr/86Sr mass-dependent isotopic fractionation and radiogenic isotope variation of 87Sr/86Sr in the Neoproterozoic Doushantuo Formation. Gondwana Res. 14, 126–133. http://dx.doi.org/10.1016/j.gr.2007.10.007.
Palmer, M., Edmond, J., 1992. Controls over the strontium isotope composition of river water. Geochim. Cosmochim. Acta 56, 2099–2111. http://dx.doi.org/10.1016/0016-7037(92)90332-D.
Palmer, M.R., Edmond, J.M., 1989. The strontium isotope budget of the modern ocean. Earth Planet. Sci. Lett. 92, 11–26. http://dx.doi.org/10.1016/0012-821X(89)90017-4.
Pearce, C.R., Parkinson, I.J., Gaillardet, J., Charlier, B.L.A., Mokadem, F., Burton, K.W., 2015a. Reassessing the stable (δ88/86Sr) and radiogenic (87Sr/86Sr) strontium isotopic composition of marine inputs. Geochim. Cosmochim. Acta 157, 125–146. http://dx.doi.org/10.1016/j.gca.2015.02.029.
Pearce, C.R., Parkinson, I.J., Gaillardet, J., Chetelat, B., Burton, K.W., 2015b. Characterising the stable (δ88/86Sr) and radiogenic (87Sr/86Sr) isotopic composition of strontium in rainwater. Chem. Geol. 409, 54–60. http://dx.doi.org/10.1016/j.chemgeo.2015.05.010.
Petit, R.J., Aguinagalde, I., de Beaulieu, J.-L., Bittkau, C., Brewer, S., Cheddadi, R., Ennos, R., Fineschi, S., Grivet, D., Lascoux, M., Mohanty, A., Müller-Starck, G., Demesure-Musch, B., Palmé, A., Martín, J.P., Rendell, S., Vendramin, G.G., 2003. Glacial refugia: hotspots but not melting pots of genetic diversity. Sci. (80-.) 300, 1563–1565. http://dx.doi.org/10.1126/science.1083264.
Petit, R.J., Brewer, S., Bordács, S., Burg, K., Cheddadi, R., Coart, E., Cottrell, J., Csaikl, U.M., Van Dam, B., Deans, J.D., Espinel, S., Fineschi, S., Finkeldey, R., Glaz, I., Goicoechea, P.G., Jensen, J.S., König, A.O., Lowe, A.J., Madsen, S.F., Mátyás, G., Munro, R.C., Popescu, F., Slade, D., Tabbener, H., De Vries, S.G.M., Ziegenhagen, B., De Beaulieu, J.L., Kremer, A., 2002a. Identification of refugia and post-glacial colonisation routes of European white oaks based on chloroplast DNA and fossil pollen evidence. For. Ecol. Manage 156, 49–74. http://dx.doi.org/10.1016/S0378-1127(01)00634-X.
Petit, R.J., Csaikl, U.M., Bordács, S., Burg, K., Coart, E., Cottrell, J., van Dam, B., Deans, J.D., Dumolin-Lapègue, S., Fineschi, S., Finkeldey, R., Gillies, A., Glaz, I., Goicoechea, P.G., Jensen, J.S., König, A.O., Lowe, A.J., Madsen, S.F., Mátyás, G., Munro, R.C., Olalde, M., Pemonge, M.-H., Popescu, F., Slade, D., Tabbener, H., Taurchini, D., de Vries, S.G.M., Ziegenhagen, B., Kremer, A., 2002b. Chloroplast DNA variation in European white oaks: phylogeography and patterns of diversity based on data from over 2600 populations. For. Ecol. Manage 156, 5–26. http://dx.doi.org/10.1016/S0378-1127(01)00645-4.
Petit, R.J., Latouche-Hallé, C., Pemonge, M.H., Kremer, A., 2002c. Chloroplast DNA variation of oaks in France and the influence of forest fragmentation on genetic diversity. For. Ecol. Manage 156, 115–129. http://dx.doi.org/10.1016/S0378-1127(01)00638-7.
Petrini, R., Sansone, L., Slejko, F.F., Buccianti, A., Marcuzzo, P., Tomasi, D., 2015. The 87Sr/86Sr strontium isotopic systematics applied to Glera vineyards: a tracer for the geographical origin of the Prosecco. Food Chem. 170, 138–144. http://dx.doi.org/10.1016/j.foodchem.2014.08.051.
Peucker-Ehrenbrink, B., Miller, M.W., Arsouze, T., Jeandel, C., 2010. Continental bedrock and riverine fluxes of strontium and neodymium isotopes to the oceans. Geochem. Geophys. Geosyst. 11, Q03016. http://dx.doi.org/10.1029/2009GC002869.
Pillonel, L., Badertscher, R., Froidevaux, P., Haberhauer, G., Hölzl, S., Horn, P., Jakob, A., Pfammatter, E., Piantini, U., Rossmann, A., Tabacchi, R., Bosset, J.O., 2003. Stable isotope ratios, major, trace and radioactive elements in emmental cheeses of different origins. LWT - Food Sci. Technol. 36, 615–623. http://dx.doi.org/10.1016/S0023-6438(03)00081-1.
Poszwa, A., Dambrine, E., Ferry, B., Pollier, B., Loubet, M., 2002. Do deep tree roots provide nutrients to the tropical rainforest? Biogeochemistry 60, 97–118. http://dx.doi.org/10.1023/A:1016548113624.
Poszwa, A., Ferry, B., Dambrine, E., Pollier, B., Wickman, T., Loubet, M., Bishop, K., 2004. Variations of bioavailable Sr concentration and 87Sr/86Sr ratio in boreal forest ecosystems. Biogeochemistry 67, 1–20.
Poszwa, A., Ferry, B., Pollie, B., Grimaldi, C., Charles-Dominique, P., Loubet, M., Dambrine, E., 2009. Variations of plant and soil 87Sr/86Sr along the slope of a tropical inselberg. Ann. For. Sci. 66, 1–13. http://dx.doi.org/10.1051/forest/2009036.
Poszwa, A., Wickman, T., Dambrine, E., Ferry, B., Dupouey, J.L., Helle, G., Schleser, G., Breda, N., 2003. A retrospective isotopic study of spruce decline in the Vosges mountains (France). Water, Air, Soil Pollut. Focus 3, 201–222. http://dx.doi.org/10.1023/A:1022176025379.
Price, T.D., Blitz, J., Burton, J., Ezzo, J.A., 1992. Diagenesis in prehistoric bone: problems and solutions. J. Archaeol. Sci. 19, 513–529. http://dx.doi.org/10.1016/0305-4403(92)90026-Y.
Price, T.D., Burton, J.H., Bentley, R.A., 2002. The characterization of biologically available strontium isotope ratios for the study of prehistoric migration. Archaeometry 44, 117–135.
Price, T.D., Grupe, G., Schröter, P., 1998. Migration in the bell beaker period of central Europe. Antiquity 72, 405–411.
Price, T.D., Grupe, G., Schröter, P., 1994a. Reconstruction of migration patterns in the Bell Beaker period by stable strontium isotope analysis. Appl. Geochem. 9, 413–417. http://dx.doi.org/10.1016/0883-2927(94)90063-9.
Price, T.D., Johnson, C.M., Ezzo, J.A., Ericson, J., Burton, J.H., 1994b. Residential mobility in the prehistoric southwest United States: a preliminary study using strontium isotope analysis. J. Archaeol. Sci. 21, 315–330.
Price, T.D., Manzanilla, L., Middleton, W.D., 2000. Immigration and the ancient city of Teotihuacan in Mexico: a study using strontium isotope ratios in human bone

and teeth. J. Archaeol. Sci. 27, 903–913. http://dx.doi.org/10.1006/jasc.1999.0504.
Price, T.D., Nielsen, J.N., Frei, K.M., Lynnerup, N., 2012. Sebbersund: isotopes and mobility in an 11th-12th c. AD Danish churchyard. J. Archaeol. Sci. 39, 3714–3720. http://dx.doi.org/10.1016/j.jas.2012.06.015.
Probst, A., El Gh'mari, A., Aubert, D., Fritz, B., McNutt, R., 2000. Strontium as a tracer of weathering processes in a silicate catchment polluted by acid atmospheric inputs, Strengbach, France. Chem. Geol. 170, 203–219. http://dx.doi.org/10.1016/S0009-2541(99)00248-X.
Raddatz, J., Liebetrau, V., Rüggeberg, A., Hathorne, E., Krabbenhöft, A., Eisenhauer, A., Böhm, F., Vollstaedt, H., Fietzke, J., López Correa, M., Freiwald, A., Dullo, W.C., 2013. Stable Sr-isotope, Sr/Ca, Mg/Ca, Li/Ca and Mg/Li ratios in the scleractinian cold-water coral Lophelia pertusa. Chem. Geol. 352, 143–152. http://dx.doi.org/10.1016/j.chemgeo.2013.06.013.
Raymo, M.E., Ruddiman, W.F., Froelich, P.N., 1988. Influence of late Cenozoic mountain building on ocean geochemical cycles. Geology 16, 649–653. http://dx.doi.org/10.1130/0091-7613(1988)016<0649:IOLCMB>2.3.CO;2.
Reynolds, A.C., Betancourt, J.L., Quade, J., Patchett, P.J., Dean, J.S., Stein, J., 2005. 87Sr/86Sr sourcing of ponderosa pine used in Anasazi great house construction at Chaco Canyon, New Mexico. J. Archaeol. Sci. 32, 1061–1075. http://dx.doi.org/10.1016/j.jas.2005.01.016.
Rich, S., Manning, S.W., Degryse, P., Vanhaecke, F., Latruwe, K., Van Lerberghe, K., 2016. To put a cedar ship in a bottle: dendroprovenancing three ancient East Mediterranean watercraft with the 87Sr/86SR isotope ratio. J. Archaeol. Sci. Rep. 9, 514–521. http://dx.doi.org/10.1016/j.jasrep.2016.08.034.
Rich, S., Manning, S.W., Degryse, P., Vanhaecke, F., Van Lerberghe, K., 2015. Provenancing East Mediterranean cedar wood with the 87Sr/86Sr strontium isotope ratio. Archaeol. Anthropol. Sci. 1–10. http://dx.doi.org/10.1007/s12520-015-0242-7.
Rich, S., Manning, S.W., Degryse, P., Vanhaecke, F., Van Lerberghe, K., 2012. Strontium isotopic and tree-ring signatures of Cedrus brevifolia in Cyprus. J. Anal. At. Spectrom. 27, 796–806. http://dx.doi.org/10.1039/c2ja10345a.
Richter, F.M., Rowley, D.B., DePaolo, D.J., 1992. Sr isotope evolution of seawater: the role of tectonics. Earth Planet. Sci. Lett. 109, 11–23. http://dx.doi.org/10.1016/0012-821X(92)90070-C.
Richter, F.M., Turekian, K.K., 1993. Simple models for the geochemical response of the ocean to climatic and tectonic forcing. Earth Planet. Sci. Lett. 119, 121–131. http://dx.doi.org/10.1016/0012-821X(93)90010-7.
Rodrigues, J., Faix, O., Pereira, H., 1998. Determination of lignin content of Eucalyptus globulus wood using FTIR spectroscopy. Holzforschung 52, 46–50. http://dx.doi.org/10.1515/hfsg.1998.52.1.46.
Rossmann, A., Haberhauer, G., Hölzl, S., Horn, P., Pichlmayer, F., Voerkelius, S., 2000. The potential of multielement stable isotope analysis for regional origin assignment of butter. Eur. Food Res. Technol. 211, 32–40. http://dx.doi.org/10.1007/s002170050585.
Rüggeberg, A., Fietzke, J., Liebetrau, V., Eisenhauer, A., Dullo, W.C., Freiwald, A., 2008. Stable strontium isotopes (δ88/86Sr) in cold-water corals - a new proxy for reconstruction of intermediate ocean water temperatures. Earth Planet. Sci. Lett. 269, 570–575. http://dx.doi.org/10.1016/j.epsl.2008.03.002.
Rummel, S., Hoelzl, S., Horn, P., Rossmann, A., Schlicht, C., 2010. The combination of stable isotope abundance ratios of H, C, N and S with 87Sr/86Sr for geographical origin assignment of orange juices. Food Chem. 118, 890–900. http://dx.doi.org/10.1016/j.foodchem.2008.05.115.
Sandak, A., Sandak, J., Babiński, L., Pauliny, D., Riggio, M., 2014. Spectral analysis of changes to pine and oak wood natural polymers after short-term waterlogging. Polym. Degrad. Stab. 99, 68–79. http://dx.doi.org/10.1016/j.polymdegradstab.2013.11.018.
Sandak, A., Sandak, J., Negri, M., 2011. Relationship between near-infrared (NIR) spectra and the geographical provenance of timber. Wood Sci. Technol. 45, 35–48. http://dx.doi.org/10.1007/s00226-010-0313-y.
Sandak, J., Sandak, A., Cantini, C., Autino, A., 2015. Differences in wood properties of Picea abies L. Karst. in relation to site of provenance and population genetics. Holzforschung 69, 385–397. http://dx.doi.org/10.1515/hf-2014-0061.
Sandström, M., Jalilehvand, F., Damian, E., Fors, Y., Gelius, U., Jones, M., Salomé, M., 2005. Sulfur accumulation in the timbers of King Henry VIII's warship Mary Rose: a pathway in the sulfur cycle of conservation concern. Proc. Natl. Acad. Sci. 102, 14165–14170. http://dx.doi.org/10.1073/pnas.0504490102.
Sandström, M., Jalilehvand, F., Persson, I., Gelius, U., Frank, P., 2002a. Acidity and salt precipitation on the Vasa: the sulfur problem. In: Proceedings of the 8th ICOM Group on Wet Organic Archaeological Materials Conference: Stockholm 2001, pp. 67–89.
Sandström, M., Jalilehvand, F., Persson, I., Gelius, U., Frank, P., Hall-Roth, I., 2002b. Deterioration of the seventeenth-century warship Vasa by internal formation of sulphuric acid. Nature 415, 893–897. http://dx.doi.org/10.1038/415893a.
Sass-Klaassen, U., Vernimmen, T., Baittinger, C., 2008. Dendrochronological dating and provenancing of timber used as foundation piles under historic buildings in The Netherlands. Int. Biodeterior. Biodegrad. 61, 96–105. http://dx.doi.org/10.1016/j.ibiod.2007.07.013.
Saurer, M., Siegenthaler, U., Schweingruber, F., 1995. The climate-carbon isotope relationship in tree rings and the significance of site conditions. Tellus B 47, 320–330. http://dx.doi.org/10.1034/j.1600-0889.47.issue3.4.x.
Sealy, J.C., van der Merwe, N.J., Sillen, A., Kruger, F.J., Krueger, H.W., 1991. 87Sr/86Sr as a dietary indicator in modern and archaeological bone. J. Archaeol. Sci. 18, 399–416. http://dx.doi.org/10.1016/0305-4403(91)90074-Y.
Seimbille, F., Négrel, P., Dupré, B., Allègre, C.J., 1989. Nature of the strontium atmospheric input in the Parisian Basin. Terra Abstr. 1, 346.
Shalev, N., Gavrieli, I., Halicz, L., Sandler, A., Stein, M., Lazar, B., 2017. Enrichment of 88Sr in continental waters due to carbonate precipitation. Earth Planet. Sci. Lett. 459, 381–393. http://dx.doi.org/10.1016/j.epsl.2016.11.042.
Shalev, N., Lazar, B., Halicz, L., Stein, M., Gavrieli, I., Sandler, A., Segal, I., 2013. Strontium isotope fractionation in soils and pedogenic processes. Procedia Earth Planet. Sci. 7, 790–793. http://dx.doi.org/10.1016/j.proeps.2013.03.074.
Shaw, H., Montgomery, J., Redfern, R., Gowland, R., Evans, J., 2016. Identifying migrants in Roman London using lead and strontium stable isotopes. J. Archaeol. Sci. 66, 57–68. http://dx.doi.org/10.1016/j.jas.2015.12.001.
Shaw, J.E., Baker, J.A., Menzies, M.A., Thirlwall, M.F., Ibrahim, K.M., 2003. Petrogenesis of the largest intraplate volcanic field on the Arabian Plate (Jordan): a mixed lithosphere–asthenosphere source activated by lithospheric extension Extension. J. Pet. 44, 1657–1679. http://dx.doi.org/10.1093/petrology/egg052.
Sillen, A., Hall, G., Richardson, S., Armstrong, R., 1998. 87Sr/86Sr ratios in modern and fossil food-webs of the Sterkfontein Valley: implications for early hominid habitat preference. Geochim. Cosmochim. Acta 62, 2463–2473.
Sillen, A., Sealy, J.C., 1995. Diagenesis of strontium in fossil bone: a reconsideration of Nelson et al. (1986). J. Archaeol. Sci. 22, 313–320. http://dx.doi.org/10.1006/jasc.1995.0033.
Slovak, N.M., Paytan, A., 2011. Applications of Sr isotopes in archaeology. Adv. Isot. Geochem. 5, 743–768. http://dx.doi.org/10.1007/978-3-642-10637-8_8.
Slovak, N.M., Paytan, A., Wiegand, B.A., 2009. Reconstructing Middle Horizon mobility patterns on the coast of Peru through strontium isotope analysis. J. Archaeol. Sci. 36, 157–165. http://dx.doi.org/10.1016/j.jas.2008.08.004.
Smith, J., Vance, D., Kemp, R.A., Archer, C., Toms, P., King, M., Zárate, M., 2003. Isotopic constraints on the source of Argentinian loess - with implications for atmospheric circulation and the provenance of Antarctic dust during recent glacial maxima. Earth Planet. Sci. Lett. 212, 181–196. http://dx.doi.org/10.1016/S0012-821X(03)00260-7.
Smith, R.H., Peloquin, R.L., Passoff, P.C., 1969. Local and Regional Variation in the Monoterpenes of Ponderosa Pine Wood Oleoresin.
Song, B.Y., Gautam, M.K., Ryu, J.S., Lee, D., Lee, K.S., 2015. Effects of bedrock on the chemical and Sr isotopic compositions of plants. Environ. Earth Sci. 74, 829–837. http://dx.doi.org/10.1007/s12665-015-4087-2.
Stein, M., Hofmann, A.W., 1992. Fossil plume head beneath the Arabian lithosphere? Earth Planet. Sci. Lett. 114, 193–209. http://dx.doi.org/10.1016/0012-821X(92)90161-N.
Stevenson, E.I., Aciego, S.M., Chutcharavan, P., Parkinson, I.J., Burton, K.W., Blakowski, M.A., Arendt, C.A., 2016. Insights into combined radiogenic and stable strontium isotopes as tracers for weathering processes in subglacial environments. Chem. Geol. 429, 33–43. http://dx.doi.org/10.1016/j.chemgeo.2016.03.008.
Stevenson, E.I., Hermoso, M., Rickaby, R.E.M., Tyler, J.J., Minoletti, F., Parkinson, I.J., Mokadem, F., Burton, K.W., 2014. Controls on stable strontium isotope fractionation in coccolithophores with implications for the marine Sr cycle. Geochim. Cosmochim. Acta 128, 225–235. http://dx.doi.org/10.1016/j.gca.2013.11.043.
Stewart, B.W., Capo, R.C., Chadwick, O.A., 1998. Quantitative strontium isotope models for weathering, pedogenesis and biogeochemical cycling. Geoderma 82, 173–195. http://dx.doi.org/10.1016/S0016-7061(97)00101-8.
Stueber, A.M., Pushkar, P., Hetherington, E.A., 1987. A strontium isotopic study of formation waters from the Illinois basin. U.S.A. Appl. Geochem. 2, 477–494. http://dx.doi.org/10.1016/0883-2927(87)90003-5.
Stuiver, M., Braziunas, T.F., 1987. Tree cellulose 13C/12C isotope ratios and climatic change. Nature 328, 58–60. http://dx.doi.org/10.1038/328058a0.
Svensson, A., Biscaye, P.E., Grousset, F.E., 2000. Characterization of late glacial continental dust in the Greenland Ice Core Project ice core. J. Geophys. Res. 105, 4637–4656. http://dx.doi.org/10.1029/1999JD901093.
Swoboda, S., Brunner, M., Boulyga, S.F., Galler, P., Horacek, M., Prohaska, T., 2008. Identification of Marchfeld asparagus using Sr isotope ratio measurements by MC-ICP-MS. Anal. Bioanal. Chem. 390, 487–494. http://dx.doi.org/10.1007/s00216-007-1582-7.
Taylor, S.R., McLennan, S.M., McCulloch, M.T., 1983. Geochemistry of loess, continental crustal composition and crustal model ages. Geochim. Cosmochim. Acta 47, 1897–1905. http://dx.doi.org/10.1016/0016-7037(83)90206-5.
Techer, I., Lancelot, J., Descroix, F., Guyot, B., 2011. About Sr isotopes in coffee "Bourbon pointu" of the Réunion island. Food Chem. 126, 718–724. http://dx.doi.org/10.1016/j.foodchem.2010.11.035.
Techer, I., Medini, S., Janin, M., Arregui, M., 2017. Impact of agricultural practice on the Sr isotopic composition of food products: application to discriminate the geographic origin of olives and olive oil. Appl. Geochem. 82, 1–14. http://dx.doi.org/10.1016/j.apgeochem.2017.05.010.
Tipper, E.T., Bickle, M.J., Galy, A., West, A.J., Pomiès, C., Chapman, H.J., 2006. The short term climatic sensitivity of carbonate and silicate weathering fluxes: insight from seasonal variations in river chemistry. Geochim. Cosmochim. Acta 70, 2737–2754. http://dx.doi.org/10.1016/j.gca.2006.03.005.
Tipper, E.T., Gaillardet, J., Galy, A., Louvat, P., Bickle, M.J., Capmas, F., 2010. Calcium isotope ratios in the world's largest rivers: a constraint on the maximum imbalance of oceanic calcium fluxes. Glob. Biogeochem. Cycles 24. http://dx.doi.org/10.1029/2009GB003574.
Torre, M., Rodroguez, A., Saura-Calixto, F., 1992. Study of the interactions of calcium ions with lignin, cellulose and pectine. J. Agric. Food Chem. 40, 1762–1766.
Traoré, M., Kaal, J., Martínez Cortizas, A., 2016. Application of FTIR spectroscopy to the characterization of archeological wood. Spectrochim. Acta Part A Mol.

Biomol. Spectrosc. 153, 63–70. http://dx.doi.org/10.1016/j.saa.2015.07.108.
Trickett, M.A., Budd, P., Montgomery, J., Evans, J., 2003. An assessment of solubility profiling as a decontamination procedure for the 87Sr/86Sr analysis of archaeological human skeletal tissue. Appl. Geochem. 18, 653–658. http://dx.doi.org/10.1016/S0883-2927(02)00181-6.
Trincherini, P.R., Baffi, C., Barbero, P., Pizzoglio, E., Spalla, S., 2014. Precise determination of strontium isotope ratios by TIMS to authenticate tomato geographical origin. Food Chem. 145, 349–355. http://dx.doi.org/10.1016/j.foodchem.2013.08.030.
Tuross, N., Behrensmeyer, A.K., Eanes, E.D., 1989. Strontium increases and crystallinity changes in taphonomic and archaeological bone. J. Archaeol. Sci. 16, 661–672. http://dx.doi.org/10.1016/0305-4403(89)90030-7.
van Bergen, P.F., Poole, I., 2002. Stable carbon isotopes of wood: a clue to palaeoclimate? Palaeogeogr. Palaeoclimatol. Palaeoecol. 182, 31–45. http://dx.doi.org/10.1016/S0031-0182(01)00451-5.
van der Hoven, S.J., Quade, J., 2002. Tracing spatial and temporal variations in the sources of calcium in pedogenic carbonates in a semiarid environment. Geoderma 108, 259–276. http://dx.doi.org/10.1016/S0016-7061(02)00134-9.
van der Merwe, N.J., Lee-Thorp, J.A., Thackeray, J.F., Hall-Martin, A., Kruger, F.J., Coetzee, H., Bell, R.H.V., Lindeque, M., 1990. Source-area determination of elephant ivory by isotopic analysis. Nature 346, 744–746. http://dx.doi.org/10.1038/346183a0.
van Zuilen, K., Müller, T., Nägler, T.F., Dietzel, M., Küsters, T., 2016. Experimental determination of barium isotope fractionation during diffusion and adsorption processes at low temperatures. Geochim. Cosmochim. Acta 186, 226–241. http://dx.doi.org/10.1016/j.gca.2016.04.049.
Vance, D., Teagle, D.A.H., Foster, G.L., 2009. Variable Quaternary chemical weathering fluxes and imbalances in marine geochemical budgets. Nature 458, 493–496. http://dx.doi.org/10.1038/nature07828.
Veizer, J., 1989. Strontium isotopes in seawater through time. Annu. Rev. Earth Planet. Sci. 17, 141–167.
Vinciguerra, V., Stevenson, R., Pedneault, K., Poirier, A., Hélie, J.-F., Widory, D., 2016. Strontium isotope characterization of wines from Quebec, Canada. Food Chem. 210, 121–128. http://dx.doi.org/10.1016/j.foodchem.2016.04.017.
Vinciguerra, V., Stevenson, R., Pedneault, K., Poirier, A., Hélie, J.-F., Widory, D., 2015. Strontium isotope characterization of wines from the Quebec (Canada) terroir. Procedia Earth Planet. Sci. 13, 252–255. http://dx.doi.org/10.1016/j.proeps.2015.07.059.
Voigt, J., Hathorne, E.C., Frank, M., Vollstaedt, H., Eisenhauer, A., 2015. Variability of carbonate diagenesis in equatorial Pacific sediments deduced from radiogenic and stable Sr isotopes. Geochim. Cosmochim. Acta 148, 360–377. http://dx.doi.org/10.1016/j.gca.2014.10.001.
Vollstaedt, H., Eisenhauer, A., Wallmann, K., Böhm, F., Fietzke, J., Liebetrau, V., Krabbenhöft, A., Farkaš, J., Tomašových, A., Raddatz, J., Veizer, J., 2014. The Phanerozoic δ88/86Sr record of seawater: new constraints on past changes in oceanic carbonate fluxes. Geochim. Cosmochim. Acta 128, 249–265. http://dx.doi.org/10.1016/j.gca.2013.10.006.
Wadleigh, M.A., Veizer, J., Brooks, C., 1985. Strontium and its isotopes in Canadian rivers: fluxes and global implications. Geochim. Cosmochim. Acta 49, 1727–1736. http://dx.doi.org/10.1016/0016-7037(85)90143-7.
Wei, G., Ma, J., Liu, Y., Xie, L., Lu, W., Deng, W., Ren, Z., Zeng, T., Yang, Y., 2013. Seasonal changes in the radiogenic and stable strontium isotopic composition of Xijiang River water: implications for chemical weathering. Chem. Geol. 343, 67–75. http://dx.doi.org/10.1016/j.chemgeo.2013.02.004.
Weinstein, Y., 2000. Spatial and temporal geochemical variability in basin-related volcanism, northern Israel. J. Afr. Earth Sci. 30, 865–886. http://dx.doi.org/10.1016/S0899-5362(00)00057-9.
Weinstein, Y., Navon, O., Altherr, R., Stein, M., 2006. The role of lithospheric mantle heterogeneity in the generation of Plio-Pleistocene alkali basaltic suites from NW Harrat Ash Shaam (Israel). J. Pet. 47, 1017–1050. http://dx.doi.org/10.1093/petrology/egl003.
Wickman, T., 1996. Weathering Assessment and Nutrient Availability in Coniferous Forests. Royal Institute of Technology, Stockholm.
Widanagamage, I.H., Griffith, E.M., Singer, D.M., Scher, H.D., Buckley, W.P., Senko, J.M., 2015. Controls on stable Sr-isotope fractionation in continental barite. Chem. Geol. 411, 215–227. http://dx.doi.org/10.1016/j.chemgeo.2015.07.011.
Widanagamage, I.H., Schauble, E.A., Scher, H.D., Griffith, E.M., 2014. Stable strontium isotope fractionation in synthetic barite. Geochim. Cosmochim. Acta 147, 58–75. http://dx.doi.org/10.1016/j.gca.2014.10.004.